論文 / 著書情報
Article / Book Information

題目(和文)	メソン-バリオン分子状態を含んだ構成子クォーク模型によるチャームバリオンのP波励起状態の解析
Title(English)	P-wave heavy baryons in a constituent quark model and their couplings to meson-baryon dynamical states
著者(和文)	吉田哲也
Author(English)	Tetsuya Yoshida
出典(和文)	学位:博士(理学), 学位授与機関:東京工業大学, 報告番号:甲第10399号, 授与年月日:2017年3月26日, 学位の種別:課程博士, 審査員:岡 眞,伊藤 克司,今村 洋介,肥山 詠美子,陣内 修
Citation(English)	Degree:Doctor (Science), Conferring organization: Tokyo Institute of Technology, Report number:甲第10399号, Conferred date:2017/3/26, Degree Type:Course doctor, Examiner:,,,,
学位種別(和文)	博士論文
Category(English)	Doctoral Thesis
種別(和文)	要約
Type(English)	Outline

P-wave heavy baryons in a constituent quark model and their couplings to meson-baryon dynamical states

Tetsuya Yoshida

Department of Physics, H-27, Tokyo Institute of Technology, Meguro, Tokyo 152-8551, Japan

February 24, 2017

A dissertation submitted to Tokyo Institute of Technology for the degree of Doctor of Science

Contents

Abstract

Recently, experiments to observe new states of excited heavy baryons are being performed at several facilities such as J-PARC, KEKB-factory, J-Lab, GSI, CERN, BES-III. It is expected both theoretically and experimentally that heavy hadrons show the specific dynamics, which is not seen in light hadrons. Hence, the study of the spectra and the dynamics of heavy hadrons are interesting topics, and clarifying the masses of excited heavy baryons and their structures are urgent issues in the modern hadron physics.

In this thesis, we study the spectrum and the structure of heavy baryon excited states using a non-relativistic potential quark model.

The model Hamiltonian is chosen as the standard one with two exceptions: (1) the color-Coulomb term depends on quark masses and (2) an antisymmetric LS (spin-orbit) force is introduced. We fix model parameters in the strange baryon sector and the masses of the observed charmed and bottomed baryons are, then, fairly well reproduced with the parameters. One of our focuses is on the low-lying negative-parity states, in which the heavy baryons show specific excitation modes reflecting the mass differences of heavy and light quarks. By changing quark masses from the SU(3) limit to the strange quark mass, and, further, to the charm and bottom quark masses, we demonstrate that the spectra change from the SU(3) symmetry patterns to the heavy-quark-symmetry ones.

Heavy baryons are predicted in the constituent quark model. However, the conventional quark model neglects the meson-baryon coupling. Thus, the meson-baryon coupling effect should be considered to predict the hadron spectrum. Moreover, hadronic model suggests that the meson-baryon molecule states realize [1]. Hence, two kinds of coupling effects on the three-quark state are considered, that is, the coupling of the three quark state with meson-baryon scattering states, and the coupling of the three-quark state with the meson-baryon molecule states. We investigate these two coupling effects by analyzing the poles in the two cases, namely in which the Weinberg-Tomozawa interaction is switched on and off.

The couplings of meson-baryon molecule state on the three-quark state are investigated by the hybrid model based on the quark model, the chiral effective theory and the Bete-Salpeter equation. We adopt the dimensional regularization scheme and we also use the 3D cut-off scheme in order to clarify the regularization scheme dependence. We determine the mass of excited heavy baryons from the constituent quark model and the effective coupling between the bare excited heavy baryon states and meson-baryon scattering state from $^3P_0$ model. We focus on $I = 0$, $J^P = 1/2^-$, $\mathcal{C} = 1$, $\mathcal{B} = 0$, $\mathcal{S} = 0$ channels to study the coupling of the ρ and λ mode states with the meson-baryon scattering states.

Our study in this thesis have the following four purposes: (1) The prediction of the spectra of excited single- and double- heavy baryons, (2) Clarifying the structure of P-wave heavy baryons in the aspect of the specific two modes, λ and ρ modes, (3) investigating the heavy hadron states in the heavy quark limit

and its relation to the $SU(3)$ state and (4) investigating the P-wave excited states of charmed baryons in a constituent quark model with the meson-baryon coupling effect through the hybrid model based on the quark model, the chiral effective theory and Bete-Salpeter equation [1].

[1]Since this thesis contains reference to unpublished work, applicable pages are omitted from the thesis. The applicable pages will be published after Apr 2017.

Part I

Introduction and Reviews

Chapter 1

Introduction

1.1 Hadron spectroscopy

Hadron is a general term for composite particles of *quarks*. The quark is one of the elementary particles in the standard model and interacts with each other by exchanging a gauge boson, called gluon. Quark and gluon are governed by the theory called Quantum Chromo-Dynamics (QCD), which describes the physics related to the strong interaction. The unique properties of QCD, such as confinement of color, asymptotic freedom, lead to difficulty to understand the physics related to the strong interaction. Since a free quark cannot be observed basically because of the confinement, experimental observations of hadrons and theoretical approaches from effective theories of hadrons become important to clarify or understand QCD.

History of the study for hadrons started by the discovery of proton by Ernest Rutherford, and now over 200 hadrons have been observed [2]. It is expected that there are still a large number of hadrons and they are waiting to be observed experimentally and described theoretically. To complete the spectroscopy and clarify its structure and properties of hadrons is one of the topics in the modern physics.

Before 1964, several hadrons composed of up, down, strange quark were discovered (See TABLE.1.3). Most hadrons, except for the pion and the neutron, were discovered in advance of theoretical predictions. Thus, hadrons were not classified systematically until 1964. In 1964, quark model suggested how to classify hadrons [3], and then we got to know which hadrons were discovered and which were not.

Recently, study of heavy hadrons, which include heavy quarks, attract attention both theoretically and experimentally. The charm and bottom quarks are much heavier than the light (up, down, strange) quarks and it implies that new dynamics of heavy quarks, which is not seen in the light hadrons, may be revealed. The heavy baryons observed at present are listed in TABLE.1.3

Now, in the experimental side, many accelerator laboratories, such as KEKB-factory (Tsukuba, Japan), CERN (Geneva, Switwerland), BES-III (Beigin, China) try to discover new hadrons and analyze their properties and the new hadron experiments are planned at J-PARC (Tokai, Japan), J-Lab (Virginia, USA) and GSI (Darmstadt, Germany), and in theoretical side, many effective theories of QCD try to predict hadron masses and show their dynamics.

	Mass [MeV]	$J^{P(C)}(I)$	Constituent	Discovery date
p	938	$1/2^+(1/2)$	uud	1919 by E. Rutherford
n	938	$1/2^+(1/2)$	udd	1932 by J. Chadwick
π	134	$0^{--}(0)$	$\bar{u}u$	1947 by C.F. Powell group
K	510	$0^{--}(1/2)$	$\bar{s}u$	1947 by G.D.Rochester
Λ^0	1116	$1/2^+(0)$	uds	1947
Ξ	1315	$1/2^+(1/2)$	uss	1964

Table 1.1: Observed hadrons discovered before 1964's.

1.2 Heavy hadrons

	Mass [MeV]	$J^{P(C)}(I)$	Constituent	Discovery date
J/ψ	2938	$1^{-+}(0)$	$\bar{c}c$	1974 [4, 5]
Υ	5500	$1^{-+}(0)$	$\bar{b}b$	1977 [6]

Table 1.2: Observed heavy quarkonia discovered in 1970's

The particle including a heavy quark discovered first is J/ψ, which is a bound state of c and $\bar{c}$, and later Υ, a $\bar{b}b$ bound state were discovered in 1973 [4–6] (See TABLE.1.2). These discoveries suggested the existence of heavy flavored quarks. Since heavy hadrons are produced at higher energy than light baryons, experimental searches are harder, and therefore less numbers of states were observed so far. Furthermore, many things are not sufficiently clear even for most of discovered heavy hadrons. Thus, the prediction of the not yet unobserved heavy hadrons and clarifying dynamics of heavy quark are an urgent issue in hadron physics.

Recent hadron physics has been stimulated by the discovery of exotic hadrons with heavy quarks. So-called X, Y, Z mesons contain most likely a hidden heavy quark and antiquark pair, either $\bar{c}c$ or $\bar{b}b$. In addition, they may contain a pair of light quark and antiquark, thus forming a multiquark configuration near the threshold region of open flavor.

For instance, $X(3872), Z_b(10610, 10850)$ are candidates of hadronic molecules of $D\bar{D}^*$, $B\bar{B}^*$ or $B^*\bar{B}^*$ via strong correlation of quark and antiquark pair [7] [8]. Furthermore, the recently discovered penta-quarks, $P_c(4380)$ and $P_c(4450)$, by LHCb [9] may also have such a structure.

Theoretically, diquark qq correlations may also play an important role, leading to the idea of compact tetraquarks [10] [11]. In fact, the diquark correlations have been considered for long time in many different contexts [12] to explain the mass ordering of light scalar mesons, weak decays of hyperons, missing nucleon resonances, novel phase structure of the quark matter and so on. In QCD, the correlation densities of the two light quarks were measured, having indicated a strong attraction in a so called good diquark pair [13]. In reality, the evidence should be also seen in masses of excited states. Charmed baryons with two light quarks may provide a good opportunity for such a study.

A pioneering work was done some time ago by Copley et al [14]. in a constituent quark model, and later elaborated by Roberts and Pervin [15]. They studied various excited states of charmed and bottomed baryons by solving three quark systems explicitly. Yet one of the motivations of the present work is to further point out the behavior of various properties of heavy baryons as functions of the heavy quark mass, smoothly interpolating the SU(3) limit of equal quark masses and the heavy quark limit. Such a study in different flavor regions is useful to systematically understand the nature of spectrum, in particular the roles of the two internal motions when baryons are regarded as three-body systems of quarks. Then the structure information must show up sensitively in various transition amplitudes of decays and productions, which can be studied experimentally at the experimental facilities like Belle, BESIII, LHCb, J-PARC and FAIR.

One important symmetry structure realized in the heavy quark hadrons is the heavy quark spin symmetry (HQS) [16]. In the heavy quark limit, the interactions which depend on the spin of the heavy quark disappear. Thus, in a single-heavy hadron the heavy quark spin $\boldsymbol{s_Q}$ is conserved, i.e., $[H, \boldsymbol{s_Q}] = 0$, and, with the conservation of the total angular momentum $\boldsymbol{J}$, one sees that $\boldsymbol{j} \equiv \boldsymbol{J} - \boldsymbol{s_Q}$, angular momentum carried by the light quarks (including all the orbital angular momenta) is also conserved. We will call j light-spin-component. Consequently, two states whose quantum number are $J = j + 1/2$ and $J = j - 1/2$ will be degenerate. They form a heavy quark spin doublet, except for $j = 0$, which yields HQS singlet. A simple example of HQS doublet is the pair of $\Sigma_Q(1/2^+)$ and $\Sigma_Q(3/2^+)$. The mass differences $\Sigma_s(3/2^+)-\Sigma_s(1/2^+)$=174 MeV, $\Sigma_c(3/2^+)-\Sigma_c(1/2^+)$=63 MeV and $\Sigma_b(3/2^+)-\Sigma_b(1/2^+)$=22 MeV decrease as m_Q becomes large.

Analysis of heavy baryons from the aspect of diquark or HQS in the quark based model gives a lot of information of heavy baryons. Yet, in a conventional quark model, the meson-baryon coupling effect basically is not taken into account. In order to reproduce complete spectroscopy, we need to consider the three quark state coupled with the meson-baryon scattering states. Furthermore, hadron based model suggests that the meson-baryon molecule state realizes. Therefore, it is expected that the three quark-state and the meson-baryon molecule state couple. We need to combine the constituent quark model with the hadron based model to investigate their couplings.

The Effective Quarntum Field Theory (EQFT) of hadron is one of the hadron based model, which looks at hadrons in a different way from the quark based model. The features of short distance scale are included in the parameters which appear in EQFT. EQFT of hadrons assumes that the hadron is a point particle. Hence, the physics of short distance, or of quark and gluon, is ignored in the theory. However, to see the system from a different standpoint sometimes leads to new discovery and expanding the understanding of hadrons.

The Chiral Effective Theory (ChET), originally introduced by Weinberg, Dashen and others in the late 60's [17–19], is one of such theories. The theory is successful in the description of resonance states of hadrons, and an especially remarkable result from ChET is about the lowest state of $\Lambda(1/2^-)$ known as $\Lambda(1405)$. It is known that $\Lambda(1405)$ is hardly reproduced by the quark model, that is to say, it predicts the mass of the first exited state of a Λ (1405) too high and cannot explain the large mass difference between $\Lambda(1405)$ and $\Lambda(1520)$.On the other hand, in ChET, $\Lambda(1405)$, located slightly below $\bar{K}N$ threshold, is well explained as the quasi-bound state of $\bar{K}N$ and show a two pole structure on a complex energy plain. Recently, ChET is applied to heavy baryons [20, 21] with the number of experimental observation of heavy

baryons increasing nowadays. To switch a strange quark in $\Lambda(1405)$ into a charm quark is a naive choice to explore whether the similar phenomena is seen in $\mathcal{C} = 1$ sector or not. $\Lambda_c(2595)$, which is located between DN threshold and $\pi\Sigma_c$ threshold, have same quantum numbers as $\Lambda(1405)$ except for flavor and hence may show a similarity with $\Lambda(1405)$.

Since, according to QCD, physical states may include all the state which have same quantum numbers, hadron molecule states in ChET and three quark state from the quark model should not be discussed separately and they are supposed to mix. However, such mixing has not been seriously discussed yet. One of our purposes is to investigate their mixing in $\mathcal{C} = 1$ sector. If the coupling between these two states is not so small, it is expected that a non-negligible shift of the mass and the width may occur.

1.3 Overview of thesis

We organize this thesis as follows: This thesis is separated into three parts. We give introduction and review to Part.1 and actual applications of the theories to Part.2 and we conclude the whole discussion in this thesis to Part.3.

In chapter 2, we review QCD and discuss its properties. QCD is the most basic theory of the strong interaction and is the starting point of effective field theories and effective models of hadrons. We discuss the basics of QCD and show a necessity of effective theories in this chapter.

In chapter 3, we review and discuss the constituent quark model which is mainly used in chapter 5. We start with a historical review of this model and show what is explained from this model with its review.

In chapter 4, the basics of chiral effective theory, which is mainly used in chapter 6, is explained. We focus on the symmetries which QCD has as a whole and in the end, we construct the effective Lagrangian of hadrons which has the same symmetry structure as QCD.

In chapter 5, we present our formulation of the non-relativistic constituent quark model. The Hamiltonian and the quark interaction are introduced in section 5.1; we employ a linear potential for quark confinement supplemented by spin-spin, tensor and spin-orbit (LS) forces. The anti-symmetric LS force is also needed to guarantee the heavy quark symmetry. In section 5.1.3, the relation of the two symmetry limits and mixings of the two internal excitation modes are discussed. In 5.2, the Gaussian expansion method is introduced to solve the many-body quark system. When the heavy quark mass is varied from $m_Q = m_q$ to $m_Q \to \infty$, then the symmetry of the spectrum changes from the SU(3) to the heavy quark spin symmetry. The results of the present work are presented in section 5.3. The results of single-heavy baryons and those of double-heavy baryons are discussed in 5.3.1 and 5.3.2, respectively. The properties of the λ and ρ modes are discussed in 5.3.3 in detail. In 5.3.4, the heavy quark limit is investigated. Finally, a summary is given in Section 5.4. Contents of 5.1 and 5.3 are the review of [22].

In appendix, we discuss the wave function in the heavy quark limit. In the heavy quark limit, the light component of the angular momentum j conserve and the basis classified by j is reasonable to discuss the heavy baryon states in that limit as we discuss in chapter 5. On the other hand, we use λ and ρ bases for the actual calculation. In this appendix, we show the relation or the transformation low of j bases and λ, ρ bases.

State	Mass [MeV]	$J^P(I)$	Constituent	Full width [MeV]	Status
Λ_c^+	2286.46 ± 0.14	$1/2^+(0)$	$1/\sqrt{2}(ud-du)c$	-	****
$\Lambda_c^+(2595)$	2592.25 ± 0.28	$1/2^-(0)$	$1/\sqrt{2}(ud-du)c$	2.6 ± 0.6	***
$\Lambda_c^+(2625)$	2628.11 ± 0.19	$3/2^-(0)$	$1/\sqrt{2}(ud-du)c$	< 0.97	***
$\Lambda_c^+ or \Sigma_c(2765)$	2766.6 ± 2.4	$?^?(?)$	$1/\sqrt{2}(ud-du)c$	50	*
$\Lambda_c^+(2880)$	2881.53 ± 0.35	$5/2^+(0)$	$1/\sqrt{2}(ud-du)c$	5.8 ± 1.1	***
$\Lambda_c^+(2940)$	$2939.3^{+1.4}_{-1.5}$	$?^?(0)$	$1/\sqrt{2}(ud-du)c$	17^{+8}_{-6}	***
$\Sigma_c^{++}(2455)$	2452.97 ± 0.4	$1/2^+(1)$	uuc	$1.89^{+0.09}_{-0.18}$	****
$\Sigma_c^+(2455)$	2452.9 ± 0.4	$1/2^+(1)$	$1/\sqrt{2}(ud+du)c$	< 4.6	****
$\Sigma_c^0(2455)$	2453.75 ± 0.14	$1/2^+(1)$	ddc	$1.89^{+0.09}_{-0.18}$	****
$\Sigma_c^{++}(2520)$	$2518.41^{+0.21}_{-0.19}$	$3/2^+(1)$	uuc	$14.78^{+0.30}_{-0.40}$	***
$\Sigma_c^+(2520)$	2517.5 ± 2.3	$3/2^+(1)$	$1/\sqrt{2}(ud+du)c$	< 17	***
$\Sigma_c^0(2520)$	2518.48 ± 0.20	$3/2^+(1)$	ddc	$15.3^{+0.4}_{-0.5}$	***
$\Sigma_c^{++}(2800)$	2801^{+4}_{-6}	$?^?(1)$	uuc	75^{+22}_{-17}	***
$\Sigma_c^+(2800)$	2792^{+14}_{-5}	$?^?(1)$	$1/\sqrt{2}(ud+du)c$	62^{+60}_{-40}	***
$\Sigma_c^0(2800)$	2806^{+5}_{-7}	$?^?(1)$	ddc	72^{+22}_{-15}	***
Ξ_c^+	$2467.93^{+0.28}_{-0.40}$	$1/2^+(1/2)$	usc	-	***
Ξ_c^0	$2470.85^{+0.28}_{-0.40}$	$1/2^+(1/2)$	usc	-	***
$\Xi_c^{+\prime}$	2575.7 ± 3.0	$1/2^+(1/2)$	usc	-	***
$\Xi_c^{0\prime}$	2577.9 ± 2.9	$1/2^+(1/2)$	usc	-	***
$\Xi_c^+(2645)$	2645.9 ± 0.5	$3/2^+(1/2)$	usc	2.6 ± 0.4	***
$\Xi_c^0(2645)$	2645.9 ± 0.5	$3/2^+(1/2)$	usc	< 5.5	***
$\Xi_c^+(2790)$	2789.1 ± 3.2	$1/2^-(1/2)$	usc	< 15	***
$\Xi_c^0(2790)$	2791.9 ± 3.3	$1/2^-(1/2)$	usc	< 12	***
$\Xi_c^+(2815)$	2816.6 ± 0.9	$3/2^-(1/2)$	usc	< 3.5	***
$\Xi_c^0(2815)$	2819.6 ± 1.2	$3/2^-(1/2)$	usc	< 6.5	***
$\Xi_c^+(2930)$	2931 ± 6	$?^?(1/2)$	usc	36 ± 13	*
$\Xi_c^+(2970)$	2970.7 ± 2.2	$?^?(1/2)$	usc	17.9 ± 3.5	***
$\Xi_c^0(2970)$	2968.0 ± 2.6	$?^?(1/2)$	usc	20 ± 7	***
$\Xi_c(3055)$	3055.1 ± 1.7	$?^?(?)$	usc	11 ± 4	***
$\Xi_c^0(3080)$	3076.94 ± 0.28	$?^?(1/2)$	usc	4.3 ± 1.5	***
$\Xi_c^+(3080)$	3079.9 ± 1.4	$?^?(1/2)$	usc	5.6 ± 2.2	***
Ω_c^0	2695.2 ± 1.7	$1/2^+(0)$	ssc	-	***
$\Omega_c^0(2770)$	2765.9 ± 2.0	$1/2^+(0)$	ssc	-	***
Λ_b^0	5619.51 ± 0.23	$1/2^+(0)$	$1/\sqrt{2}(us-du)b$	-	***
$\Lambda_b^0(5912)$	2912.11 ± 0.26	$1/2^-(0)$	$1/\sqrt{2}(ud-du)b$	< 0.66	***
$\Lambda_b^0(5920)$	2919.81 ± 0.23	$3/2^-(0)$	$1/\sqrt{2}(ud-du)b$	< 0.63	***
Σ_b^+	5811.3 ± 1.9	$1/2^+(1)$	uub	-	***
Σ_b^-	5815.5 ± 1.8	$1/2^+(1)$	$1/\sqrt{2}(ud+du)b$	-	***
Σ_b^{*+}	5832.1 ± 1.9	$3/2^+(1)$	uub	11.5 ± 2.8	***
Σ_b^{*-}	5835.1 ± 1.9	$3/2^+(1)$	$1/\sqrt{2}(ud+du)b$	21.2 ± 2.0	***
Ξ_b^-	5794.5 ± 1.4	$1/2^+(1/2)$	usb	-	***
Ξ_b^0	5791.9 ± 0.5	$1/2^+(1/2)$	usb	-	***
$\Xi_b^{-\prime}(5935)$	5935.02 ± 0.05	$1/2^+$	usb	< 0.08	***
$\Xi_b^0(5945)$	5948.9 ± 1.6	$3/2^+$	usb	2.1 ± 1.7	***
$\Xi_b^{-*}(5955)$	5955.33 ± 0.13	$3/2^+$	usb	1.65 ± 0.33	***
Ω_b^-	6046.4 ± 1.9	$1/2^+(0)$	ssb	-	***
$P_c(4380)$	4380 ± 30	$J = 3/2$ or $J = 5/2$	$uudc\bar{c}$?	205 ± 90	*
$P_c(4380)$	4449.8 ± 3.0	$J = 3/2$ or $J = 5/2$	$uudc\bar{c}$?	39 ± 20	*

Table 1.3: Observed heavy flavored baryons [2]. The name, mass, quantum number, constituent, full decay width and status are shown respectively.

Chapter 2

Review of QCD

The system, where strong interaction is dominated, is described by Quantum Chromo Dynamics (QCD). The analysis of QCD leads to the elucidation of hadron level structure, QCD phase structure, vacuum structure, color confinement etc. We do not directly use QCD to describe hadrons in our study, but at least, we have to mention what is the theory which is related to the interaction inside hadrons, why we cannot directly apply the theory to investigate the structure of hadrons and why we need effective theories in substitution for QCD.

In this section, we introduce non-Abelian gauge theory first, and then we discuss QCD after we show that non-Abelian theory itself suggests the theory of the strong force.

2.1 Non-Aberian gauge theory and Asymptotic freedom

The physical quantity, which is mainly related to electro-magnetic force, is described under the principle of local gauge invariance. Namely, the Lagrangian of Quantum Electro-Dynamics (QED) is constructed so that the system is invariant under a local gauge transformation. The system, in which the strong interaction is dominated and have additional internal symmetries, is described by a more complicated gauge transformation. Before we move to QCD, we give a general discussion of non-Abelian gauge theory on the analogy of QED.

We start with the $SU(N)$ gauge transformation:

$$\psi(x) \to \psi' = U(x)\psi(x). \tag{2.1}$$

where $U \in SU(N)$, ψ is the Dirac field and $U(x)$ is defined as

$$U(x) = \exp[i\alpha^a t^a] \quad (a = 1 \sim N-1) \tag{2.2}$$

where t_a is the generator of Lie algebra and it satisfies the relation:

$$[t^a, t^b] = i f_{abc} t^c. \tag{2.3}$$

f_{abc} is the structure constant for $SU(N)$. Then, we assume the covariant derivative which takes the form

$$D_\mu = \partial_\mu - ig \sum_{a=1}^{N^2-1} A_\mu^a t^a. \tag{2.4}$$

In Eq.(2.4), we introduce the gauge field, A^a, which belongs to the adjoint representation of the $SU(N)$ gauge group. In order to construct the gauge invariant Lagrangian, we assume that the $A_\mu = \sum_a t^a A_\mu^a$ transform as $A_\mu \to A'_\mu$ under the gauge transformation, then one finds that covariant derivative transform under gauge transformation as follows

$$\mathcal{D}_\mu \psi \to U(x)\partial_\mu \psi(x) + (\partial_\mu U(x))\psi(x) + igA'_\mu U(x)\psi(x). \tag{2.5}$$

In the same way as constructing QED Lagrangian, we require that the covariant derivative satisfy the transformation low:

$$\mathcal{D}_\mu \psi \to U(x)\mathcal{D}_\mu \psi, \tag{2.6}$$

then the transformation low of the gauge field is determined:

$$A'_\mu = U(x)A_\mu U^\dagger(x) + \frac{i}{g}(\partial_\mu U(x))U(x). \tag{2.7}$$

In the end, we finds that the Lagrangian in the type of

$$\mathcal{L} = \bar{\psi}\left[i\not{\mathcal{D}} - m\right]\psi \tag{2.8}$$

is invariant under $SU(N)$ gauge transformation. However, Eq.(2.8) is not the complete one. There are additional terms which have gauge invariance. To construct complete Lagrangian, we discuss the term which depends only on A_μ, namely the kinetic term of vector field. From an analogy of QED, we define the field strength tensor

$$\begin{aligned} G_{\mu\nu}(x) &= -\frac{i}{g}\left[\mathcal{D}_\mu, \mathcal{D}_\nu\right] \\ &= \partial_\mu A_\nu(x) - \partial_\nu A_\mu(x) + ig[A_\mu(x), A_\nu(x)] \end{aligned} \tag{2.9}$$

The field strength tensor, which is expressed as Eq.2.9, shows the same transformation low as covariant derivative, $G_{\mu\nu}(x) \to U(x)G_{\mu\nu}(x)U^\dagger(x)$, so the kinetic term of gauge field, which is invariant under gauge transformation, is constructed as follows

$$\mathcal{L}_G = -\frac{1}{2}Tr[G_{\mu\nu}(x)G^{\mu\nu}(x)]. \tag{2.10}$$

Finally, one reaches at the full Lagrangian:

$$\begin{aligned} \mathcal{L} &= \bar{\psi}(i\not{\mathcal{D}} - m)\psi - \frac{1}{2}Tr[G_{\mu\nu}G^{\mu\nu}] \\ \mathcal{D}_\mu &\equiv \partial_\mu + igA_\mu(x) \end{aligned} \tag{2.11}$$

We can also add another additional term, θ term, which takes the form

$$\begin{aligned} \mathcal{L}_\theta &= \theta\frac{g^2}{32\pi^2}G^{a,\mu\nu}\tilde{G}^a_{\mu\nu} \\ \tilde{G}^a_{\mu\nu} &\equiv \frac{1}{2}\epsilon_{\mu\nu\alpha\beta}G^{a,\alpha\beta}, \quad \epsilon^{0123} = 1 \end{aligned} \tag{2.12}$$

This term violates C and CP, or T, invariance of QCD, but experimental estimates show that $\theta < 10^{-9}$ [23, 24], so we neglect this term for our purpose, namely we set $\theta = 0$ in the later discussion. This term is related to the topological properties of QCD vacuum.

The specific feature of the Lagrangian in Eq.(2.12), $N = 3$ case, is three point and four point vertex of gauge field. It is shown in Fig.2.1. These vertex is not seen in QED and leads the theory to getting complex.

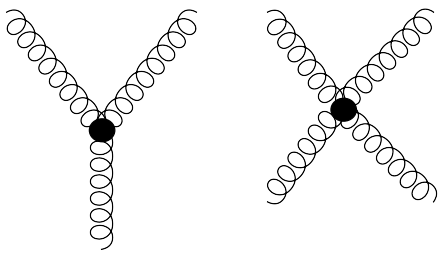

Figure 2.1: Three point and four point vertex appearing in gauge SU(3) invariant Lagrangian

Highly important conclusion from the Non-Abelian gauge theory is the *asymptotic freedom*. The difficulty of analysis of QCD is caused by this feature. To see behavior of coupling in SU(N) non-Abelian gauge field theory, we start with β function obtained in this theory.

The β function for the SU(N) non-Abelian gauge group is given by

$$\beta(g) = -\frac{g^3}{(4\pi)^2}\left[\frac{11}{3}N - \frac{2}{3}n_f\right]. \tag{2.13}$$

up to one-loop perturbation where n_f is the number of fermion species. In SU(3) gauge group, the sign of the beta function is negative at small g for $n_f < \frac{33}{2}$. Thus $g = 0$ is the UV fixed point so that SU(3) non-Abelian gauge group is asymptotic free. One of the specific feature of non-Abelian gauge is seen in coupling constant. Renormalization group equation makes correlation between β function and the coupling

constant, which is given by

$$\frac{d}{d\log(\mathrm{Q}^2/\mu^2)}g = \beta(g). \tag{2.14}$$

where g is the coupling constant in SU(N) non-Abelian gauge field theory, μ is renormalization scale. Inserting the explicit form of β function, we find the coupling α_s in non-Abelian gauge theory takes the form;

$$\begin{aligned} \alpha_s(Q^2) &= \frac{\alpha_s}{1+\frac{\alpha_s}{4\pi}(11-\frac{2}{3}n_f)\log(Q^2/\mu^2)} \\ &= \frac{4\pi}{(11-\frac{2}{3}n_f)\log(Q^2/\Lambda^2)} \end{aligned} \tag{2.15}$$

where $\Lambda = \frac{1}{M}\exp[-g^2(11-\frac{2}{3}n_f)/8\pi^2]$ and we focus on $SU(3)$ gauge theory. Eq.(2.15) implies that running coupling α_s become much large at small Q and perturbation theory is valid in the region of the energy scale which is much larger than Λ, which is estimated $\Lambda \sim 200$ MeV from experimental analysis of coupling constant (See Fig.2.2).

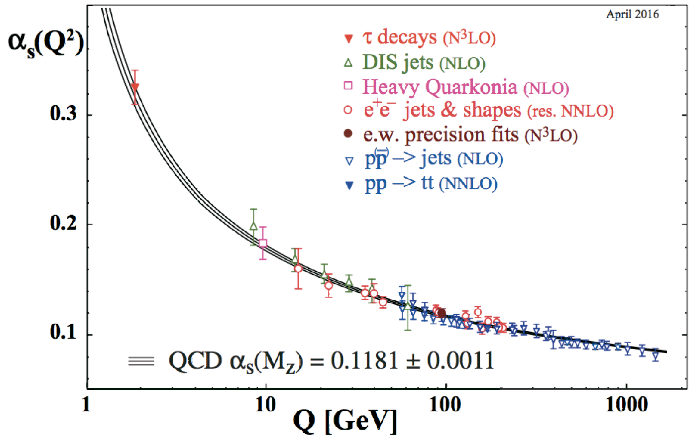

Figure 2.2: Running coupling constant α_s as a function of the energy scale Q, which is taken form [2]

2.2 Parton model and Bjorken scaling

Experiments by hadron or lepton accelerators give much information on the strong interaction. Especially, *Deep Inelastic Scattering* (DIS) clarifies the property of QCD cross section, where an lepton e, μ, which interacts with the proton p, emits highly off-shell photon, $ep \to e + X$. DIS is described theoretically in a simple picture where quarks are treated as noninteracting point fermions. In fact, this behavior of quarks in DIS gives the hint for what is the theory of strong force.

In the high energy region, the strong interaction shows an unexpectedly weak effect. For instance, it is known experimentally that the pion, which is produced by proton-proton high energy collisions, has limited transverse momentum. This phenomenon leads to the picture where hadrons is a loosely bound assemblage of many components. Bjorken and Feynman introduced *parton model* to investigate what is occurring. This model assumes that the proton is a loosely bound assemblage of number of a small constituents.

The differential cross section in terms of the kinematic variable Q^2, $x = Q^2/2P \cdot q$, and the parton distribution function, $f_i(x)$, is

$$\frac{d^2\sigma}{dxdQ^2} = \sum_i f_i(x) Q_i^2 \cdot \frac{2\pi\alpha^2}{Q^4} \left[1 + \left(1 - \frac{Q^2}{xs} \right)^2 \right]. \tag{2.16}$$

where Q_i is the quark charge and s is the Mandelstam variable. Eq.(2.16) surprisingly suggests that the differential cross section after dividing by the factor

$$\frac{1 + \left(1 - \frac{Q^2}{xs} \right)^2}{Q^4} \tag{2.17}$$

is independent of Q^2. This behavior, which generally called *Bjorken Scaling*, is seen in Fig. 2.3.

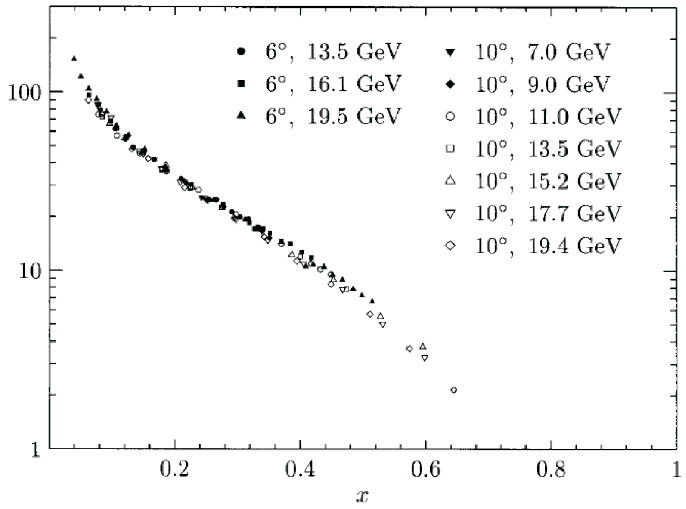

Figure 2.3: The Bjorken scaling observing from deep inelastic cross section measured by SLAC-MIT. It is take form [25]

The Bjorken scaling implies that the theory of strong interaction is an asymptotic free quantum field theory in the four dimension of space time. We have already shown that non-Abelian theory is just such kind of theory. Now, we have obtained the materials to construct the theory of strong interaction, QCD. In the next section, we discuss QCD itself.

2.3 QCD

The key to construct the theory of strong force is in an asymptotic freedom. Last two section suggests that non-Abelian gauge theory satisfies the condition to construct such theory. When we discussed the running coupling, we assumed $SU(3)$ non-Abelian gauge theory. But, why $SU(3)$? To answer this question, we discuss *quark model*, which is originally pointed out by Gell-mann and Zweig, and *color* degrees of freedom.

2.3.1 Quark Model

In 1964, Gell-Mann and Zweig introduced *quark model* [3] to classify the hadrons which were discovered in that time. Quarks are constituents of hadrons and strongly interacting in the hadron through a vector boson, called *gluon*. The quark has spin 1/2 and is positive parity while its anti-particleqnti-quark, has spin 1/2 and negative parity. Once we assume that hadrons are bound states of quarks and anti-quarks, spectroscopy of mesons and baryons, which are discovered at that time, are explained well. The existence of six kines of quarks is known so far. TABLE.2.1 shows the quantum numbers of the quarks. They are related to Gell-mann Nishijima formula [26, 27];

$$\mathcal{Q} = I_z + \frac{\mathcal{B} + S + C + B + T}{2}. \tag{2.18}$$

Gell-mann and Zweig assumed only first three flavors quarks, up, down, strange and considered $SU_f(3)$

	d	u	s	c	b	t
$\mathcal{Q}$	$-1/3$	$+2/3$	$-1/3$	$+2/3$	$-1/3$	$+2/3$
I	$+1/2$	$+1/2$	0	0	0	0
I_z	-1/2	$+1/2$	0	0	0	0
S	0	0	-1	0	0	0
C	0	0	0	1	0	0
B	0	0	0	0	-1	0
T	0	0	0	0	0	1

Table 2.1: Quantum numbers of each flavored quark.

symmetry. Heavy flavored quarks are introduced after the charmonium and the bottomonium, which are heavy flavored hadron, were discovered.

Mesons have baryon number $\mathcal{B} = 0$, and they are quark-anti-quark bound states in the quark model. They are classified by the total angular momentum J, parity P, $P = (-)^{\ell+1}$, and the charge conjugation C, $C = (-)^{\ell+s}$. The S-wave states, which are defined by $\ell = 0$, are classified into the pseudo-scalars ($J^{PC} = 0^{-+}$) and the vectors ($J^{PC} = 1^{--}$). The P-wave states, which are defined by $\ell = 1$, are classified into the scalars ($J^{PC} = 0^{++}$), the axial vectors ($J^{PC} = 1^{++}$) or ($J^{PC} = 1^{+-}$) and the tensors ($J^{PC} = 2^{++}$). Quarks are introduced as the fundamental representation of flavor $SU(3)$ in the quark model. The possible

nine $\bar{q}q$ states are grouped into flavor octet and flavor singlet;

$$\mathbf{3} \otimes \bar{\mathbf{3}} = \mathbf{1} \oplus \mathbf{8}. \tag{2.19}$$

Since the mass of charm quark is much larger than light quarks, the flavor $SU(4)$ symmetry is badly broken. However, it is convenient for the classification of charm hadrons to extend flavor $SU(3)$ to flavor $SU(4)$;

$$\mathbf{4} \otimes \bar{\mathbf{4}} = \mathbf{15} \oplus \mathbf{1}. \tag{2.20}$$

One finds that $q\bar{q}$ 16-states are grouped into a 15-plet and a singlet (See Fig.2.4). The multiplets in Eq.(2.20) have $SU(3)$ subgroups, which is given by

$$\mathbf{15} = \mathbf{8} \oplus \mathbf{1} \oplus \mathbf{3} \oplus \bar{\mathbf{3}}. \tag{2.21}$$

Octet and a singlet in Eq.(2.21) have $\mathcal{C} = 0$, a triplet has $\mathcal{C} = -1$ and an anti-triplet has $\mathcal{C} = 1$.

Baryons are the fermions of which baryon number $\mathcal{B} = 1$. Baryons are constructed from three quarks (qqq), and in the same way as meson, the possible 27 states are grouped into a decuplet, two octets and a singlet:

$$\mathbf{3} \otimes \mathbf{3} \otimes \mathbf{3} = \mathbf{10}_S \oplus \mathbf{8}_M \oplus \mathbf{8}_M \oplus \mathbf{1}_A. \tag{2.22}$$

One can extend the discussion to flavor $SU(4)$ symmetry including charm quark or flavor $SU(5)$ including both charm and bottom quarks although they are strongly broken (See Fig.2.5). The baryons which include heavy flavor quarks (heavy baryons) are recently of interest. Because of their narrow widths compared with light hadrons, intricate partial wave analysis is not necessary. The small cross section of heavy flavored hadron was the problem on the experimental side before. But, heavy baryon state, including exited states, has gradually observed recently.

In the spin-flavor $SU(6)$ representation with the spin and $SU(3)$ flavor combined, baryons are decomposed into the multiplets:

$$\mathbf{6} \otimes \mathbf{6} \otimes \mathbf{6} = \mathbf{56}_S \oplus \mathbf{70}_M \oplus \mathbf{70}_M \oplus \mathbf{20}_A. \tag{2.23}$$

These multiplets are decomposed into the $SU(3)$ multiplets as follows:

$$\mathbf{56} = {}^4\mathbf{10} \oplus^2 \mathbf{8} \tag{2.24}$$

$$\mathbf{70} = {}^2\mathbf{10} \oplus^4 \mathbf{8} \oplus^2 \mathbf{8} \oplus^2 \mathbf{1} \tag{2.25}$$

$$\mathbf{20} = {}^2\mathbf{8} \oplus^4 \mathbf{1} \tag{2.26}$$

where the subscripts $(2S+1)$ give the net spin S of the quarks. 56-multiplet represent ground state, or S-wave state, 70 and 20-multiplet represent the excited states. The Nucleon is in ${}^2\mathbf{8}$, $J^P = 1/2^+$ octet, of 56-multiplets and Δ particles, Δ^-, Δ^0, Δ^+, Δ^{++} are in ${}^4\mathbf{10}$, $J^P = 3/2^+$ decuplet, of 56-multiplets. As we will see in the next, this classification leads to necessity of introducing new symmetry, global $SU_{color}(3)$.

In the way as the discussion of flavor $SU(4)$ for meson, it is useful to discuss flavor $SU(4)$ including

charm flavored quark also for baryons in order to classify charmed baryons. The multiplet for $SU(4)$ is

$$\mathbf{4} \otimes \mathbf{4} \otimes \mathbf{4} = \mathbf{20}_S \oplus \mathbf{20}_M \oplus \mathbf{20}_M \oplus \mathbf{4}_A. \tag{2.27}$$

Spin-flavor $SU(8)$ multiplet is also considered, which is described as

$$\mathbf{8} \otimes \mathbf{8} \otimes \mathbf{8} = \mathbf{120}_S \oplus \mathbf{168}_M \oplus \mathbf{168}_M \oplus \mathbf{56}_A. \tag{2.28}$$

Subgroups of the multiplets are

$$\mathbf{120} = {}^2\mathbf{20}_S \oplus^4 \mathbf{20}_M \tag{2.29}$$
$$\mathbf{56} = {}^4\mathbf{4} \oplus^2 \mathbf{20}_M \tag{2.30}$$
$$\mathbf{168} = {}^2\mathbf{20}_S \oplus^4 \mathbf{20}_M \oplus^2 \mathbf{20}_M \oplus^2 \mathbf{4}. \tag{2.31}$$

Lowest lying charmed baryons are included in **120** since **120** is totally symmetric (all the quarks in the baryon should be s-wave). Λ_c, Σ_c, Ξ_c, Ξ_c', Ω_c, Ξ_{cc}, Ω_{cc} and Σ_c^* are in ${}^2\mathbf{20}_S$ and Ξ_c^*, Ω_c^*, Ω_{cc}^*, Ξ_{cc}^* and Ω_{ccc} are in ${}^4\mathbf{20}_M$. Orbital excited states are in other multiplets.

2.3.2 Color degrees of freedom

Since quarks are fermions, they must obey the Fermi statistics. But, the decuplet baryons, Δ, Σ^*, Ξ^*, Ω clearly contradict the statistics. Therefore, we have to introduce an extra internal symmetry, $SU_c(3)$. Introducing *color* degrees of freedom or $SU_c(3)$ solves this problem.

We assume that all the quarks have colors:

$$\begin{pmatrix} r \\ b \\ g \end{pmatrix}. \tag{2.32}$$

The color was introduced by Han and Nambu, Greenberg and Gell-Mann [3, 28] just as *ad hoc* assumption. But, now it is shown by many experimental data that its existence are highly probable. One of the evidence of the existence of color is seen int the reaction of $e^-e^+ \to$ hadron. Without the color degrees of freedom, the total cross section is described as

$$\sigma(e^+e^- \to \text{hadrons}) = \sigma_0 \sum_{\text{f}} \text{Q}_\text{f}^2 \tag{2.33}$$

where Q_f is the charge of quarks, σ_0 is the cross section of the reaction $e^-e^+ \to \mu^-\mu^+$, which is represented as

$$\sigma_0 = \frac{4\pi\alpha^2}{3s}. \tag{2.34}$$

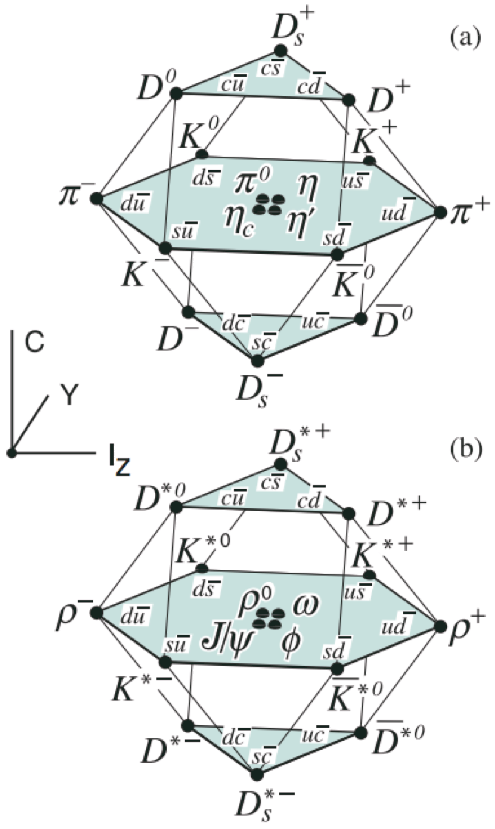

Figure 2.4: SU(4) weight diagram showing the 16-plets for the pseudo-scalar (a) and the vector mesons (b). This figure is taken from [2]

In the energy region which is as large as the $b\bar{b}$ pair is created,

$$\sigma(e^+e^- \to \text{hadrons})/\sigma_0 = \sum_{\text{f}} \text{Q}_{\text{f}}^2 = \frac{11}{9} \tag{2.35}$$

where we use TABLE.2.1. But, the observed value is approximately 11/3 [29–31]. Therefore, it suggests that quarks have the color degree of freedom. Color degrees of freedom has never observed directly. It leads the fact that all hadrons are color singlet and no other multiplets, such as octet, decuplet state, are realized. Quarks transform as 3 representation under global $SU_c(3)$ and anti-quark transform as $\bar{3}$ under global $SU_c(3)$. Since all hadrons are invariant under $SU_c(3)$ transformation, the following combination are allowed:

$$\bar{q}^i q_i, \quad \epsilon^{ijk} q_i q_j q_k, \quad \epsilon_{ijk} \bar{q}^i \bar{q}^j \bar{q}^k. \tag{2.36}$$

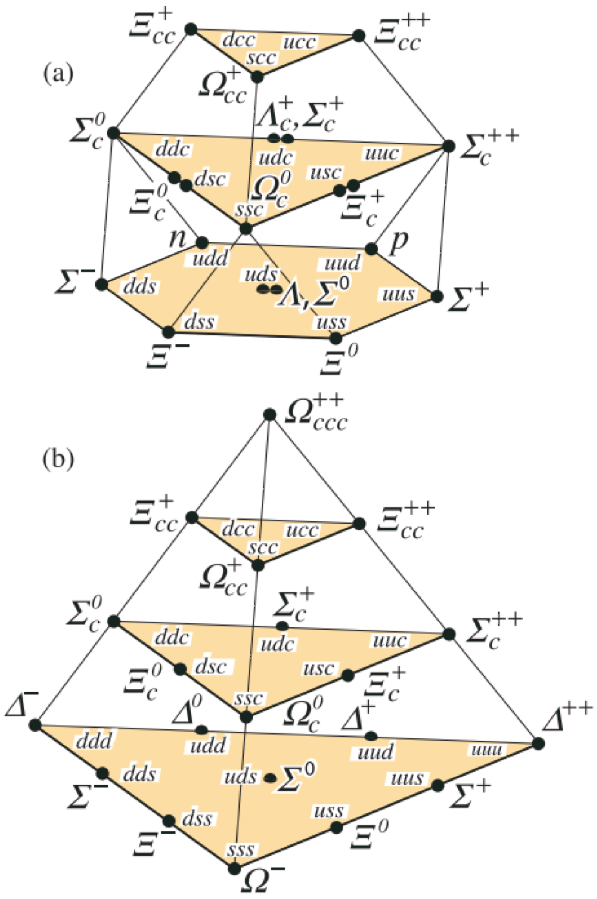

Figure 2.5: SU(4) multiplets of baryons. (a) The 20-plets with SU(3) octet and (b) The 20-plets with SU(3) decuplet. This figure is taken from [2]

where $i, j, k = 1, 2, 3$ is the color index. Namely, only baryon, anti-baryon, meson are possible state with the assumption that all the hadrons must be color singlet. So-called *exotic* states, i.e. tetra quark, penta quark, hadron molecule state, glueballs, hybrid hadrons, are also possible to exist. The study of exotic hadrons is much important in hadron physics recently and is on going both experimentally and theoretically.

After taking into account color, one finds that QCD Lanrangian takes the form:

$$\mathcal{L}_{QCD} = \sum_f \bar{\psi}^i \left[i\not{D} - m_f \right] \psi_i - \frac{1}{2} Tr[G^a_{\mu\nu} G^{a\mu\nu}] \tag{2.37}$$

where f is flavor index, $i = 1, 2, \cdots N_c$, $a = 1, 2, \cdots N_c^2 - 1$ are the color index and D_μ is the covariant

derivative which is defined as

$$D_\mu = \partial_\mu + ig \sum_a A^a_\mu t^a.$$

The field strength tensor $G^a_{\mu\nu}$ is given by

$$G^a_{\mu\nu} = \partial_\mu A^a_\nu - \partial_\nu A^a_\mu + igf^{abc} A^b_\mu A^c_\nu$$

where f^{abc} is the structure constant of $SU(3)$ gauge group.

In principle, we can calculate all the physical quantities which are related to the strong interaction from Eq.(2.37). However, the crucial problem is that QCD is the theory which is asymptotic free. In the low energy region which is lower than $\Lambda \sim 200$ MeV, the theory cannot be treated perturbatively, for coupling constant in this region become much larger because of asymptotic freedom. We know almost only the perturbative way to obtain the physical quantity in the field theory, so we need some models or accurate numerical method to solve the QCD. It does not mean that there are no theories which approaches non-perturbatively. QCD-sum rules [32, 33] and non-perturbative Schwinger-Dyson equation [34] enable to treat QCD Lagrangian in a non-perturbative way. These theories leads to qualitative understanding of QCD. However, the main purpose of our work lie in clarifying the structure of hadrons, especially excited heavy baryons, and the prediction of hadron spectra. These theories have not so small uncertainty, so do not sufficiently satisfy our purpose.

Lattice QCD calculation is also the theory which can treat QCD non-perturbatively. In our work, we do not use Lattice QCD theory directly, but since it is important for the later discussion, we have to mention the treatment of hadron from Lattice QCD theory briefly without touching its detail.

2.3.3 Lattice QCD and confinement potential

Lattice QCD is the method which enables to evaluate the physical quantity, or expectation values, from the *first principle*. In Lattice QCD, action S is formulated in discretized four dimension Euclidean space-time separated by the lattice spacing a. One can get exact result in the limit of $a \to 0$ and the infinite volume. The accuracy of actual calculation depends on the machine power of the computer. In order to obtain accurate result, the physical quantity is obtained by extrapolating to the physical point. It is known that Lattice QCD is still powerful and much accurate method especially for hadron spectroscopy.

Quark or anti-quark field is defined at lattice points, or site, and two separated points is connected by link. Link variable is defined as

$$U_{x,\mu} = \mathcal{P}\left[\exp\left(i\int dx'_\mu A_\mu(x')\right)\right]. \tag{2.38}$$

Under gauge transformation link variable transform as follows

$$\begin{aligned} U^\Omega_{x,\mu} &\to \Omega_x U_{x,\mu} \Omega_{x+a\hat{\mu}}. \\ \Omega &\in SU(3) \end{aligned} \tag{2.39}$$

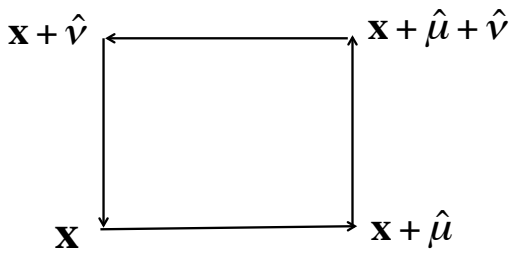

Figure 2.6: Closed loop in Lattice space. It is the example of the object that is gauge invariant.

One immediately notices that the trace of a product of link variable in closed loop, such as $U_{x,\mu\nu} = U_{x,\mu}U_{x+a\hat{\mu},\nu}U^{\dagger}_{x+a\hat{\nu},\mu}U^{\dagger}_{x,\nu}$ (See Fig.2.6), is gauge invariant. The expectation value of the operator $\mathcal{O}$ is defined by

$$\langle\mathcal{O}\rangle = \frac{1}{Z}\int [dU][dq][d\bar{q}]\mathcal{O}[U]e^{-S[U,q,\bar{q}]}. \tag{2.40}$$

The partition function Z is defined so that $\langle\mathbf{1}\rangle = 1$. Enormous amount of integrals in Eq.(2.40) is performed by the Monte-Carlo method in actual computation. Color confinement is related to $Wilson$ loop which is originally introduced by Wegner. The Wilson loop is defined as

$$W(C) = Tr\left\{\mathcal{P}\left[\exp\left(i\int_{\delta c} dx^{'}_{\mu}A_{\mu}(x^{'})\right)\right]\right\} = Tr\left(\prod_{(x,\mu)\in\delta C} U_{x,\mu}\right). \tag{2.41}$$

Wilson, and later Brown and Weisberger have pointed out that the Wilson loop is related to the potential energy between very heavy quark and anti-quark as color sources. The expectation value of the Wilson loop in the limit of $T\to\infty$ is given by

$$\langle W\rangle = \lim_{T\to\infty} F(R)e^{-V(R)T} \sim e^{-\sigma RT} \tag{2.42}$$

where sigma is the parameter called *string tension*. Actual calculation of $V(r)$ is shown in Fig.2.7. It is known that quark anti-quark potential $V(R)$ calculated from Lattice QCD is fitted well by $Cornell$ potential, which takes the form

$$V(r) = V_0 + \sigma r - \frac{A}{r}. \tag{2.43}$$

The linear type potential between quarks implies the picture where, in hadrons, quarks behaved as they are connected by *string* and it is the reason why color have been never observed yet. QCD calculation give a clue to the explanation of color confinement numerically although complete verification on the phenomena of color confinement has not given yet theoretically.

In the above analysis, we assumed ideally much heavy quarks, but the effective potential between quarks should depend on the energy scale. Recent study of the potential between quarks by Lattice QCD shows the quark mass dependence for the effective potential between quarks, which is shown in Fig.2.8. One finds that string tension does not show the dependence of quark mass and color-Coulomb force has relatively large dependence on the quark mass.

The feature of confinement, which became clear by Lattice QCD calculation, reinforces effective theories or models. As we will mention in the next section, constituent quark model, which is one of the powerful models to predict the spectra of hadrons and its structure, describe hadrons by using Cornell potential model. Constituent quark model has achieved success on the prediction of hadron level structures while first application of Cornell potential on the constituent quark model is before the effective potential between quarks is evaluated by Lattice QCD calculation.

One of the outstanding point of Lattice QCD is the vasy accurate prediction of hadron mass. Ideally, Lattice QCD can clarify all the mass spectra of hadrons described by QCD if the machine power of computer is infinity. Processing power of actual computers are finite, but Lattice QCD calculation still give accurate mass spectra of ground states of hadrons. However, Lattice QCD have difficulty about the analysis of exited state and structure of hadrons at present. Excited states of hadrons, especially heavy hadrons, become important for the understanding of QCD, or understanding of heavy flavored dynamics. Furthermore, the in-depth theoretical understanding of the structure of hadrons have a crucial meaning experimentally. The concept of constituent quark model is very simple. Nevertheless, this model gives the prediction of the level structure of hadrons and other plentiful information of hadrons. In the next section we review constituent quark model briefly.

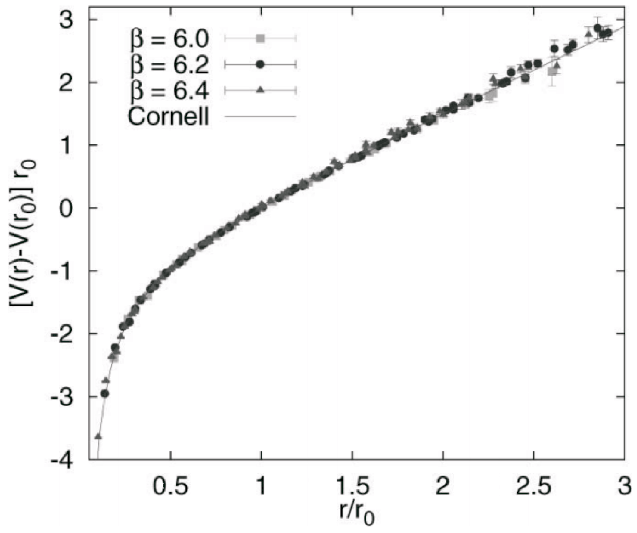

Figure 2.7: The quark-anti-quark potential resulted in Lattice QCD calculation [35].

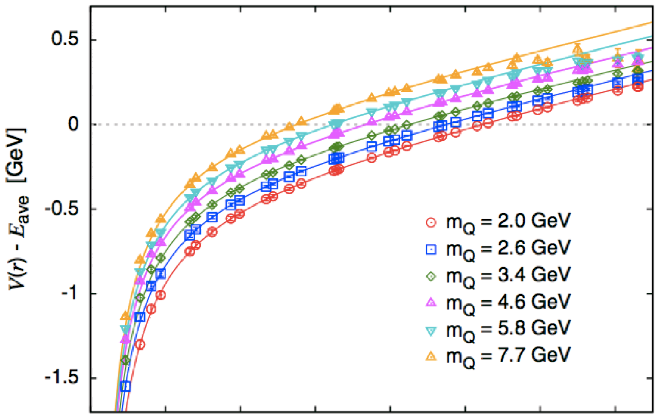

Figure 2.8: The quark mass dependence of Cornell potential resulted in Lattice QCD calculation [36].

Chapter 3

Constituent Quark Model

3.1 Mass relations based on $SU_f(3)$ symmetry

As is seen in the previous chapter, we need some models to predict hadron level structure. The $SU(3)$ flavor symmetry leads to relations between hadron masses.

Okubo and Gurey and Radicati formulated a mass formula [37, 38] by using matrix elements of the mass operator:

$$M = a_1 + a_2 Y + a_3 \left[I(I+1) - Y^2/4 \right] + a_4 J(J+1). \tag{3.1}$$

where Y is the hyper-charge, I is the isospin and J is the total angular momentum of hadrons. This mass formula leads to the relations between hadron masses:

$$\frac{M_N + M_\Xi}{2} = \frac{3M_\Lambda + M_\Sigma}{4}, \tag{3.2}$$

and

$$M_\Delta - M_{\Sigma^*} = M_{\Sigma^*} - M_{\Xi^*} = M_{\Xi^*} - M_\Omega. \tag{3.3}$$

These relations reproduce experimental data surprisingly well within 1 %. This is a first step to hadron spectroscopy. The mass-formula does work for the prediction of mass splitting of ground states, but the level structure of exited states and the origin of the splittings $\Sigma{-}\Lambda$ and $N{-}\Delta$ is still unclear. Developments of QCD led to the effective models to describe hadron mass. Among them, *constituent quark model* is known as a powerful method to predict the hadron level structure including excited states and their structures.

3.2 Constituent Quarks

The constituent quark model is a simple model where it is assumed that hadron is a 'bound' state of *constituent quark* (the word 'bound' is sometimes used in this model although a free constituent quark state does not exist). Existence of the constituent quark as fundamental degrees of freedom is a basic assumption of the constituent quark model. They have finite sizes, larger masses than the current quarks

appearing in the QCD and they are interpreted as the quarks dressed by gluons and sea quarks. All the quantum numbers of constituent quark are the same as the current quarks. No rigorous derivation of the constituent quark from QCD is not achieved yet, while the constituent quark model reproduces various experimental data and also gives information on the hadron structure. The mass of constituent quark is parameter which has to be fitted to some experimental data, but in some models, such as Dyson-Schwinger equation (DSE), Lattice QCD, NJL model, the mass of constituent quarks has been computed. The calculation mass, or the self-energy of the quark, depends on the (Euclidean) momentum. The DSE model calculation of the mass of constituent quark gives $M_q \sim 300$ MeV at $p = 0$ (See Fig.3.1).

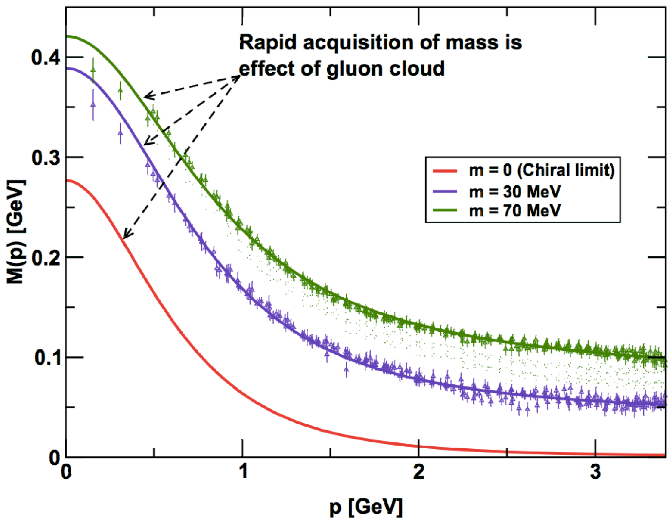

Figure 3.1: The mass of constituent quark. Solid lines is the result from DSE. Data point represent lattice QCD simulations. m is current quark mass. This figure is taken from [39]

3.3 Isgur Karl model and Heavy quarkonia

One of the success of the constituent quark model is the reproduction of experimental data of the charmonium spectra and prediction of the charmonium level structure by Eichten et al [40]. The equation to be solved in non-relativistic constituent quark model is a Schrodinger equation equation of a few body system of constituent quarks:

$$\left[\frac{\boldsymbol{p}^2}{2\mu} - T_G + V(\boldsymbol{r})\right]\psi(\boldsymbol{r}) = E\psi(\boldsymbol{r}) \tag{3.4}$$

where μ is reduced mass of quark and anti-quark and T_G is the kinetic energy of the center of mass of the system. Eichten assumed The Cornell potential in their work:

$$V(\boldsymbol{r}) = -\frac{\kappa}{r} + \frac{r}{a^2}. \tag{3.5}$$

In their work, they neglect relativistic corrections in the potential, namely the terms in the order of $\mathcal{O}((v/c)^2)$ is neglected. This assumption is reasonable for the heavy quarkonia because a heavy quark is heavy enough to neglect the corrections, which is to say v is much smaller compared to M_Q ($Q = c, b$). In the later study, Godfrey et al. [41] gave a complete level structure of the charmonim, which is shown in Fig.3.2. In their work, They take into account spin-spin force in order to reproduce the hyperfine splitting. In the next section we give a short discussion of the hyperfine splitting.

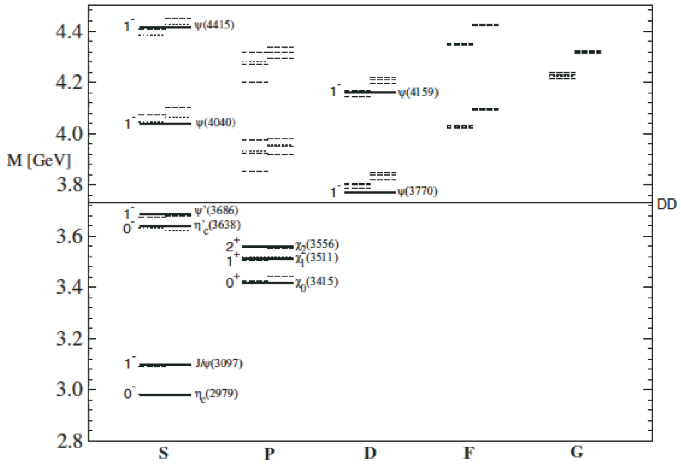

Figure 3.2: The quark model prediction of charmonium mass spectra [42]. Solid line denotes experimental data, left dashed line shows the calculated result from non-relativestic quark model, right hand dashed line shows the calculated result of Godfrey-Isgur model where relativistic kinetic energy, $T = \sqrt{\boldsymbol{p}_q + M_p} + \sqrt{\boldsymbol{p}_{\bar{q}} + M_{\bar{p}}}$, is applied.

3.4 Hyperfine splitting

The N-Δ, Λ-Σ and χ_c-h splittings are not reproduced only with the Cornell potential. De Rujula, Georgi, and Glashow introduced One-Gluon-Exchange (OGE) potential to reproduce these splittings [43]. The short rage parts o the potential which come from the OGE takes the form:

$$H_{OGE} = \sum_{j>i} (\alpha Q_i Q_j + k\alpha_s) S_{ij} \tag{3.6}$$

where

$$\begin{aligned} S_{ij} &= \frac{1}{r_{ij}} - \frac{1}{2m_i m_j}\left[\frac{\boldsymbol{p_i}\cdot\boldsymbol{p_j}}{r_{ij}} + \frac{\boldsymbol{r}_{ij}\cdot(\boldsymbol{r}_{ij}\cdot\boldsymbol{p_i})\boldsymbol{p_j}}{r_{ij}^3}\right] - \frac{\pi}{2}\delta^3(\boldsymbol{r}_{ij})\left(\frac{1}{m_i^2}+\frac{1}{m_j^2}+\frac{16\boldsymbol{s_i}\cdot\boldsymbol{s_j}}{3m_i m_j}\right) \\ &- \frac{1}{2r_{ij}^3}\left[\frac{1}{m_i^2}\boldsymbol{r}_{ij}\times\boldsymbol{p}_i\cdot\boldsymbol{s}_i - \frac{1}{m_j^2}\boldsymbol{r}_{ij}\times\boldsymbol{p}_j\cdot\boldsymbol{s}_j + \frac{1}{m_i m_j}\left(\boldsymbol{r}_{ij}\times\boldsymbol{p}_i\cdot\boldsymbol{s}_i - \boldsymbol{r}_{ij}\times\boldsymbol{p}_j\cdot\boldsymbol{s}_j\right)\right. \\ &- \left. 2\boldsymbol{s}_i\cdot\boldsymbol{s}_j + 6\frac{(\boldsymbol{s}_i\cdot\boldsymbol{r}_{ij})(\boldsymbol{s}_j\cdot\boldsymbol{r}_{ij})}{r_{ij}^2}\cdots\right] \end{aligned} \tag{3.7}$$

where $\boldsymbol{r}_{ij} = \boldsymbol{r}_j - \boldsymbol{r}_i$, $\boldsymbol{s}_i$ is the spin of i-th quark, $\cdots$ means higher order terms of the relativistic correction. This expression is derived from one-gluon-exchange diagram of the constituent quarks (See.3.3). We consider the expectation value of total Hamiltonian with the zeroth order wave function, which is defined as $H_0\left|\Psi_0\right\rangle = M_0\left|\Psi_0\right\rangle$ where

$$H_0 = \sum_i\left(\frac{\boldsymbol{p_i}^2}{2\mu} + m_i\right) + V_{\rm Conf}. \tag{3.8}$$

This is the Hamiltonian where the short range force is not taken into account. Using the wave function which is the eigenstate of the zeros order Hamiltonian, we employ the first order perturbation theory, and the first order mass formula is obtained:

$$M = \left\langle\Psi_0\,|\,H\,|\,\Psi_0\right\rangle = M_0 + \sum_{i>j}(\alpha Q_i Q_j - 2\alpha_s/3)\left[b - \frac{c}{m_i m_j} - d\left(\frac{1}{m_i^2}+\frac{1}{m_j^2}+\frac{16\boldsymbol{s_i}\cdot\boldsymbol{s_j}}{3m_i m_j}\right)\right]. \tag{3.9}$$

with

$$a = \frac{1}{2}\left\langle\Psi_0\,\middle|\,p_i^2\,\middle|\,\Psi_0\right\rangle \tag{3.10}$$

$$b = \left\langle\Psi_0\,\middle|\,\frac{1}{r_{ij}}\,\middle|\,\Psi_0\right\rangle \tag{3.11}$$

$$c = \frac{1}{2}\left\langle\Psi_0\right|\frac{r_{ij}^2\boldsymbol{p}_i\cdot\boldsymbol{p}_j + \boldsymbol{r}_{ij}\cdot(\boldsymbol{r}_{ij}\cdot\boldsymbol{p}_1)\cdot\boldsymbol{p}_2}{r_{ij}^3}\left|\Psi_0\right\rangle \tag{3.12}$$

$$d = \frac{\pi}{2}\left\langle\Psi_0\,\middle|\,\delta^3(\boldsymbol{r}_{ij})\,\middle|\,\Psi_0\right\rangle \tag{3.13}$$

where $\boldsymbol{L}\cdot\boldsymbol{S}$ and tensor type force are neglected for simplicity.

Using Eq.(3.9), the ratio of strange quark and light quark mass can be estimated:

$$\frac{M_q}{M_s} = \frac{2\Sigma^* - 2\Sigma}{2\Sigma^* + \Sigma - 3\Lambda} \sim 0.6. \tag{3.14}$$

Thus, we can estimate the mass of the constituent strange quark from this relation and Fig.3.1, M_s∼0.5 GeV. The force from OGE provides also a qualitative explanation on baryon masses. The decuplet baryons should be heavier than octet baryons because two quarks have a higher energy when the spins of quarks

is aligned than when the directions of their spin are opposite. Therefore, we can naively understand why $M_\Delta > M_N$ and $M_{\Sigma^*} > M_\Sigma$. The splitting of $\Sigma - \Lambda$ is also understood as follows. Diquark in Σ must be spin triplet state because Σ is isotriplet particle and one finds

$$\boldsymbol{s_{q_1}} \cdot \boldsymbol{s_{q_2}} = \frac{1}{4} \tag{3.15}$$

and, from the fact that total spin is 1/2,

$$\boldsymbol{s_{q_1}} \cdot \boldsymbol{s_{q_2}} + \boldsymbol{s_{q_1}} \cdot \boldsymbol{s_s} + \boldsymbol{s_s} \cdot \boldsymbol{s_{q_2}} = -\frac{3}{4}. \tag{3.16}$$

Thus, thw contribution of the spin-spin interaction, which is proportional to $-1/m_q m_s$, in OGE potential of $q - s$ pair should be negative. Similarly, since Λ has a spin 0 diquark, the spin-spin interaction of $q - q$ pair is

$$\boldsymbol{s_{q_1}} \cdot \boldsymbol{s_{q_2}} = -\frac{3}{4}, \tag{3.17}$$

and form Eq.(3.16), the contribution from the $q - s$ pair is zero and the contribution from the spin 0 qq diquark is proportional to $-3/2m_q^2$. Since all the other interactions of Λ and Σ are the same, one obtains

$$M_\Sigma - M_\Lambda \sim \left(\frac{1}{4m_q^2} - \frac{1}{m_q m_s}\right) - \left(-\frac{3}{4m_q^2}\right) = \frac{1}{m_q}\left(\frac{1}{m_q} - \frac{1}{m_s}\right). \tag{3.18}$$

Thus, the mass of Σ must be heavier than Λ and its splitting comes from the mass difference of a strange constituent quark and a light constituent quark.

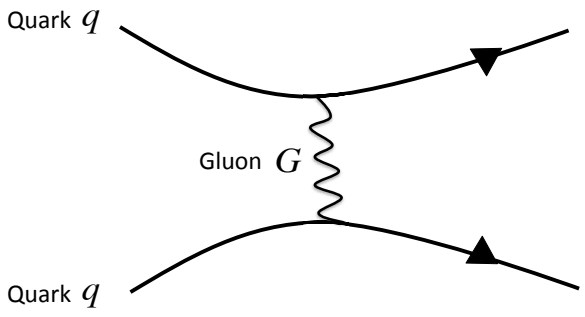

Figure 3.3: Feynmann diagram of one-gluon-exchange. solid line denote constituent quarks. not current quarks.

3.5 Orbital excited states of baryons

P-wave baryons belong to a $SU(3)$ 70-plet with $L = 1$ in the Eq.(2.26). The splitting between $\Lambda(J^-)-\Sigma(J^-)$ is mainly determined by the spin-spin term of the Hamiltonian. It is understood by the same discussion as spin-spin splitting of S-wave baryons, but the discussion of P-wave baryons is a little more complicated thanthe S-wave baryons. In this section, we discuss the level structure of P-wave baryons and show how to understand the splittings of P-wave baryons.

The level structure of the baryon state in this multiplet is naively understood well with harmonic oscillator potential. In the harmonic oscillator potential, the two degrees of freedom decouple and the Hamiltonian can be written simply as a sum the two parts,

$$\begin{aligned} H &= \sum_i \left(\frac{\boldsymbol{p}_i^2}{2m_i} + m_i \right) + \sum_{i<j} \frac{k}{2} |\boldsymbol{r}_i - \boldsymbol{r}_j|^2 \\ &= \frac{\boldsymbol{p}_\rho^2}{2m_\rho} + \frac{\boldsymbol{p}_\lambda^2}{2m_\lambda} + \frac{m_\rho {\omega_\rho}^2}{2} \boldsymbol{\rho}^2 + \frac{m_\lambda {\omega_\lambda}^2}{2} \boldsymbol{\lambda}^2, \end{aligned} \tag{3.19}$$

where, m_ρ and m_λ denote the reduced masses

$$m_\rho = \frac{m_1 + m_2}{2} \quad , \quad m_\lambda = \frac{m_\rho m_3}{m_\rho + m_3}. \tag{3.20}$$

and the oscillator frequencies ω_ρ and ω_λ are given by

$$\omega_\rho = \sqrt{\frac{3k}{2m_\rho}} \quad \omega_\lambda = \sqrt{\frac{2k}{m_\lambda}}. \tag{3.21}$$

It is convenient to introduce the Jacobi coordinates, $\boldsymbol{\lambda} = \boldsymbol{r_3} - \frac{\boldsymbol{r_{q1}} + \boldsymbol{r_{q2}}}{2}$ and $\boldsymbol{\rho} = \boldsymbol{r_{q2}} - \boldsymbol{r_{q1}}$, with obvious notations (see Fig.3.4). One of the advantage of the discussion with harmonic oscillator type potential is to be able to obtain analytic solution of Schrodinger equation of a quark three body system. From the Hamiltonian Eq.(3.19), one immediately finds

$$E = \hbar\omega_\rho \left(l_\rho + 2n_\rho + \frac{3}{2} \right) + \hbar\omega_\lambda \left(l_\lambda + 2n_\lambda + \frac{3}{2} \right) + \sum_i m_i \tag{3.22}$$

and

$$\psi_{lm}(\boldsymbol{\rho}, \boldsymbol{\lambda}) = \psi_{00}(\boldsymbol{\rho}, \boldsymbol{\lambda}) = \left(\frac{\omega_\rho}{\sqrt{\pi}} \right)^{3/2} \left(\frac{\omega_\lambda}{\sqrt{\pi}} \right)^{3/2} \exp\left[-\frac{\omega_\rho^2 \boldsymbol{\rho}^2}{2} - \frac{\omega_\lambda^2 \boldsymbol{\lambda}^2}{2} \right] \tag{3.23}$$

$$\psi_{11}^\lambda(\boldsymbol{\rho}, \boldsymbol{\lambda}) = -\left(\frac{\omega_\rho^2}{\sqrt{\pi}} \right)^{3/2} \left(\frac{\omega_\lambda}{\sqrt{\pi}} \right)^{3/2} (l_\rho^{(x)} + i l_\rho^{(y)}) \exp\left[-\frac{\omega_\rho^2 \boldsymbol{\rho}^2}{2} - \frac{\omega_\lambda^2 \boldsymbol{\lambda}^2}{2} \right] \tag{3.24}$$

$$\psi_{11}^\rho(\boldsymbol{\rho}, \boldsymbol{\lambda}) = -\left(\frac{\omega_\lambda^2}{\sqrt{\pi}} \right)^{3/2} \left(\frac{\omega_\rho}{\sqrt{\pi}} \right)^{3/2} (l_\lambda^{(x)} + i l_\lambda^{(y)}) \exp\left[-\frac{\omega_\rho^2 \boldsymbol{\rho}^2}{2} - \frac{\omega_\lambda^2 \boldsymbol{\lambda}^2}{2} \right] \tag{3.25}$$

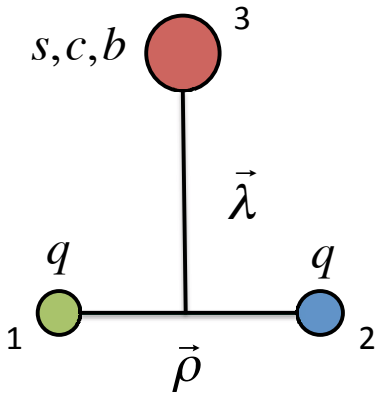

Figure 3.4: Jacobi coordinate in the three body system. Non-light quark is assigned as third quark.

In the $SU(3)$ limit, $m_u = m_d = m_s$, it is well known that ψ^ρ and ψ^λ is associated with a 70-supermultiplet of SU(6) which break into the multiplets ^{2}1, ^{2}8, ^{4}8, ^{2}10, where the superscripts indicate a total quark spin. A list of the states in the $SU(6)$ bases is shown in TABLE.3.1.

		^{2}8	^{4}8	^{2}10	^{2}1
$S=0$:	$J=1/2$	N	N	Δ	$\cdots$
	$J=3/2$	N	N	Δ	$\cdots$
	$J=5/2$		N		
$S=-1$:	$J=1/2$	Λ,Σ	Λ,Σ	Σ	Λ
	$J=3/2$	Λ,Σ	Λ,Σ	Σ	Λ
	$J=5/2$	$\cdots$	Λ,Σ	$\cdots$	$\cdots$
$S=-2$:	$J=1/2$	Ξ	Ξ	Ξ	$\cdots$
	$J=3/2$	Ξ	Ξ	Ξ	$\cdots$
	$J=5/2$	$\cdots$	Ξ	$\cdots$	$\cdots$
$S=-3$:	$J=1/2$	$\cdots$	$\cdots$	Ω^-	$\cdots$
	$J=3/2$	$\cdots$	$\cdots$	Ω^-	$\cdots$

Table 3.1: Low lying negative parity baryons in the SU(3) bases.

In the non-relativistic constituent quark model, the total wave function is defined by the multiplication

by the color wave function, the flavor wave function, the spin wave function and the space wave function. The space wave function with the harmonic oscillator potential have already been given in Eq.(3.25). However, in a realistic case, the orbital wave function is derived by the numerical calculation, which is discussed in Chapter 5.

The spin wave function of the baryon is given by

$$\chi^S_{+3/2} = |\uparrow\uparrow\uparrow\rangle \tag{3.26}$$

$$\chi^\rho_{+1/2} = \frac{1}{\sqrt{2}}(|\uparrow\downarrow\uparrow\rangle - |\downarrow\uparrow\uparrow\rangle) \tag{3.27}$$

$$\chi^\rho_{-1/2} = \frac{1}{\sqrt{2}}(|\uparrow\downarrow\downarrow\rangle - |\downarrow\uparrow\downarrow\rangle) \tag{3.28}$$

$$\chi^\lambda_{+1/2} = \frac{1}{\sqrt{6}}(|\uparrow\downarrow\uparrow\rangle + |\downarrow\uparrow\uparrow\rangle - 2\,|\uparrow\uparrow\downarrow\rangle) \tag{3.29}$$

$$\chi^\lambda_{-1/2} = \frac{1}{\sqrt{6}}(|\uparrow\downarrow\downarrow\rangle + |\downarrow\uparrow\downarrow\rangle - 2\,|\downarrow\downarrow\uparrow\rangle) \tag{3.30}$$

and the flavor wave functions with $\mathcal{S} \neq 0$ are

$$\Sigma^+ = uus,\ \ \Sigma^0 = = \frac{1}{\sqrt{2}}(ud+du)s,\ \ \Sigma_c^- = dds \tag{3.31}$$

$$\Lambda^0 = \frac{1}{\sqrt{2}}(ud-du)s \tag{3.32}$$

for $\mathcal{S} = -1$ and

$$\Xi^- = ssd,\ \Xi^0 = ssu \tag{3.33}$$

$$\Omega = sss \tag{3.34}$$

for $\mathcal{S} = -2$, $\mathcal{S} = -3$. We also mention about the charmed flavored wave function to smoothly understand the inclusion of the later chapter. Flavor wave functions with a charm flavored quark are

$$\Sigma_c^{++} = uuc,\ \ \Sigma_c^+ = = \frac{1}{\sqrt{2}}(ud+du)c,\ \ \Sigma_c^0 = ddc \tag{3.35}$$

$$\Xi_c^{\prime+} = \frac{1}{\sqrt{2}}(us+su)c,\ \ \Xi_c^{\prime+} = \frac{1}{\sqrt{2}}(ds+sd)c \tag{3.36}$$

$$\Omega_c^0 = ssc \tag{3.37}$$

$$\Lambda_c^+ = \frac{1}{\sqrt{2}}(ud-du)c\ \ \Xi_c^{\prime+} = \frac{1}{\sqrt{2}}(us-su)c,\ \ \Xi_c^{\prime+} = \frac{1}{\sqrt{2}}(ds-sd)c \tag{3.38}$$

for $\mathcal{C} = -1$ and

$$\Xi_{cc}^{++} = ccu,\ \ \Omega_{cc}^+ = ccs\ \ \Omega_{ccc}^{++} = ccc \tag{3.39}$$

for $\mathcal{C} = -2$ and $\mathcal{C} = -3$.

In the $SU(3)$ limit, $SU(3)$ states and the states $\left|\Lambda;^4\,\rho\right\rangle$, $\left|\Sigma;^4\,\lambda\right\rangle$ are connected by the relation:

$$\left|\Lambda;^4\,\mathbf{8}\right\rangle = \left|\Lambda;^4\,\rho\right\rangle \tag{3.40}$$

$$\left|\Sigma;^4\,\mathbf{8}\right\rangle = \left|\Sigma;^4\,\lambda\right\rangle . \tag{3.41}$$

The other states $\left|\Lambda;^2\,\rho\right\rangle$, $\left|\Lambda;^2\,\lambda\right\rangle$, $\left|\Sigma;^2\,\rho\right\rangle$ and $\left|\Sigma;^2\,\rho\right\rangle$ are not diagonalized in the $SU(3)$ limit, but these state are expressed by $SU(3)$ state in the relation:

$$\left|\Lambda;^2\,\mathbf{1}\right\rangle = \frac{1}{\sqrt{2}}(\left|\Lambda;^2\,\lambda\right\rangle - \left|\Lambda;^2\,\rho\right\rangle) \tag{3.42}$$

$$\left|\Lambda;^2\,\mathbf{8}\right\rangle = \frac{1}{\sqrt{2}}(\left|\Lambda;^2\,\lambda\right\rangle + \left|\Lambda;^2\,\rho\right\rangle) \tag{3.43}$$

$$\left|\Sigma;^2\,\mathbf{8}\right\rangle = \frac{1}{\sqrt{2}}(\left|\Sigma;^2\,\lambda\right\rangle - \left|\Sigma;^2\,\rho\right\rangle) \tag{3.44}$$

$$\left|\Sigma;^2\,\mathbf{10}\right\rangle = \frac{1}{\sqrt{2}}(\left|\Sigma;^2\,\lambda\right\rangle + \left|\Sigma;^2\,\rho\right\rangle). \tag{3.45}$$

We touch more detail of the relation between SU(3) state and the baryon state in heavy quark limit in 5.1.3.

The hadron states are neither pure $SU(3)$ state and ρ (λ) mode state and should be described by the superposition of these states which have the same quantum number. However, to investigate the hadron state in SU(3) limit and the heavy quark limit is useful to understand the hadron level structure and spectroscopy.

One of the consequences from a naive analysis of P-wave state in the quark model is the mass ordering of $\Lambda(5/2^-)$ and $\Sigma(5/2^-)$. We have already mentioned from the analysis of the spin-spin interaction that it should be $M_\Sigma > M_\Lambda$. However, the mass ordering of $\Lambda(5/2^-)$ and $\Sigma(5/2^-)$ is opposite, $M_{\Sigma(5/2^-)} < M_{\Lambda(5/2^-)}$, which is seen in experimental data. It is explained from the analysis of ρ and λ states as follows.

In the system where $m_3 \neq m_q$, subscript 3 denote s or c or b quark, from the analysis using harmonic oscillator potential, the ratio of the two excited energy is given by

$$\frac{\omega_\lambda}{\omega_\rho} = \sqrt{\frac{1}{3}(1 + 2m_q/m_3)} \leq 1. \tag{3.46}$$

where we set $m_1 = m_2 = m_q$. In the SU(3) limit, $m_q = m_3$, the λ and ρ modes degenerate, $\omega_\lambda = \omega_\rho$. However, when $m_3 > m_q$, the excited energy of the λ mode is always lower than that of the ρ mode, $\omega_\lambda < \omega_\rho$. The quark mass dependence of each excited energy is shown in Fig.3.5. In general, ρ and λ states mix for the physical system, but $\Lambda(5/2^-)$ and $\Sigma(5/2^-)$ are the exceptions, namely these state are either pure ρ state or pure λ state (see TABLE.3.2). Therefore, although the spin average of the masses for $\Sigma(J^-)$ is still higher than that for $\Lambda(J^-)$, the mass of $\Lambda(5/2^-)$ is heavier than that of $\Sigma(5/2^-)$ because of the energy gap of ρ state and λ state. In the discussion above, the higher partial waves are neglected. However, since higher states are well isolated from the lowest states in the quark model, the effect of these states on the energy of lowest state is small. The analysis of ρ and λ states is important for clarifying the

	$^4\rho$	$^2\rho$	$^2\lambda$
$\Lambda(5/2^-)$	$\psi^\rho_{11}\chi^S_{3/2}\phi_0$		
$\Lambda(3/2^-)$	$\psi^\rho_{1m}\chi^S_{3/2-m}\phi_0$	$\psi^\rho_{1m}\chi^\lambda_{3/2-m}\phi_0$	$\psi^\lambda_{1m}\chi^\rho_{3/2-m}\phi_0$
$\Lambda(1/2^-)$	$\psi^\rho_{1m}\chi^S_{1/2-m}\phi_0$	$\psi^\rho\chi^\lambda_{1/2-m}\phi_0$	$\psi^\rho_{1m}\chi^\rho_{3/2-m}\phi_0$
$\Sigma(5/2^-)$	$\psi^\lambda_{11}\chi^S_{3/2}\phi_1$		
$\Sigma(3/2^-)$	$\psi^\lambda_{1m}\chi^S_{3/2-m}\phi_1$	$\psi^\rho_{1m}\chi^\rho_{3/2-m}\phi_0$	$\psi^\rho_{1m}\chi^\lambda_{1/2-m}\phi_1$
$\Sigma(1/2^-)$	$\psi^\lambda_{1m}\chi^S_{1/2-m}\phi_1$	$\psi^\rho_{1m}\chi^\rho_{1/2-m}\phi_0$	$\psi^\rho_{1m}\chi^\lambda_{1/2-m}\phi_1$

Table 3.2: Classification of single strange baryons into $^4\rho$, $^2\rho$, $^2\lambda$.

structure of the exited heavy baryons. Fig.3.5 shows that the excited energy of ρ and λ is separated well in the charm sector, $m_c \sim 2.0$ GeV. Thus, we expect that in the heavy quark sector, the λ excitation modes become dominant for the low lying states of singly heavy quark baryons. In contrast, when $m_Q < m_q$, which corresponds to doubly heavy-quark baryons, we have $\omega_\lambda > \omega_\rho$, and therefore, the ρ excitation modes become dominant. It is shown that this feature is rather general for non-relativistic potential models except for the case when the Coulomb type potential of $1/r$ dominates the binding. We give detailed analysis of ρ and λ state for heavy baryon to Chapter 5.

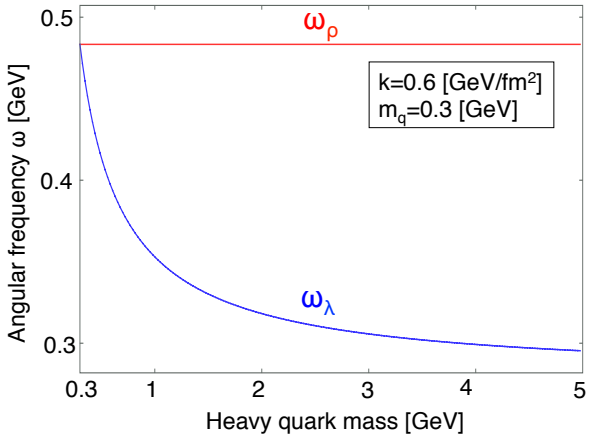

Figure 3.5: Heavy quark mass dependence of excited energies of the λ-mode(red solid line) and the ρ-mode(blue solid line) in Eq.(3.19)

Chapter 4

Chiral effective theory

In this chapter, we discuss the effective theory of hadrons which is valid in the low energy scale. The basic concept is that we construct the effective Lagrangian which has the same symmetry as the QCD Lagrangian, such as chiral symmetry, and heavy quark spin symmetry and the fundamental degrees of freedom are mesons and baryons in this theory. We assume that the effect of high energy scale is included in the parameters in the effective theory. We start with discussion of chiral symmetry and spontaneous symmetry breaking which are the properties of QCD and our final goal is to construct the effective Lagrangian for meson and baryon.

4.1 Chiral symmetry and spontaneous symmetry breaking

QCD Lagrangian has an approximate symmetry called *Chiral symmetry*. In order to discuss chiral symmetry, we introduce left-hand and right-hand fermion, which are defined as

$$q_R = P_R q, \quad q_L = P_L q \tag{4.1}$$

where subscript L and R denote left-hand and right-hand, and projection operator P_R and P_L is defined by

$$P_R = \frac{1+\gamma_5}{2}, \quad P_L = \frac{1-\gamma_5}{2}. \tag{4.2}$$

These operators satisfy completeness

$$P_R + P_L = 1 \tag{4.3}$$

and idempotent

$$P_R^2 = P_R, \quad P_L^2 = P_L \tag{4.4}$$

and the orthogonality relation

$$P_R P_L = P_L P_R = 0. \tag{4.5}$$

The QCD Lagrangian given in Eq.(2.37) can be decomposed into left-hand part and right-hand part in the chiral limit, namely $m_i \to 0$ for N_f flavors

$$\mathcal{L}_{QCD} = \sum_f \bar{\psi}\left[i\not{D} - m_f\right]\psi - \frac{1}{4}G^a_{\mu\nu}G^{a\mu\nu} \tag{4.6}$$

$$\underset{m_f\to 0}{=} \sum_f \left(\bar{\psi}_L \not{D}\psi_L + \bar{\psi}_R \not{D}\psi_R\right) - \frac{1}{4}G^a_{\mu\nu}G^{a\mu\nu}. \tag{4.7}$$

The QCD Lagrangian is invariant under unitary transformations, $U_L(N_f) \otimes U_R(N_f)$. In the $U_L(N_f) \otimes U_R(N_f)$ symmetry, $U_A(1)$ is broken because of $U_A(1)$ anomaly, while $U_V(1)$ symmetry is satisfied. After Removing subgroups $U_A(1)$, the remaining symmetry is $SU_R(N_f) \otimes SU_L(N_f)$, which is defined as

$$q_L \to Lq_L \quad L \equiv e^{i\theta^a_L T^a} \in SU_L(N_f) \tag{4.8}$$

$$q_R \to Rq_R \quad R \equiv e^{i\theta^a_R T^a} \in SU_R(N_f). \tag{4.9}$$

The QCD Lagrangian is invariant under $SU_R(N_f) \otimes SU_L(N_f)$ in the chiral limit. These symmetries are exactly satisfied for QCD Lagrangian in the chiral limit while real quark have finite mass. While the QCD Lagrangian is invariant under the chiral transformation, it is known that QCD vacuum does not have such a symmetry, which leads to the spontaneous broken chiral symmetry in QCD. We give the two indirect evidence of the spontaneous broken chiral symmetry in QCD below.

The $SU_V(N_f)$ is an approximate symmetry that the QCD vacuum has, which is related to the existence of $SU(N_f)$ multiplet in a hadron spectra. If the QCD vacuum is symmetric under $SU_R(N_f) \otimes SU_L(N_f)$, there should be degenerate states which have opposite parity, which is called *chiral partner*, such as $N(1/2^+) - N^*(1/2^-)$, but it is not the case in nature. Thus, one expects that $SU_R(N_f) \otimes SU_L(N_f)$ is broken in a QCD vacuum, and actually it is related to non-vanishing quark condensate $\langle\bar{q}q\rangle$ which is not invariant under $SU_L(N_f) \otimes SU_R(N_f)$ transformation.

Another evidence of the spontaneous broken chiral symmetry in QCD is that the pion have outstandingly light mass. Nambu-Goldstone theorem [44] [45] [46] ensures that the existence of massless bosons in the system where chiral symmetry is spontaneously broken, thus it is expected that the pion is Gold-Stone boson in the two flavor case and a small mass of pion comes from the explicit chiral symmetry breaking term in the QCD Lagrangian, namely the quark mass term. From above two discussion, it is strongly expected that chiral symmetry is spontaneously broken in QCD.

4.2 Chiral Lagrangian

In this section, we construct the chiral Lagragian of mesons and baryons which is based on a chiral symmetry, $SU_R(3) \otimes SU_L(3)$ and its spontaneous breaking to $SU_V(3)$.

4.2.1 Chiral Lagrangian for meson at lowest order

In the chiral limit, the QCD Lagrangian is invariant under a group $G = SU(N_f)_L \otimes SU(N_f)_R$ and the QCD vacuum is not invariant under G, but invariant under a subgroup $H = SU(N_f)_V \in G$. This situation

is expressed as follows. Let $|\Omega\rangle$ be a vacuum in a system, then the following equation is satisfied:

$$U(g)\,|\Omega\rangle \neq |\Omega\rangle \tag{4.10}$$
$$U(h)\,|\Omega\rangle = |\Omega\rangle \tag{4.11}$$

where $g \in G$ and $h \in H$. NG thorem says that the total number of massive bosons are equal to the number of generator of H and the number of Goldstone bosons are equal to the difference between the number of generator of G and the number of generator of H, i.e. $n_{NB} = n_G - n_H$. In other words, Nambu-Goldstone bosons are in the *coset* space G/H. $g \in G$ is decomposed as $g = (g_L, g_R) = qh$ where $g = (g_L, g_R) \in G$, $h = (V, V) \in H$ and q is a representative in the coset space G/H satisfying $q \in G/H$. The choice of q is arbitrary. One finds that one of possible choices for q are

$$g = (g_L, g_R) = (g_L g_R^{-1}, 1)(g_R . g_R) \equiv qh \tag{4.12}$$

with the definition of the operation:

$$gg' = (g_1, g_2)(g_3, g_4) \equiv (g_1 g_3, g_2 g_4), \tag{4.13}$$

where we use $(g_R, g_R) \in H$. Thus, the NG boson is expressed as $SU(N)$ matrix $U(x) = g_L g_R^{-1}$. G operate on G/H as

$$(L, R)(g_L g_R^{-1}, 1) = (L g_L g_R^{-1}, R) = (L g_L g_R^{-1} R^{-1}, 1)(R, R), \tag{4.14}$$

and the transformation property of U under G is

$$U \xrightarrow{G} L U(x) R^{-1} = L U(x) R^{\dagger} \tag{4.15}$$

where we use the unitarity of matrix R.

In general, any element of $g \in G$ can be uniquely decomposed as

$$g = e^{V^a \Psi^a} e^{X^b \Phi^b} \tag{4.16}$$

where V^a is the generator of Lie group H and X^b is the remaining generators, namely the generator of the coset space G/H, and V^a and X^b form a complete set of G. Now, we consider $N_f = 3$ case as an example. Form Eq.4.16, one of the expressions of $SU(3)$ matrix U defined above in the exponential representation is

$$U(x) = \exp\left[\frac{i\sqrt{2}\Phi^a(x)\lambda^a/2}{f}\right] \equiv \exp\left[\frac{i\sqrt{2}\Phi(x)}{f}\right] \tag{4.17}$$

where λ^a is the Gell-mann matrix and f is the constant which is introduced to make the exponential dimensionless. f is related to the pion decay and called *pion decay constant*. $\Phi(x)$ in the Eq. (4.17) is expressed by NG fields:

$$\Phi = \begin{pmatrix} \frac{1}{\sqrt{2}}\pi^0 + \frac{1}{\sqrt{6}}\eta & \pi^+ & K^+ \\ \pi^- & -\frac{1}{\sqrt{2}}\pi^0 + \frac{1}{\sqrt{6}}\eta & K^0 \\ K^- & \bar{K}^0 & -\frac{2}{\sqrt{6}}\eta \end{pmatrix}. \tag{4.18}$$

We define the origin $\Phi = 0$ as ground state of a system, which corresponds to U=U_0=1. A vacuum, which is defined as ground state, transform under $H \in SU(3)_V$, as

$$U_0 \xrightarrow{H} V U_0 V^\dagger = 1 = U_0. \tag{4.19}$$

Thus, a vacuum is invariant under $SU(N_f)_V$. On the other hand, a vacuum is not invariant under an axial transformation G_A, which is defined as $G_A = (A, A^\dagger)$:

$$U_0 \xrightarrow{G_A} A^\dagger U_0 A^\dagger \neq U_0. \tag{4.20}$$

One notice that This properties of U reflect spontaneous symmetry breaking.

From the transformation property of U (See Eq.4.15), one can easily construct the *globally* invariant chiral Lagrangian:

$$\mathcal{L}_{\text{eff}} = \frac{f^2}{4} Tr\left[\partial_\mu U (\partial_\mu U)^\dagger\right] \tag{4.21}$$

For more general discussion, we consider the QCD Lagrangian with the external fields and quark mass term in QCD Lagrangian:

$$\mathcal{L}^{ext}_{QCD} = \mathcal{L}^0_{QCD} + \bar{q}_L \gamma^\mu l_\mu q_L + \bar{q}_R \gamma^\mu r_\mu q_R - \bar{q}(s - i\gamma_5 p) q \tag{4.22}$$

where l_μ, r_μ, p are left-handed vector, right-handed vector and pseudo-calar scalar field respectively, and quark mass matrix s is given by

$$s = \begin{pmatrix} m_u & & \\ & m_d & \\ & & m_s \end{pmatrix}. \tag{4.23}$$

In the formalism of the chiral perturbation theory, a new field χ is introduced for its convenience:

$$\chi \equiv 2B_0(s + ip), \quad \chi^\dagger \equiv 2B_0(s - ip) \tag{4.24}$$

where B_0 is the constant. In the chiral limit, $s \to 0$, the Lagrangian given in Eq.(4.22) have chiral symmetry, if all the external fields transform under $SU_R(3) \otimes SU_L(3)$ as follows:

$$\chi \to R\chi L^\dagger, \quad l_\mu \to L l_\mu L^\dagger + iL\partial_\mu L^\dagger, \quad r_\mu \to R r_\mu R^\dagger + R\partial_\mu R^\dagger. \tag{4.25}$$

Before showing the chiral Lagrangian, we have to mention shortly about the order counting in ChET. It was shown that loop diagram and meson momentum q^μ have one-to-one correspondence. Therefore, an order counting in ChET is performed by $\mathcal{O}(q^n)$, called chiral order [47–50]. One easily notice that

$$U : \mathcal{O}(q^0), \quad D_\mu U : \mathcal{O}(q), \quad \chi : \mathcal{O}(q^2). \tag{4.26}$$

The chiral Lagrangian, in which the $SU_L(3) \otimes SU_R(3)$ is *locally* imposed, is constructed with the external fields:

$$\mathcal{L}_{\text{eff}} = \frac{f^2}{4} Tr\left[D_\mu U (D^\mu U)^\dagger\right] + \frac{f^2}{4} Tr\left[\chi U^\dagger + U\chi^\dagger \cdots\right] \tag{4.27}$$

where $\cdots$ denote higher order terms in the chiral counting and only the terms at the order of q^2 are explicitly shown. In the chiral Lagrangian of meson, covariant derivative D_μ is given by

$$D_\mu U \equiv \partial_\mu U - i r_\mu U + i U l_\mu. \tag{4.28}$$

4.2.2 Chiral Lagrangian for baryon at lowest order

In the last section, we discuss the transformation properties only of mesons, but once baryon field is taken into account, meson and baryon field should be transformed simultaneously, and thus discussion become more complicated than meson case. We start with $N_f = 2$ as a simple case. We define $G = SU(2)_R \otimes SU(2)_L$. Let N denote isospin-doublet field representing proton and neutron

$$N = \begin{pmatrix} p \\ n \end{pmatrix}. \tag{4.29}$$

As we have seen, chiral field U transform as $U \to RUL^\dagger$ under G and the field u, which is defined by $u^2 = U$, transform as

$$u \xrightarrow{G} u' = \sqrt{RUL^\dagger} \equiv RuK^{-1}(L, R, U) \tag{4.30}$$

where the $SU(2)$-valued function K is given by

$$K = u'^{-1} R u = \sqrt{RUL^\dagger}^{-1} R \sqrt{U}. \tag{4.31}$$

We consider a set $\{(U, \Psi)\}$. One finds that the following transformation define an operation of G on the set:

$$\phi(g) : \begin{pmatrix} U \\ N \end{pmatrix} \longrightarrow \begin{pmatrix} U' \\ N' \end{pmatrix} = \begin{pmatrix} RUL^\dagger \\ K(R, L, U)N \end{pmatrix}. \tag{4.32}$$

because

$$\phi(g_1)\phi(g_2)\begin{pmatrix}U\\N\end{pmatrix} =\phi(g_1)\begin{pmatrix}R_2UL_2^\dagger\\K(L_2,R_2,U)N\end{pmatrix}=\begin{pmatrix}R_1R_2UL_2^\dagger L_1^\dagger\\K(L_1,R_1,R_2UL_2^\dagger)K(L_2,R_2,U)N\end{pmatrix} \tag{4.33}$$

$$=\begin{pmatrix}(R_1R_2)U(L_1L_2)^\dagger\\K((L_1L_2),(R_1R_2),U)N\end{pmatrix}=\phi(g_1g_2)\begin{pmatrix}U\\N\end{pmatrix}. \tag{4.34}$$

where we use

$$\begin{aligned}K(L_1,R_1,R_2UL_2^\dagger)K(L_2,R_2,U) &= \left(\sqrt{R_1(R_2UL_2^\dagger)L_1^\dagger}^{-1}R_1\sqrt{R_2UL_2^\dagger}\right)\left(\sqrt{R_2UL_2^\dagger}^{-1}R_2\sqrt{U}\right)\\ &= \sqrt{(R_1R_2)U(L_1L_2)^\dagger}^{-1}(R_1R_2)\sqrt{U}\\ &= K((L_1L_2),(R_1R_2),U).\end{aligned} \tag{4.35}$$

The chiral field U transform under an isospin transformation, i.e. in the case of $R=L=V$, as

$$U'=VUV^\dagger. \tag{4.36}$$

Thus, N transform as an isospin doublet under $SU(2)_V\in H$, because Eq. (4.36) implies $K^{-1}(V,V,U)=V^\dagger$ and $K(V,V,U)=V$.

We can extendthe above discussion to the $SU(3)$ case. Here, we focus on an octet of $J=1/2^+$ baryons. In this case, an operation of G on the set $\{U,B\}$ is expressed by

$$\phi(g):\begin{pmatrix}U\\B\end{pmatrix}\longrightarrow\begin{pmatrix}U'\\B'\end{pmatrix}=\begin{pmatrix}RUL^\dagger\\K(R,L,U)BK(R,L,U)^\dagger\end{pmatrix}. \tag{4.37}$$

where B denotes a 3×3 complex, traceless matrix, which is related to octet baryon fields of $J=1/2$:

$$B=\sum_{a=1}^{8}\frac{B^a\lambda^a}{\sqrt{2}}=\begin{pmatrix}\frac{1}{\sqrt{2}}\Sigma^0+\frac{1}{\sqrt{6}}\Lambda & \Sigma^+ & p\\ \Sigma- & -\frac{1}{\sqrt{2}}\Sigma^0+\frac{1}{\sqrt{6}}\Lambda & n\\ \Xi^- & \Xi^0 & -\frac{2}{\sqrt{6}}\Lambda\end{pmatrix}. \tag{4.38}$$

Since transformation property of the set $\{(U,B)\}$ was revealed, we now got prepared for constructing the chiral Lagrangian with baryon. We again start with $N_f=2$ and consider the Lagrangian which is invariant under *local* $SU(2)_L\otimes SU(2)_R\otimes U_V(a)$. As discussed above, nucleon doublet N and U transform under $G\in SU(2)_L\otimes SU(2)_R\otimes U_V(1)$ as

$$\begin{pmatrix}U(x)\\N(x)\end{pmatrix}\xrightarrow{G}\begin{pmatrix}V_R(x)UV_L(x)^\dagger\\\exp[-i\Theta(x)]K(V_R(x),V_L(x),U(x))N(x)\end{pmatrix}. \tag{4.39}$$

We define covariant derivative D_μ so that it obey the transformation low as follows

$$D_\mu N(x) \longrightarrow [D_\mu N(x)]' = \exp[-i\Theta(x)]K(V_R(x), V_L(x), U(x))D_\mu N(x). \tag{4.40}$$

In order to construct the covariant derivative which satisfy the relation, it is convenient to introduce following quantity called chiral connection:

$$\Gamma_\mu = \frac{1}{2}[u^\dagger(\partial_\mu - ir_\mu)u + u(\partial_\mu - il_\mu)u^\dagger]. \tag{4.41}$$

Then, we reach at explicit form of the covariant derivative with chiral connection:

$$D_\mu B(x) = \partial_\mu B(x) + [\Gamma_\mu, B(x)]. \tag{4.42}$$

The also axial vector coupling term should be taken into account, which is invariant under G and it is given by

$$\frac{\mathcal{G}_A}{2}\gamma^\mu\gamma_5 u_\mu \tag{4.43}$$

with

$$u_\mu = \frac{1}{2}[u^\dagger(\partial_\mu - ir_\mu)u - u(\partial_\mu - il_\mu)u^\dagger]. \tag{4.44}$$

The axial vector coupling constant $\mathcal{G}_A$ is estimated experimentally from the neutron beta decay and the physical value is $\mathcal{G}_A = 1.2694 \pm 0.0028$ [51].

Since baryon is not NG boson, baryon mass M_B does not vanish in the chiral limit. The power counting for baryon sector is understood by the plane wave solution of the free Dirac particle and one finds that $\not{p} - m$ corresponds to the order of q [52]. The order of each components appearing in baryon sector are

$$\bar{B}, B : \mathcal{O}(q^0), \quad D_\mu B : \mathcal{O}(q^0), \quad (i\not{D} - m)B : \mathcal{O}(q), \tag{4.45}$$

$$\gamma_\mu, \gamma_5\gamma_\mu : \mathcal{O}(q^0), \quad \gamma_5 : \mathcal{O}(q^0) \tag{4.46}$$

From the discussion so far, the meson-baryon term of the chiral Lagrangian at lowest order is given by [53]:

$$\mathcal{L}_{\pi N} = \bar{B}\left(i\not{D} - M + \frac{\mathcal{G}_A}{2}\gamma^\mu\gamma_5 u_\mu\right)B, \tag{4.47}$$

moreover, from Eq.(4.27), the full meson-baryon Lagrangian which satisfies local $SU(2)_L \otimes SU(2)_R \otimes U_V(2)$ at lowest order is written by

$$\mathcal{L}_{eff} = \bar{\Psi}\left(i\not{D} - M + \frac{\mathcal{G}_A}{2}\gamma^\mu\gamma_5 u_\mu\right)\Psi + \frac{f^2}{4}Tr\left[D_\mu U(D^\mu U)^\dagger\right] + \frac{f^2}{4}Tr\left[\chi U^\dagger + U\chi^\dagger\right]. \tag{4.48}$$

In the SU(3) sector, the transformation property of baryon fields is given in Eq.(4.37). Thus, one obtains the effective Lagrangian for baryons in a similar way as SU(2) case:

$$\mathcal{L}_{MB} = \mathrm{Tr}[\bar{\mathrm{B}}\,(\mathrm{i}\not{D} - \mathrm{M}_0)\,\mathrm{B}] + \frac{\mathrm{D}}{2}\mathrm{Tr}\left(\bar{\mathrm{B}}\gamma^\mu\gamma_5\{\mathrm{u}_\mu, \mathrm{B}\}\right) + \frac{\mathrm{F}}{2}\mathrm{Tr}\left(\bar{\mathrm{B}}\gamma^\mu\gamma_5\{\mathrm{u}_\mu, \mathrm{B}\}\right) \tag{4.49}$$

where

$$D_\mu B = \partial_\mu B + [\Gamma_\mu, B]. \tag{4.50}$$

New constants F and D appear in Eq.(4.49) as an axial vector constant, which are determined by the semi-leptonic decays and from the experimental analysis, these constants take [54]

$$D = 0.8, \quad F = 0.5. \tag{4.51}$$

Part II

Applications

Chapter 5

Heavy baryons in a constituent quark model

In this chapter, we discuss our model Hamiltonian in detail. In the non-relativistic quark model, baryons are formed by three valence (constituent) quarks. They are confined by a confining potential and interact with each other by residual two-body interactions. Their internal motions are then described by the two spatial variables $\boldsymbol{\rho}$ and $\boldsymbol{\lambda}$. In other models of baryons, non-quark degrees of freedom are considered such as constituent gluons and confining fields. Their signals in baryon excitations are, however, not yet confirmed in experiments, and are expected to lie at higher energies than the low lying quark excitation modes. Empirically these justify the applicability of the quark model, especially for low lying excitation modes.

5.1 Formalism

5.1.1 Hamiltonian

Our Hamiltonian is written as

$$H = K + V_{\rm con} + V_{\rm short}, \tag{5.1}$$

where the kinetic energy, K, the confinement potential, $V_{\rm con}$, and the short range interaction, $V_{\rm short}$, are given as

$$K = \sum_i \left(m_i + \frac{\boldsymbol{p}^2{}_i}{2m_i} \right) - K_G \ , \tag{5.2}$$

$$V_{\rm con} = \sum_{i<j} \frac{br_{ij}}{2} + C \tag{5.3}$$

$$
\begin{aligned}
V_{\rm short} &= \sum_{i<j}\Bigg[-\frac{2\alpha^{\rm Coul}}{3r_{ij}}+\frac{16\pi\alpha^{\rm ss}}{9m_im_j}\boldsymbol{s}_i\cdot\boldsymbol{s}_j\frac{\Lambda^2}{4\pi r_{ij}}\exp(-\Lambda r_{ij})+\frac{\alpha^{\rm so}(1-\exp(-\Lambda r_{ij}))^2}{3{r_{ij}}^3} \\
&\times \left[(\frac{1}{m_i^2}+\frac{1}{m_j^2}+4\frac{1}{m_im_j})\boldsymbol{L}_{ij}\cdot(\boldsymbol{s}_i+\boldsymbol{s}_j)+(\frac{1}{m_i^2}-\frac{1}{m_j^2})\boldsymbol{L}_{ij}\cdot(\boldsymbol{s}_i-\boldsymbol{s}_j)\right] \\
&+ \frac{2\alpha^{\rm ten}(1-\exp(-\Lambda r_{ij}))^2}{3m_im_j{r_{ij}}^3}\left(\frac{3(\boldsymbol{s}_i\cdot\boldsymbol{r_{ij}})(\boldsymbol{s}_j\cdot\boldsymbol{r_{ij}})}{{r_{ij}}^2}-\boldsymbol{s}_i\cdot\boldsymbol{s}_j\right)\Bigg]. \qquad (5.4)
\end{aligned}
$$

In Eq.(5.2), m_i is the constituent quark mass of the i-th quark, and the center of mass energy, K_G, is subtracted so that the kinetic energy consists only of the ρ and λ-kinetic energies. In Eq.(5.3), we employ the linear confinement potential with the b parameter corresponding to the string tension and $\boldsymbol{r}_{ij}=\boldsymbol{r}_i-\boldsymbol{r}_j$ is the relative coordinate. In Eq.(5.4), $\boldsymbol{L}_{ij}=(\boldsymbol{r}_i-\boldsymbol{r}_j)\times(m_j\boldsymbol{p}_i-m_i\boldsymbol{p}_j)/(m_i+m_j)$ is the relative orbital angular momentum and $\boldsymbol{s}_i(=\sigma_i/2)$ is the spin operators of the i-th quark. The components of Eq.(5.4) are inferred by the one-gluon-exchange (OGE), which requires only one coupling constant common to the four terms. Practically, however, they may have different origins other than the OGE, and therefore, we treat the four coupling strengths, $\alpha^{\rm Coul}$, $\alpha^{\rm ss}$, $\alpha^{\rm so}$ and $\alpha^{\rm ten}$ as independent parameters for better description of baryon masses.

In order to guarantee the heavy quark symmetry, we introduce anti-symmetric LS force (ALS). The terms dependent on the heavy quark spin $\boldsymbol{s_Q}$ of the $V_{\rm SLS}$ and $V_{\rm ALS}$ in a single-heavy baryon are given by

$$
\begin{aligned}
V_{\rm SLS} &\to \sum_{i=1,2}\frac{\alpha^{\rm so}(1-\exp(-\Lambda r_{iQ}))^2}{3r_{iQ}^3} \\
&\times \left(\frac{1}{m_i^2}+\frac{1}{m_Q^2}+\frac{4}{m_im_Q}\right)\boldsymbol{L}_{iQ}\cdot\boldsymbol{s}_Q \qquad (5.5) \\
V_{\rm ALS} &\to \sum_{i=1,2}\frac{\alpha^{\rm so}(1-\exp(-\Lambda r_{iQ}))^2}{3r_{iQ}^3} \qquad (5.6) \\
&\times \left(\frac{1}{m_i^2}-\frac{1}{m_Q^2}\right)\boldsymbol{L}_{iQ}\cdot(-\boldsymbol{s}_Q) \qquad (5.7)
\end{aligned}
$$

where we choose $i=3$ for the heavy quark. Then by summing the parts from SLS and ALS, the $\boldsymbol{L_Q}\cdot\boldsymbol{s_Q}$ is always proportional to $1/m_Q$ or higher. Thus the $\boldsymbol{s}_Q$ dependence disappear in the $m_Q\to\infty$ limit, and the heavy quark symmetry is guaranteed.

Recently, it was suggested by a Lattice QCD calculation [36] that the strength, $\alpha^{\rm Coul}$, of the color Coulomb force depends significantly on the quark mass. In our study, we therefore assume that $\alpha^{\rm Coul}$ for the $i-j$ pair of quarks depends on the reduced mass, $\mu_{ij}=\frac{m_im_j}{m_i+m_j}$, as follows,

$$\alpha^{\rm Coul}=\frac{K}{\mu_{ij}}. \qquad (5.8)$$

We summarize 10 parameters in the Hamiltonian employed here in TABLE 5.1. The parameters are determined from experimental data of the strange baryon spectrum (See TABLE 5.2). First, we switch off the LS and tensor force to determine the parameters C, $\alpha_{\rm ss}$, m_q, m_s and Λ, K from the positive parity

state. Then, we determine $\alpha^{\rm so}$, b from negative parity states. The details how to determine the parameters are as follows.

- The constant term C

  In the constituent quark models, we can predict mass differences between different states, but the absolute values can not be determined. In our work, we introduce the constant C to reproduce the ground state of $\Lambda(1115)$ and we assume that the constant C is independent of the constituent quark mass. Namely, we use the same value for the charmed baryons.

- Spin-spin term

  The spin-spin term in the hamiltonian is responsible for the splitting among Λ, Σ and Σ^*. This term depends on $\alpha^{\rm ss}$, m_q, m_s and Λ. Because we have four parameters for three states to be fitted, we fix $m_q = 300$ MeV which is the standard value suggested from the magnetic moment of the baryon in the constituent quark model and then we determine the other parameters to reproduce the masses of Λ, Σ, Σ^*.

- The parameter K

  In our calculation, we introduce $\alpha^{\rm Coul}$ as a quark mass dependent form as given by Eq (5.8). Thus, the Coulomb force can contribute to the mass splitting between the ground states of $\Lambda_s(\Sigma_s)$, Ξ_{ss}, Ω_{sss}. This force also contributes to the mass differences between the ground state and the excited states. We determine the parameter K to reproduce $\Xi(1/2^+)$ and the mass difference between the ground state and the excited states.

- The linear confinement b

  Our emphasis in the present study is on the P wave states. The parameters which mainly determine the mass differences are b and K. K is determined from $\Xi(1/2^+)$ as mentioned above and we determine the parameter b to reproduce the splitting between ground state and P-wave state.

- The spin-orbit coupling $\alpha^{\rm so}$

  The strength $\alpha^{\rm so}$ of the spin-orbit force may be determined by the splitting of the P-wave baryons, such as $\Lambda(1/2^-)$ and $\Lambda(3/2^-)$. However, we do not use the lowest $\Lambda(1/2^-)$, $=\Lambda(1405)$, because various recent studies on the $\Lambda(1405)$ resonance suggests that this is not simply a pure three-quark state, but rather a $N\bar{K}$ molecular-like state. Therefore, we determine the parameter $\alpha^{\rm so}$ to reproduce the splitting between the second $\Lambda(1/2^-)$ and $\Lambda(3/2^-)$, namely $\Lambda(1670)$ and $\Lambda(1690)$. Thus, as expected, $\alpha_{\rm so}$ becomes very small, much smaller than α_{ss}. If the spin-spin and LS forces come only from the OGE, then their values are not consistent. However, other sources of quark interactions including the relativistic correlations to the confinement and instanton induced interaction(III) may contribute

also the LS interaction shown [55] that the LS force from OGE and III are opposite. Then the discrepancy between $\alpha^{\rm ss}$ and $\alpha^{\rm so}$ can be explained.

- The strength $\alpha^{\rm ten}$

  The tensor force in the hamiltonian contributes mainly to the positive parity $\Sigma(1/2^+)$, $\Sigma(3/2^+)$ and the lowest negative states. It has been known that the tensor force is weak and does not contribute much except for generating mixings of $S = 1/2$ and $3/2$ states. We choose $\alpha^{\rm ten}$ equal to $\alpha^{\rm so}$

- Charm and bottom quark mass, m_c, m_b

  We fit the charm quark mass m_c (bottom quark mass m_b) to the ground state of Λ_c (Λ_b). These values contribute to the mass splittings as well as the absolute values, but once we determine the other parameters in the strange sector, m_c and m_b are determined uniquely.

From Table 5.2, we find that our results reproduce most of the known strange baryon masses, except for the second $J^P = 1/2^+$ state and the first $J^P = 1/2^-$. It is well known that the Roper resonance $N(1440)$, the second $J^P = 1/2^+$ state, is lighter than lowest $J^P = 1/2^-$ state, which is incompatible with the quark model predictions. Similarly, in the strange sector, the Roper-like states $\Lambda(1600)$ and $\Sigma(1660)$, are predicted at higher masses than experiment. The origin of these discrepancies may reside outside the simple three quark picture of the baryons in the quark model. We therefore omit these states from the fitting in the present analysis.

m_q [MeV]	m_s [MeV]	m_c [MeV]	m_b [MeV]	b [GeV^2]	K [MeV]	$\alpha^{\rm ss}$	$\alpha^{\rm so}(=\alpha^{\rm ten})$	C [MeV]	Λ [fm^{-1}]
300	510	1750	5112	0.165	90	1.2	0.077	-1139	3.5

Table 5.1: Parameters in the Hamiltonian. We determine m_q, m_s, b, K, α^{ss} and Λ to reproduce strange baryons and m_c and m_b are determined from the ground state of Λ_c and Λ_b.

5.1.2 Baryon wave function

We here consider three quark systems (TABLE.5.3) with one heavy quark, $Q = (c$ or $b)$, with two or three heavy quarks with the same flavor, i.e., $QQ = (cc$ or $bb)$ and $QQQ = (ccc$ or $bbb)$. The remaining quarks are u, d or s. We classify the baryons according to the number of heavy quarks, and the strangeness, $\mathcal{S}$ and the total isospin, T. The last column of the TABLE.5.3 shows the isospin wave function where $\eta_0 = 1$.

In expressing three-quark wave functions, we introduce three sets of Jacobi coordinates, which we call channels (Fig. 5.1).

The Jacobi coordinates in each channel c ($c = 1, 2, 3$) are defined as

$$\boldsymbol{\lambda}_c = \boldsymbol{r_k} - \frac{m_i \boldsymbol{r_i} + m_j \boldsymbol{r_j}}{m_i + m_j}, \tag{5.9}$$

$$\boldsymbol{\rho}_c = \boldsymbol{r_j} - \boldsymbol{r_i}, \tag{5.10}$$

(a)Λ_s

J^P	Theory [MeV]	Exp. [MeV]
$\frac{1}{2}^+$	1116	1116
	1799	1560-1700
	1922	1750-1850
$\frac{3}{2}^+$	1882	1850-1910
	2030	
	2100	
$\frac{5}{2}^+$	1891	1815-1825
	2045	2090-2140
	2143	
$\frac{1}{2}^-$	1526	1405
	1665	1660-1680
	1777	1720-1850
$\frac{3}{2}^-$	1537	1520
	1685	1685-1695
	1810	
$\frac{5}{2}^-$	1814	1810-1830
	2394	
	2448	

(b)Σ_s

J^P	Theory [MeV]	Exp. [MeV]
$\frac{1}{2}^+$	1197	1192
	1895	1630-1690
	2016	
$\frac{3}{2}^+$	1391	1385
	2004	
	2028	
$\frac{5}{2}^+$	2012	1900-1935
	2085	
	2091	
$\frac{1}{2}^-$	1654	(≈1620)
	1734	1730-1800
	1751	
$\frac{3}{2}^-$	1660	1665-1685
	1755	1900-1950
	1760	
$\frac{5}{2}^-$	1762	1770-1780
	2324	
	2427	

(c)Ξ_{ss}

J^P	Theory [MeV]	Exp. [MeV]
$\frac{1}{2}^+$	1325	1314
	1962	
	2131	
$\frac{3}{2}^+$	1525	1530
	2034	
	2115	
$\frac{5}{2}^+$	2040	
	2166	
	2211	
$\frac{1}{2}^-$	1778	
	1875	
	1910	
$\frac{3}{2}^-$	1782	1820
	1877	
	1920	
$\frac{5}{2}^-$	1933	
	2460	
	2518	

Table 5.2: Calculated energy spectra and corresponding experimental data of Λ_s,Σ_s and Ξ_{ss}. We take the 3-star and 4-star resonances in PDG except for the first $1/2^-$ state of Σ_s which has only two stars

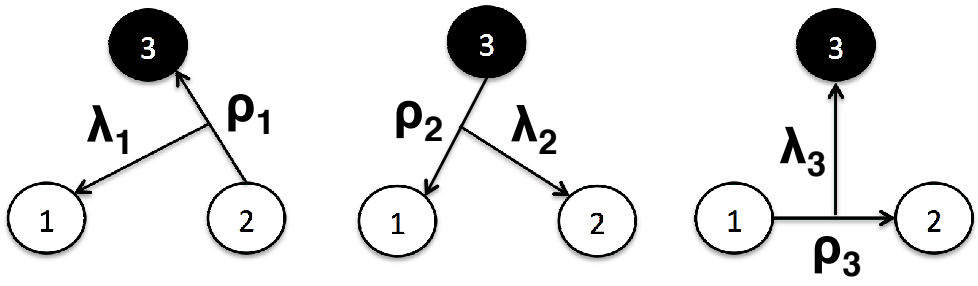

Figure 5.1: Jacobi coordinates for the three body system. We place the heavy quark as the 3rd particle in the case of single-heavy baryons, while the 1st and 2nd particles are heavy quarks in double-heavy baryons.

Heavy baryons	Isospin $\mathcal{S}$	Strangeness T	isospin wave function
$\Lambda_Q = [qq]_{T=0}Q$	0	0	$\Big[\big[\eta_{1/2}\eta_{1/2}\big]_{\mathrm{t}=0}\,\eta_0\Big]_{T=0}$
$\Sigma_Q = [qq]_{T=1}Q$	0	1	$\Big[\big[\eta_{1/2}\eta_{1/2}\big]_{\mathrm{t}=1}\,\eta_{1/2}\Big]_{T=1}$
$\Xi_Q = sqQ$	-1	1/2	$\Big[\big[\eta_0\eta_{1/2}\big]_{\mathrm{t}=1/2}\,\eta_0\Big]_{T=1/2}$
$\Omega_Q = ssQ$	-2	0	1
$\Xi_{QQ} = QQq$	0	1/2	$\big[\big[\eta_0\eta_0\big]_{\mathrm{t}=0}\,\eta_{1/2}\big]_{T=1/2}$
$\Omega_{QQ} = QQs$	-1	0	1
$\Omega_{QQQ} = QQQ$	0	0	1

Table 5.3: Heavy baryons and their flavor contents. We use the isopin classification so that q stands collectively for the u and d quarks. Q denotes a c or b quark.We do not consider mixing of c and b
.

where (i, j, k) are given by Table 5.4.

channel	i	j	k
1	2	3	1
2	3	1	2
3	1	2	3

Table 5.4: The quark assignments (i,j,k) for the Jacobi channels.

The total wave function is given as a superposition of the channel wave functions as

$$\Phi^{JM}_{\mathrm{total}} = \sum_{c\alpha} C_{c,\alpha}\Phi^{(c)}_{JM,\alpha}(\boldsymbol{\rho_c}, \boldsymbol{\lambda_c}), \tag{5.11}$$

where the index α represents $\{s, S, \ell, L, I, n, N\}$. Here s is the spin of the (i, j) quark pair, S is the total spin, ℓ and L are the orbital angular momentum for the coordinate ρ and λ, respectively, and I is the total orbital angular momentum. The coupling scheme of the spin and angular momenta is as

$$\boldsymbol{s} = \boldsymbol{s}_i + \boldsymbol{s}_j;\ \boldsymbol{s} + \boldsymbol{s}_k = \boldsymbol{S};\ \boldsymbol{\ell} + \boldsymbol{L} = \boldsymbol{I};\ \boldsymbol{S} + \boldsymbol{I} = \boldsymbol{J}. \tag{5.12}$$

The wave function for channel c is given by

$$\Phi^{(c)}_{JM}(\boldsymbol{\rho_c}, \boldsymbol{\lambda_c}) = \phi_c \otimes \Big[X^{(c)}_{S,s} \otimes \Phi^{(c)}_{\ell,L,I}\Big]_{JM} \otimes H^{(c)}_{T,t}, \tag{5.13}$$

where the color wave function, ϕ_c, the spin wave function, X_S, the orbital wave function, Φ_I, and the

isospin wave function, H_T, are given by

$$\phi_{\rm c} = \frac{1}{\sqrt{6}}(rgb - rbg + gbr - grb + brg - bgr) \tag{5.14}$$

$$X^{(c)}_{S,s} = \Big[\big[\chi_{1/2}(i)\chi_{1/2}(j)\big]_s \chi_{1/2}(k)\Big]_S \tag{5.15}$$

$$H^{(c)}_{T.t} = \big[\big[\eta_{\tau_i}(i)\eta_{\tau_j}(j)\big]_t \eta_{\tau_k}(k)\big]_T \tag{5.16}$$

$$\Phi^{(c)}_{\ell,L,I} = \Big[\phi^{(c)}_\ell(\boldsymbol{\rho_c})\phi^{(c)}_L(\boldsymbol{\lambda_c})\Big]_I \tag{5.17}$$

$$\phi^{(c)}_\ell(\boldsymbol{\rho_c}) = N_{n\ell}\rho_c^\ell e^{-\beta_n\rho_c^2}Y_{\ell m}(\hat{\boldsymbol{\rho}}_{\boldsymbol{c}}) \tag{5.18}$$

$$\phi^{(c)}_L(\boldsymbol{\lambda_c}) = N_{NL}\lambda_c^L e^{-\gamma_N\lambda_c^2}Y_{LM}(\hat{\boldsymbol{\lambda}}_{\boldsymbol{c}}). \tag{5.19}$$

In Eq. (5.14), r, g, b denote the color of the quark, and the color-singlet wave function is totally anti-symmetric. In Eq.(5.15), $\chi_{1/2}$ is the spin wave function of the quark, while η_τ in Eq.(5.16) is the isospin wave function with τ defined by

$$\tau = \begin{cases} 1/2 & \text{for } u,\, d \\ 0 & \text{for } s,\, c,\, b \end{cases} \tag{5.20}$$

We consider the quark antisymmetrization for the light quarks, u and d, and the heavy quarks, s, c, b, separately. Then for single-heavy baryons, antisymmetrization is applied only to the light quarks. As the color wave function is always totally anti-symmetric, the spin, isospin and the orbital angular momentum in the channel (3) should satisfy

$$\ell + s + t = \text{even} \quad \text{for } \Lambda_Q,\, \Sigma_Q \tag{5.21}$$

where ℓ, s, t are the orbital angular momentum, total spin and isospin of the two light quarks. Similarly, the heavy quarks are antisymmetrized in the double-heavy baryons as

$$\ell + s + 1 = \text{even} \quad \text{for } \Xi_{QQ},\, \Omega_Q,\, \Omega_{QQ} \tag{5.22}$$

where ℓ, s, t are the corresponding ones for the heavy quarks. Considering the antisymmetrization and the combinations of the angular momenta, we obtain possible assignments of the angular momenta for the low-lying $\Lambda_Q(1/2^+)$ in Table 5.5, where we take all the combinations satisfying $\ell + L \leq 2$.

In solving the Schrödinger equation, we use the Gaussian expansion method [56], where the orbital wave functions are expanded, in Eqs. (5.18) and (5.19), by Gaussian functions with the range parameters,

β_n and γ_N, chosen as:

$$\beta_n = 1/r_n^2,\ r_n = r_1 a^{n-1}\ (n = 1, \ldots, n_{\max}), \tag{5.23}$$

$$\gamma_N = 1/R_N^2,\ R_N = R_1 b^{N-1}\ (N = 1, \ldots, N_{\max}). \tag{5.24}$$

In Eqs (5.18) ans (5.19), $N_{n\ell}(N_{NL})$ denotes the normalization constant of the Gaussian basis. The coefficients $C_{c,\alpha}$ of the variational wave function, Eq.(5.11), are determined by the Rayleigh-Ritz variational principle. We see the more detail of numerical method in 5.2.

In order to check that the energy converges to the required precision, we change the number of bases and plot the eigen-energy of the lowest lying $\Lambda_c(3/2^-)$ in Fig.5.2. The filled points are the results from the calculation only using the channel 3, while the open circles are the results from the three channel calculation (Fig.5.1). One sees that when we take only one channel, the convergence is slow and has not yet reached the required precision at $N_{\max} = n_{\max} = 10$.

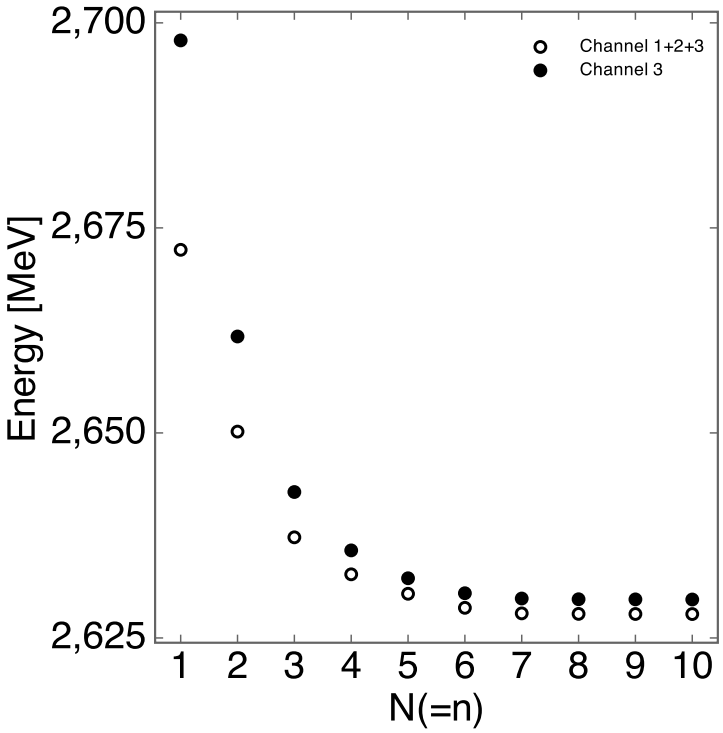

Figure 5.2: Convergence of the energy of the lowest $\Lambda_c(3/2^-)$ for increasing the number of bases functions.

5.1.3 Heavy quark limit

One of the aims of this paper is to see how the heavy baryon spectrum changes when the heavy quark mass m_Q changes. Two limits are important: the SU(3) limit with $m_Q = m_q$, and the heavy quark (HQ) limit, $m_Q \to \infty$.

channel	ℓ	L	I	s	S
3	0	0	0	0	1/2
3	1	1	0	1	1/2
3	1	1	1	1	1/2
3	1	1	1	1	3/2
3	1	1	2	1	3/2

Table 5.5: Combinations of the spin and orbital angular momenta in channel 3 of the low-lying $\Lambda(1/2^+)$. In our study, we restrict the total angular momentum up to 2, $\ell + L = 0, 2$.

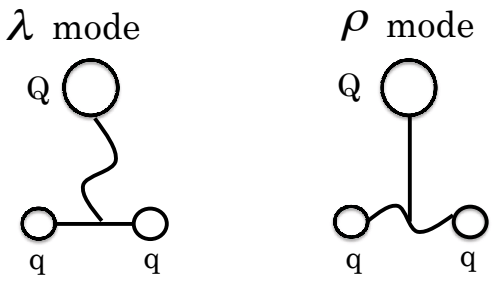

Figure 5.3: The ρ- and λ-modes excitations of the single-heavy baryon.

In the limit $m_Q \to m_q$, the spectrum is classified by the SU(3) representations. For instance, the lowest P-wave baryons are expected to belong to the SU(6) 70-dimensional representation, which contains ${}^2\mathbf{1}$, ${}^2\mathbf{8}$, ${}^4\mathbf{8}$, and ${}^2\mathbf{10}$. Here the upper index number is the spin multiplicity and the bold number represents the SU(3) multiplicity. On the other hand, in the HQ limit, $m_Q \to \infty$, as we have discussed in sect.I, the P-wave baryons are better classified by the ρ- and λ-excitation modes (Fig.5.3). Here we derive relations between the two pictures.

Let us consider single-heavy Λ_Q and Σ_Q baryons. We put the heavy quark Q as the 3rd quark. Then the orbital-spin wave functions of Λ_Q and Σ_Q in the SU(3) limit are given by

$$\Psi(\Lambda_Q; {}^2\mathbf{1}) = \frac{1}{\sqrt{2}}(X_{1/2,1}\Phi_{1,0,1} - X_{1/2,0}\Phi_{1,1,0}). \tag{5.25}$$

$$\Psi(\Lambda_Q; {}^2\mathbf{8}) = \frac{1}{\sqrt{2}}(X_{1/2,1}\Phi_{1,0,1} + X_{1/2,0}\Phi_{1,1,0}) \tag{5.26}$$

$$\Psi(\Lambda_Q; {}^4\mathbf{8}) = X_{3/2,1}\Phi_{1,0,1} \tag{5.27}$$

and

$$\Psi(\Sigma_Q;{}^2\mathbf{10}) = \frac{1}{\sqrt{2}}(X_{1/2,1}\Phi_{1,1,0} + X_{1/2,0}\Phi_{1,0,1}) \quad (5.28)$$

$$\Psi(\Sigma_Q;{}^2\mathbf{8}) = \frac{1}{\sqrt{2}}(X_{1/2,1}\Phi_{1,1,0} - X_{1/2,0}\Phi_{1,0,1}) \quad (5.29)$$

$$\Psi(\Sigma_Q;{}^4\mathbf{8}) = X_{3/2,1}\Phi_{1,1,0}. \quad (5.30)$$

In the SU(3) limit, the ${}^2\mathbf{8}(S=1/2)$ and ${}^4\mathbf{8}(S=3/2)$ can be mixed with the spin-spin/spin-orbit forces (If we further argue SU(6), they do not mix). For $m_q < m_Q$, $\Psi(\Lambda_Q;{}^2\mathbf{1})$ and $\Psi(\Lambda_Q;{}^2\mathbf{8})$ may mix with each other and in the large m_Q limit, they are reduced to the λ-mode, $\Phi_{1,1,0}$, and the ρ-mode, $\Phi_{1,0,1}$, excitations. Representing the $\lambda(\rho)$-mode with the total spin S by ${}^{2S+1}\lambda({}^{2S+1}\rho)$, we obtain

$$\begin{aligned}\Psi(\Lambda_Q;{}^2\lambda) &= X_{1/2,0}\Phi_{1,1,0} \\ &= \frac{1}{\sqrt{2}}(\Psi(\Lambda_Q;{}^2\mathbf{8}) - \Psi(\Lambda_Q;{}^2\mathbf{1})) \quad (5.31)\\ \Psi(\Lambda_Q;{}^2\rho) &= X_{1/2,1}\Phi_{1,0,1} \\ &= \frac{1}{\sqrt{2}}(\Psi(\Lambda_Q;{}^2\mathbf{8}) + \Psi(\Lambda_Q;{}^2\mathbf{1})) \quad (5.32)\\ \Psi(\Lambda_Q;{}^4\rho) &= X_{3/2,1}\Phi_{1,0,1} = \Psi(\Lambda_Q;{}^4\mathbf{8}). \quad (5.33)\end{aligned}$$

for the Λ_Q baryons and

$$\begin{aligned}\Psi(\Sigma_Q;{}^2\lambda) &= X_{1/2,1}\Phi_{1,1,0} \\ &= \frac{1}{\sqrt{2}}(\Psi(\Sigma_Q;{}^2\mathbf{10}) + \Psi(\Sigma_Q;{}^2\mathbf{8})) \quad (5.34)\\ \Psi(\Sigma_Q;{}^2\rho) &= X_{1/2,0}\Phi_{1,0,1} \\ &= \frac{1}{\sqrt{2}}(\Psi(\Sigma_Q;{}^2\mathbf{10}) - \Psi(\Sigma_Q;{}^2\mathbf{8})) \quad (5.35)\\ \Psi(\Sigma_Q;{}^4\lambda) &= X_{3/2,1}\Phi_{1,1,0} = \Psi(\Sigma_Q;{}^4\mathbf{8}), \quad (5.36)\end{aligned}$$

for the Σ_Q baryons.

Generally, the λ-modes appear lower in energy than the ρ-modes and they do not mix with each other in the heavy quark limit. The two states which are in the same mode but have different spin, ($\Lambda_Q;{}^2\rho$, $\Lambda_Q;{}^4\rho$ and $\Sigma_Q;{}^2\lambda$, $\Sigma_Q;{}^4\lambda$) may mix even in the heavy quark limit, because the light quark spin-spin force is still alive in this limit. For intermediate heavy quark masses, all these states may mix and the wave functions of energy eigenstates show how the mixings change as the heavy quark mass increases.

A similar analysis can be done for other heavy quark baryons. We tabulate, in Table 5.6, the λ- and ρ-modes classification of the P-wave heavy quark baryons and their quantum numbers in the Jacobi coordinate channel 3.

In the heavy quark limit, $m_Q \to \infty$, HQS symmetry becomes exact, where the spin degeneracy of

$J = j \pm 1/2$ appears. In this limit, the light component $\boldsymbol{j} = \boldsymbol{J} - \boldsymbol{s}_Q$ and the heavy quark spin $\boldsymbol{s_Q}$ are conserved independently, $[H, \boldsymbol{s_Q}] = 0 \to [H, \boldsymbol{J} - \boldsymbol{s_Q}] = [H, \boldsymbol{j}] = 0$. The basis in which j becomes diagonal can be written in terms of the Jacobi-coordinate basis states Eq.(5.13) for the channel $c = 3$ as

$$\begin{aligned}\Psi(qqQ; j; J) &= [[\chi_{1/2}(q)\chi_{1/2}(q)]_s \Phi_{\ell L I}]_j \chi_{1/2}(Q)]_J \\ &= \sum_S (-)^{(s+S+1/2)} \sqrt{(2S+1)(2j+1)} \left\{ \begin{array}{ccc} 1/2 & s & S \\ I & J & j \end{array} \right\} [X_{S,s} \otimes \Phi_{I\ell L}]_J \end{aligned} \tag{5.37}$$

flavor	ℓ	L	I	s	S	mode	J
Λ_Q	0	1	1	0	1/2	$^2\lambda$	$1/2^-, 3/2^-$
	1	0	1	1	1/2	$^2\rho$	$1/2^-, 3/2^-$
	1	0	1	1	3/2	$^4\rho$	$1/2^-, 3/2^-, 5/2^-$
Σ_Q	0	1	1	1	1/2	$^2\lambda$	$1/2^-, 3/2^-$
	0	1	1	1	3/2	$^4\lambda$	$1/2^-, 3/2^-, 5/2^-$
	1	0	1	0	1/2	$^2\rho$	$1/2^-, 3/2^-$
Ξ_Q	0	1	1	0	1/2	$^2\lambda$	$1/2^-, 3/2^-$
	1	0	1	1	1/2	$^2\rho$	$1/2^-, 3/2^-$
	1	0	1	1	3/2	$^4\rho$	$1/2^-, 3/2^-, 5/2^-$
	0	1	1	1	1/2	$^2\lambda$	$1/2^-, 3/2^-$
	0	1	1	1	3/2	$^4\lambda$	$1/2^-, 3/2^-, 5/2^-$
	1	0	1	0	1/2	$^2\rho$	$1/2^-, 3/2^-$
Ξ_{QQ}	0	1	1	1	1/2	$^2\lambda$	$1/2^-, 3/2^-$
	0	1	1	1	3/2	$^4\lambda$	$1/2^-, 3/2^-, 5/2^-$
	1	0	1	0	1/2	$^2\rho$	$1/2^-, 3/2^-$
Ω_{QQ}	0	1	1	1	1/2	$^2\lambda$	$1/2^-, 3/2^-$
	0	1	1	1	3/2	$^4\lambda$	$1/2^-, 3/2^-, 5/2^-$
	1	0	1	0	1/2	$^2\rho$	$1/2^-, 3/2^-$
Ω_{QQQ}	0	1	1	1	1/2	$^2\lambda$	$1/2^-, 3/2^-$
	1	0	1	0	1/2	$^2\rho$	$1/2^-, 3/2^-$

Table 5.6: The λ- and ρ-mode assignments of the P-wave excitations of Λ_Q, Σ_Q, Ξ_Q, Ξ_{QQ}, Ω_{QQ} and Ω_{QQQ}. The quantum numbers are given in the Jacobi coordinate channel 3.

5.2 Numerical method

In this section, we explain the numerical method we use in our work. We employ the Gaussian Ecpansion Method (GEM) , originally proposed by Kamimura [57], which is based on the Rayleigh-Ritz variational principle. The method we introduce here is widely applied to many body system such as nuclear many-body system [58–62] and many-body quark systems [22, 63–66]. It is known empirically that the GEM is one of the most accurate calculation methods for solving many-body Schrodinger equation. Numerical method is important for an actual calculation, but is less related to the physics. Therefore, we mention

numerical method briefly and do not touch its detail in this section.

5.2.1 Rayleigh-Ritz variational principle

We assume H is the Hamiltonian of many body quantum system, E_0 denotes the energy of the ground state and Ψ is a trial function. Then, the following equation is satisfied in general:

$$E_0 \leqq \frac{\langle \Psi \,|\, H \,|\, \Psi \rangle}{\langle \Psi \,|\, \Psi \rangle}. \tag{5.38}$$

This is the well known Rayleigh-Ritz variational principle. Eq.(5.38) gives an approximate solution, but it is not sufficient because of the following two reasons: (i) excited states are not obtained from Eq.(5.38) (ii) the mixing among different channels is not taken into account. Hence, E_0 obtained from Eq.(5.38) is possible to be far from exact solution.

Excited states and the mixing among the states can be taken into account by introducing N *linearly independent* bases in the trial function:

$$|\Psi\rangle = \sum_{n=1}^{N} A_n \,|\psi_n\rangle \tag{5.39}$$

where A_n is a complex number. After we apply variational principle with this trial function, namely we consider the condition that functional $E[\Psi]$ take a minimum value for Ψ:

$$\frac{\partial}{\partial A_m}\left[\frac{\langle \Psi \,|\, H \,|\, \Psi \rangle}{\langle \Psi \,|\, \mathbf{1} \,|\, \Psi \rangle}\right] = 0 \quad \frac{\partial}{\partial A_m^*}\left[\frac{\langle \Psi \,|\, H \,|\, \Psi \rangle}{\langle \Psi \,|\, \mathbf{1} \,|\, \Psi \rangle}\right] = 0 \quad (m = 1 \cdots N), \tag{5.40}$$

we obtain a generalized eigenvalue problem

$$\begin{pmatrix} H_{11} & H_{21} & \dots & H_{1n} \\ H_{21} & H_{22} & \dots & H_{2n} \\ \vdots & \vdots & \ddots & \vdots \\ H_{n1} & H_{n2} & \dots & H_{nn} \end{pmatrix} \begin{pmatrix} A_1 \\ A_2 \\ \vdots \\ A_n \end{pmatrix} = E \begin{pmatrix} N_{11} & N_{12} & \dots & N_{1n} \\ N_{21} & N_{22} & \dots & N_{2n} \\ \vdots & \vdots & \ddots & \vdots \\ N_{n1} & N_{n2} & \dots & N_{nn} \end{pmatrix} \begin{pmatrix} A_1 \\ A_2 \\ \vdots \\ A_n \end{pmatrix} \tag{5.41}$$

where

$$\{H_{ij}\} = \langle \psi_i \,|\, H \,|\, \psi_j \rangle\,, \quad \{N_{ij}\} = \langle \psi_i \,|\, \mathbf{1} \,|\, \psi_j \rangle\,. \tag{5.42}$$

5.2.2 Gaussian expansion method

When we solve the many-body Schroedinger equation, an important thing is to determine the bases functions. Even if we choose *bad* bases, we can reproduce the true wave function ideally with large enough N. However, it is practically impossible to take such a large N. Although we can mathematically solve variational problem even if some two bases are linear dependence, it is known that the numerical calculation

is collapse if some two bases are approximately linear dependence. As N increase, some basis functions show approximate linear dependence and the computation fail at some N. In that sense, N is limited and we need a *good* bases to calculate accurately. It is much difficult, or almost impossible, to determine good bases with no any information. Yet we have already had several information of the physical wave function: (i) angular part should be the spherical harmonics, $Y_{lm}(\theta,\phi)$, if potential satisfy $V(\boldsymbol{r}) = V(|\boldsymbol{r}|)$ (ii) it is a smooth function and in a long range, it exponentially decrease and is close to 0 (iii) $\Psi(\boldsymbol{r}=\boldsymbol{0}) = 0$ except for S-wave states.

Now, we consider two-body cases as example. From the above discussion, one notices that the following form is one of the reasonable choices of basis functions:

$$\psi_{nlm}(\boldsymbol{r}) = N_{n,lm} r^l e^{-\nu_n r^2} Y_{lm}(\theta,\phi) \tag{5.43}$$

where $N_{n,lm}$ is a normalization constant and ν_n is a variational parameter which is determined so as to minimize the energy and we choose ν_n as geometric progression:

$$\nu_n = 1/r_n^2, \quad r_n = r_1 a^{n-1} \text{ (n = 1, ..., N)}. \tag{5.44}$$

This choice is one of better ways to reproduce the short range strong correlation between particles and the long range tail of the wave function. The method using the bases of Eq.(5.43) for a trial function is called *Gaussian Expansion Method* (GEM).

The matrix elements which is defined in Eq.(5.42) is calculated straightforwardly and one obtain

$$\begin{aligned} N_{ij} &= \langle \psi_i \,|\, \mathbf{1} \,|\, \psi_j \rangle = \int d\boldsymbol{r} d\boldsymbol{r'} \langle \psi_i \,|\, \boldsymbol{r} \rangle \left\langle \boldsymbol{r} \,\middle|\, \boldsymbol{r'} \right\rangle \left\langle \boldsymbol{r'} \,\middle|\, \psi_j \right\rangle \\ &= \int d\boldsymbol{r} d\boldsymbol{r'} \psi_i^*(\boldsymbol{r}) \delta^3(\boldsymbol{r}-\boldsymbol{r'}) \Psi_j(\boldsymbol{r'}) \\ &= \left(\frac{2\sqrt{\nu_i \nu_j}}{\nu_i + \nu_j} \right)^{l+\frac{3}{2}}, \end{aligned} \tag{5.45}$$

$$\begin{aligned} T_{ij} &= \left\langle \psi_i \,\middle|\, \hat{T} \,\middle|\, \psi_j \right\rangle \\ &= \int d\boldsymbol{r} \psi_i^*(\boldsymbol{r}) \left[-\frac{1}{2\mu} \left(\frac{1}{r^2} \frac{\partial}{\partial r} r^2 \frac{\partial}{\partial r} - \frac{\hat{L}^2}{r^2} \right) \right] \psi_j(\boldsymbol{r'}) \\ &= \frac{1}{\mu} \frac{(2l+3)\nu_i \nu_j}{\nu_i + \nu_j} N_{ij}, \end{aligned} \tag{5.46}$$

$$\begin{aligned} V_{ij} &= \left\langle \psi_i \,\middle|\, \hat{V} \,\middle|\, \psi_j \right\rangle \\ &= \int d\boldsymbol{r} \psi_i^*(\boldsymbol{r}) V(\boldsymbol{r}) \psi_j(\boldsymbol{r}) \\ &= N_{i,lm} N_{j,lm} \int_0^\infty dr r^{2l+2} e^{-(\nu_i+\nu_j)r^2} V(\boldsymbol{r}) \end{aligned} \tag{5.47}$$

where $\hat{T}$ is the kinetic energy part of the Hamiltonian and $\hat{V}$ is the potential energy part of the Hamiltonian, i.e. $H_{ij} = T_{ij} + V_{ij}$.

Numerical calculation of three-body systems is formulated in a similar way, this is to say, we prepare the Gaussian type bases functions which has been already given in Eq.(5.18), (5.19) and calculate matrix elements as two body case. However, transformation between channels, which is needed to calculate three body matrix elements, leads to the complexity of whole calculation especially when the interaction become complicated. To avoid them, we apply the computational method using $Infinitesimally-Shifted\ Gaussian\ bases\ functions$ (ISG) which is proposed by Hiyama and Kamimura [56], which is the powerful method to calculate many body system in a more simple way. We introduce ISG in the next subsection.

5.2.3 Infinitesimally-Shifted Gaussian bases functions (ISG)

The basic concept is that we rewrite the basis function given in Eq.(5.43) in terms of pure Gaussian functions without r^l and $Y_{lm}(\hat{\boldsymbol{r}})$ in order to simplify the calculation and make the computation faster. To see that it is possible, we consider one-body Gaussian function, ze^{-ar^2}, as a most simple example. ze^{-ar^2} can be rewritten into pure Gaussian form as follows:

$$ze^{-ar^2} = \lim_{\epsilon\to 0} \frac{1}{4\epsilon a} e^{-a(x^2+y^2)}[e^{-a(z-\epsilon)^2} - e^{-a(z+\epsilon)^2}]. \tag{5.48}$$

Eq.(5.48) is generalized to the following form:

$$(\boldsymbol{c}\cdot\boldsymbol{r})^n e^{-ar^2} = \lim_{\epsilon\to 0} \left(\frac{n}{4\epsilon a}\right) \left[e^{-\frac{a}{n}(\boldsymbol{r}-\epsilon\boldsymbol{c})^2} - e^{-\frac{a}{n}(\boldsymbol{r}+\epsilon\boldsymbol{c})^2}\right]^n. \tag{5.49}$$

where $\boldsymbol{c}$ is an arbitrary complex vector.

The $r^l Y_{lm}(\theta,\phi)$ part of Gaussian bases function given in Eq.(5.43) can be expanded in the form of a polynomial as follows:

$$\begin{aligned} r^l Y_{lm}(\theta,\phi) &= \left[\frac{(2l+1)!(l-m)!}{4\pi(l+m)!}\right]^{\frac{1}{2}} r^l P_l^m(\cos\theta) e^{im\phi} \\ &= \left[\frac{(2l+1)!(l-m)!}{4\pi(l+m)!}\right]^{\frac{1}{2}} \frac{(l+m)!}{2^m} r^l (\sin\theta e^{i\phi})^m \sum_{j=0}^{\left[\frac{l-m}{2}\right]} \frac{(-1)^j \cos^{l-m-2j}\theta \sin^{2j}\theta}{4^j j!(m+j)!(l-m-2j)!} \\ &= \sum_j^{\left[\frac{l-m}{2}\right]} A_{lm,j} z^{l-m-2j}(x+iy)^{m+j}(x-iy)^j \end{aligned} \tag{5.50}$$

where

$$A_{lm,j} = \left[\frac{(2l+1)!(l-m)!}{4\pi(l+m)!}\right]^{\frac{1}{2}} \frac{(l+m)!}{2^m} \frac{(-1)^j}{4^j j!(m+j)!(l-m-2j)!}. \tag{5.51}$$

In order to transform Eq.(5.50) into a Gaussian form as Eq.(5.49), we define a shift vector $\boldsymbol{a}$:

$$\boldsymbol{a}\cdot\boldsymbol{r} = \begin{cases} z \ \text{ for } \ \boldsymbol{a}=\boldsymbol{a}_z \equiv (0,0,1) \\ x+iy \ \text{ for } \ \boldsymbol{a}=\boldsymbol{a}_{xy} \equiv (1,i,0) \\ x-iy \ \text{ for } \ \boldsymbol{a}=\boldsymbol{a}^\star_{xy} \equiv (1,-i,0). \end{cases} \tag{5.52}$$

From the above discussion, one notice that Gaussian bases function in Eq.(5.43) is rewritten into a pure Gaussian form:

$$\begin{aligned}
\psi_{nlm}(\boldsymbol{r}) &= N_{n,lm} r^l e^{-\nu_n r^2} Y_{lm}(\theta,\phi) \\
&= N_{n,lm} \lim_{\epsilon\to 0} \left(\frac{l}{4\nu\epsilon}\right)^l \sum_j^{\left[\frac{l-m}{2}\right]} A_{lm,j} \left[e^{\frac{\nu}{l}(\boldsymbol{r}-\epsilon\boldsymbol{a}_z)^2} - e^{\frac{\nu}{l}(\boldsymbol{r}+\epsilon\boldsymbol{a}_z)^2}\right]^{l-m-2j} \\
&\times \left[e^{\frac{\nu}{l}(\boldsymbol{r}-\epsilon\boldsymbol{a}_{xy})^2} - e^{\frac{\nu}{l}(\boldsymbol{r}+\epsilon\boldsymbol{a}_{xy})^2}\right]^{m+j} \left[e^{\frac{\nu}{l}(\boldsymbol{r}-\epsilon\boldsymbol{a}^\star_{xy})^2} - e^{\frac{\nu}{l}(\boldsymbol{r}+\epsilon\boldsymbol{a}^\star_{xy})^2}\right]^{j} \\
&= N_{n,lm} \lim_{\epsilon\to 0} \left(\frac{l}{4\nu\epsilon}\right)^l \sum_j^{\left[\frac{l-m}{2}\right]} A_{lm,j} r^{-\nu r^2} \sum_{s=0}^{l-m-2j} \begin{pmatrix} l-m-2j \\ s \end{pmatrix} e^{2(2s-l+m+2j)\epsilon\nu\boldsymbol{a}_z\cdot\boldsymbol{r}/l} \\
&\times \sum_{t=0}^{m+j} \begin{pmatrix} m+j \\ t \end{pmatrix} e^{2(2t-m-j)\epsilon\nu\boldsymbol{a}_{xy}\cdot\boldsymbol{r}/l} \sum_{u=0}^{j} \begin{pmatrix} j \\ u \end{pmatrix} e^{2(2u-j)\epsilon\nu\boldsymbol{a}^\star_{xy}\cdot\boldsymbol{r}/l} \\
&= N_{n,lm} \lim_{\epsilon\to 0} \left(\frac{l}{4\nu\epsilon}\right)^l \sum_j^{\left[\frac{l-m}{2}\right]} A_{lm,j} \sum_{s=0}^{p}\sum_{t=0}^{q}\sum_{u=0}^{j} \begin{pmatrix} p \\ s \end{pmatrix}\begin{pmatrix} q \\ t \end{pmatrix}\begin{pmatrix} j \\ u \end{pmatrix} e^{-\nu(\boldsymbol{r}-\epsilon\boldsymbol{D})^2} \\
&\equiv N_{n,lm} \lim_{\epsilon\to 0} \frac{1}{(\nu\epsilon)^l} \sum_{k=1}^{k_{\max}} C_{lm,k} e^{-\nu(\boldsymbol{r}-\epsilon\boldsymbol{D}_{lm,k})^2}
\end{aligned} \tag{5.53}$$

where

$$p = l-m-2j, \quad q = l+m \tag{5.54}$$

$$\boldsymbol{D} = \frac{2}{l}\left[(2s-p)\boldsymbol{a}_z + (2t-q)\boldsymbol{a}_{xy} + (2u-j)\boldsymbol{a}^\star_{xy}\right]. \tag{5.55}$$

In order to see how the calculation of matrix element with ISG function is performed, we consider Gaussian type potential, i.e. $V(\boldsymbol{r}) = v_0 e^{-\mu r^2}$ for example. The matrix elements of the Gaussian type potential by

using ISG functions is given by

$$V_{nn'} = \left\langle \psi_{nlm} \left| \hat{V} \right| \psi_{n'lm} \right\rangle = \int d\boldsymbol{r} d\boldsymbol{r'} \psi^*_{nlm}(\boldsymbol{r}) v_0 e^{-\mu r^2} \psi_{nlm}(\boldsymbol{r'})$$
$$= N_{nl} N_{n'l} \lim_{\epsilon,\epsilon' \to 0} \frac{1}{(\nu_n \epsilon)^l} \frac{1}{(\nu'_n \epsilon')^l} \sum_{k,k'} C^\star_{lm,k} C_{lm,k} \int d\boldsymbol{r} e^{-\nu(\boldsymbol{r}-\epsilon \boldsymbol{D}_{lm,k})^2} e^{-\nu(\boldsymbol{r}-\epsilon \boldsymbol{D}_{lm,k'})^2} v_0 e^{-\mu r^2}$$
$$= N_{nl} N_{n'l} \lim_{\epsilon,\epsilon' \to 0} \frac{1}{(\nu_n \epsilon)^l} \frac{1}{(\nu'_n \epsilon')^l} \sum_{k,k'} C^\star_{lm,k} C_{lm,k} \left(\frac{\pi}{\nu_n + \nu'_n + \mu} \right)^{\frac{3}{2}} \exp \left[\frac{2\nu_n \nu'_n \epsilon \epsilon' \boldsymbol{D}^\star_{lm,k} \boldsymbol{D}^\star_{lm,k'}}{\nu_n + \nu'_n} \right]. \quad (5.56)$$

Since only the terms which have $(\epsilon\epsilon')^l$ survive after the limit is taken, one gets

$$V_{nn'} = N_{nl} N_{n'l} \lim_{\epsilon,\epsilon' \to 0} \frac{1}{(\nu_n \epsilon)^l} \frac{1}{(\nu'_n \epsilon')^l} \sum_{k,k'} C^\star_{lm,k} C_{lm,k} \left(\frac{\pi}{\nu_n + \nu'_n + \mu} \right)^{\frac{3}{2}} \frac{1}{(\nu_n + \nu'_n)^l} \frac{1}{l!} (2\nu_n \nu'_n \epsilon \epsilon' \boldsymbol{D}^\star_{lm,k} \boldsymbol{D}^\star_{lm,k'})^l$$
$$= N_{nl} N_{n'l} \sum_{k,k'} C^\star_{lm,k} C_{lm,k} \left(\frac{\pi}{\nu_n + \nu'_n + \mu} \right)^{\frac{3}{2}} \frac{1}{(\nu_n + \nu'_n)^l} \frac{2^l}{l!} (\boldsymbol{D}^\star_{lm,k} \boldsymbol{D}^\star_{lm,k'})^l. \quad (5.57)$$

5.3 Results and Discussion

5.3.1 Energy spectra of single-heavy systems

We first discuss energy spectra of the single-charmed baryons, Λ_c, Σ_c and Ω_c. The energies of the charmed baryons are listed in Table 5.7 and are illustrated in Fig 5.4. The mass of the lowest Λ_c is used to fix the charm quark mass m_c. The energy differences among the lowest $\Lambda_c(1/2^+)$, $\Sigma_c(1/2^+)$, $\Sigma_c{}^*(3/2^+)$ are given by $\Sigma_c(1/2^+)-\Lambda_c(1/2^+)$=175 MeV (exp. 170 MeV), $\Sigma_c{}^*(3/2^+)-\Sigma_c(1/2^+)$=71 MeV (exp. 65 MeV), which agree very well to the experimental data. The mass of the other single-charmed baryons are also well reproduced within 50 MeV deviation.

The energies of the lowest $\Lambda_c(1/2^-)$ and $\Lambda_c(3/2^-)$ states are consistent with the experimental data within 40 MeV, while the spin-orbit splitting between them is smaller than the observed ones. This tendency is also seen in the previous quark model calculations. One possible cause for the discrepancy is the coupling to the meson-baryon scattering states. As in the case of $\Lambda(1405)$, $\Lambda_c(2595)$ and $\Lambda_c(2628)$ may couple to DN and D^*N states [67] [68]. We discuss the meson-baryon coupling effect on the three quark state in chapter 5.

There are two observed states, $\Lambda_c(2940)$ and $\Sigma_c(2800)$, whose spin and parity have not been assigned. The present calculation indicates that $\Lambda_c(2940)$ can be assigned to one of the following states, $3/2^+_1$ (2920MeV), $5/2^-_1$ (2960MeV), $1/2^-_2$ (2890MeV), $1/2^-_3$ (2933MeV), $3/2^-_2$ (2917MeV), and $3/2^-_3$ (2956MeV), while $\Sigma_c(2800)$ may be assigned to one of $1/2^-_1$ (2802MeV), $3/2^-_1$ (2807MeV), $1/2^-_2$ (2826MeV), $3/2^-_2$ (2837MeV) and $5/2^-_1$ (2839MeV). Here, J^P_n denotes the n-th J^P state. Further experimental information,

such as decay branching ratios and production rates, will be necessary to determine the quantum numbers of these states.

For $S = -2$ baryons, the lowest states of $\Omega_c(1/2^+)$ and $\Omega_c(3/2^+)$ have been experimentally observed. We underestimate the mass difference between them by about 20 MeV.

The masses of the single-bottom baryons are listed in Table 5.8 and illustrated in Fig 5.5. The ground state Λ_b is fitted to the experimental data of Particle Data Group . The mass differences among Λ_b, Σ_b, and $\Sigma_b{}^*$ are $\Sigma_b(1/2^+)-\Lambda_b(1/2^+)$=188MeV, $\Sigma_b{}^*(3/2^+)-\Sigma_b(1/2^+)$=21 MeV experimentally, while our calculation gives $\Sigma_b(1/2+)-\Lambda_b(1/2^+)$=195MeV, and $\Sigma_b{}^*(3/2^+)-\Sigma_b(1/2^+)$=22 MeV. Thus, we find that the low lying positive-parity states are reproduced within 10 MeV deviation.

The negative parity Λ_b states, $\Lambda_b(5912)$ and $\Lambda_b(5920)$, have been discovered recently. Their mass difference is about 8 MeV in experiment while it is 1 MeV in our prediction. For $S = -2$ bottom baryons, $\Omega_b(1/2^+)$, our estimate of the mass is 6076 MeV, which is higher than the experimental value, 6015 MeV.

(a)Λ_c

J^P	Theory [MeV]	Exp. [MeV]
$\frac{1}{2}^+$	2285	2285
	2857	
	3123	
$\frac{3}{2}^+$	2920	
	3175	
	3191	
$\frac{5}{2}^+$	2922	2881
	3202	
	3230	
$\frac{1}{2}^-$	2628	2595
	2890	
	2933	
$\frac{3}{2}^-$	2630	2628
	2917	
	2956	
$\frac{5}{2}^-$	2960	
	3444	
	3491	

(b)Σ_c

J^P	Theory [MeV]	Exp. [MeV]
$\frac{1}{2}^+$	2460	2455
	3029	
	3103	
$\frac{3}{2}^+$	2523	2518
	3065	
	3094	
$\frac{5}{2}^+$	3099	
	3114	
	3191	
$\frac{1}{2}^-$	2802	
	2826	
	2909	
$\frac{3}{2}^-$	2807	
	2837	
	2910	
$\frac{5}{2}^-$	2839	
	3316	
	3521	

(c) Ω_c

J^P	Theory [MeV]	Exp. [MeV]
$\frac{1}{2}^+$	2731	2698
	3227	
	3292	
$\frac{3}{2}^+$	2779	2768
	3257	
	3285	
$\frac{5}{2}^+$	3288	
	3299	
	3359	
$\frac{1}{2}^-$	3030	
	3048	
	3110	
$\frac{3}{2}^-$	3033	
	3056	
	3111	
$\frac{5}{2}^-$	3057	
	3477	
	3620	

Table 5.7: Calculated energy spectra and experimental result of Λ_c, Σ_c, Ω_c

5.3.2 Energy spectra of double-heavy baryon systems

TABLE 5.9, 5.10 and Figs.5.6 and 5.7 show the calculated energy spectra and experimental data for double-heavy baryons. Lattice QCD [69] [70] and quark models [15] [71] predicted the masses of double-heavy baryons and variations among the model calculations are large, compared to those in the single-heavy baryons.

The calculated mass of the lowest Ξ_{cc} state is 3685 MeV, which is much higher than the experimental

(a) Λ_b

J^P	Theory [MeV]	Exp. [MeV]
$\frac{1}{2}^+$	5618	5624
	6153	
	6467	
$\frac{3}{2}^+$	6211	
	6488	
	6511	
$\frac{5}{2}^+$	6212	
	6530	
	6539	
$\frac{1}{2}^-$	5938	5912
	6236	
	6273	
$\frac{3}{2}^-$	5939	5920
	6273	
	6285	
$\frac{5}{2}^-$	6289	
	6739	
	6786	

(b)Σ_b

J^P	Theory [MeV]	Exp. [MeV]
$\frac{1}{2}^+$	5823	5815
	6343	
	6395	
$\frac{3}{2}^+$	5845	5835
	6356	
	6393	
$\frac{5}{2}^+$	6397	
	6402	
	6505	
$\frac{1}{2}^-$	6127	
	6135	
	6246	
$\frac{3}{2}^-$	6132	
	6141	
	6246	
$\frac{5}{2}^-$	6144	
	6592	
	6834	

(c) Ω_b

J^P	Theory [MeV]	Exp. [MeV]
$\frac{1}{2}^+$	6076	6048
	6517	
	6561	
$\frac{3}{2}^+$	6094	
	6528	
	6559	
$\frac{5}{2}^+$	6561	
	6566	
	6657	
$\frac{1}{2}^-$	6333	
	6340	
	6437	
$\frac{3}{2}^-$	6336	
	6344	
	6438	
$\frac{5}{2}^-$	6345	
	6728	
	6919	

Table 5.8: Calculated energy spectra and experimental result of Λ_b, Σ_b, Ω_b

(a) Ξ_{cc}

J^P	Theory [MeV]	Exp. [MeV]	[69]	[15]
$\frac{1}{2}^+$	3685	3512	3603±15±16	3674
	4079			4029
	4159			
$\frac{3}{2}^+$	3754		3706±22±16	3753
	4114			4042
	4131			
$\frac{5}{2}^+$	4115			4047
	4164			4091
	4348			
$\frac{1}{2}^-$	3947			3910
	4135			4074
	4149			
$\frac{3}{2}^-$	3949			3921
	4137			4078
	4159			
$\frac{5}{2}^-$	4163			4092
	4488			
	4534			

(b)Ξ_{bb}

J^P	Theory [MeV]	[15] [MeV]
$\frac{1}{2}^+$	10314	10340
	10571	
	10612	
$\frac{3}{2}^+$	10339	10367
	10592	
	10593	
$\frac{5}{2}^+$	10592	10676
	10613	
	10809	
$\frac{1}{2}^-$	10476	10493
	10703	
	10740	
$\frac{3}{2}^-$	10476	10495
	10704	
	10742	
$\frac{5}{2}^-$	10759	10713
	10973	
	11004	

Table 5.9: Calculated energy spectra and experimental result of Ξ_{cc} and Ξ_{bb}

(a) Ω_{cc}

J^P	Theory [MeV]	[69]	[15]
$\frac{1}{2}^+$	3832	3704±5±16	3815
	4227		4180
	4295		
$\frac{3}{2}^+$	3883	3779±6±17	3876
	4263		4188
	4265		
$\frac{5}{2}^+$	4264		4202
	4299		4232
	4410		
$\frac{1}{2}^-$	4086		4046
	4199		4135
	4210		
$\frac{3}{2}^-$	4086		4052
	4201		4140
	4218		
$\frac{5}{2}^-$	4220		4152
	4555		
	4600		

(b)Ω_{bb}

J^P	Theory [MeV]	[15]
$\frac{1}{2}^+$	10447	10454
	10707	10693
	10744	
$\frac{3}{2}^+$	10467	10486
	10723	10721
	10730	
$\frac{5}{2}^+$	10729	10720
	10744	10734
	10937	
$\frac{1}{2}^-$	10607	10616
	10796	10763
	10803	
$\frac{3}{2}^-$	10608	10619
	10797	10765
	10805	
$\frac{5}{2}^-$	10808	10766
	11028	
	11059	

Table 5.10: Calculated energy spectra and experimental result of Ω_{cc} and Ω_{bb}

observations by SELEX [72], 3519 MeV. However, the other experimental searches by BARBAR [73], Belle [74] and LHCb [75], could not confirm this state. Our prediction is consistent with the recent lattice result as well as the other quark model calculations.

We predict that the lowest Ξ_{bb} state is $\Xi_{bb}(\frac{1}{2}^+)$=10314 MeV followed by $\Xi_{bb}(\frac{3}{2}^+)$=10339 MeV.

5.3.3 λ mode and ρ mode structures in heavy baryon systems

Now we compare the heavy baryon spectra for the strange sector and the heavier sector (c and b) and clarify the quark dynamics in the heavy baryon. Strange baryons are conventionally analyzed by the $SU(3)_f$ symmetry. When the strange quark is replaced by a heavier quark, c or b, we can study the dynamics of the two light quarks, which may be regarded as a diquark. From this point of view, one sees two distinct excitation modes, λ and ρ modes. The λ-mode state is composed of the $(qq)_{\ell=0}$ diquark with L=1 excitation relative to the heavy quark, Q, while the ρ-mode state has an excited diquark $(qq)_{\ell=1}$ in the $L=0$ orbit around Q.

As is discussed in Sec.I, the λ- and ρ-modes are largely mixed in the SU(3) limit in the light quark sector. This mixing is induced mainly by the spin-spin interaction. Because the spin dependent interaction for the heavy quark is weak, the λ- and ρ-modes are well separated for the charm and bottom baryons. Then, each P-wave state is dominated and characterized either by the λ-mode or ρ-mode.

In order to demonstrate these properties quantitatively, we change the heavy quark mass, m_Q, from 300 MeV to 6 GeV and analyze the excitation energies and wave functions. Fig. 5.12 shows the spectra

of Λ_Q and Σ_Q as functions of m_Q. One sees that the splitting between the 1st and 2nd $1/2^-$ state of Λ_Q increases rapidly from 100 MeV in the SU(3) limit to 300 MeV in the heavy quark limit when m_Q increases. This behavior is due to the $\lambda - \rho$ splitting as demonstrated by the harmonic osillator model (in Fig.3.5). Namely, the lowest state becomes dominated by the λ-mode as m_Q becomes large. This is confirmed in Fig.5.14, where the λ- and ρ-mode probabilities of the lowest $1/2^-$ state are plotted as functions of m_Q. One sees that the state is almost purely in the λ mode at $m_Q \geq 1.5$ GeV; the λ dominance is seen even at $m_Q = 510$ MeV. As is classified in TABLE 5.6, the quark model predicts seven P-wave Λ_Q excitations, $(1/2^-)^3$, $(3/2^-)^3$, $(5/2^-)$. They split into the $(1/2^-, 3/2^-)$ λ modes and $(1/2^-)^2$, $(3/2^-)^2$, $5/2^-$ ρ modes. In Fig. 5.12, one sees clear splitting ($\approx$350 MeV) of two low lying λ-modes and five higher ρ mode states.

The P-wave Σ_Q has also seven states in the quark model, $(1/2^-)^3$, $(3/2^-)^3$, $(5/2^-)$. One sees that they are classified into the $(1/2)^2$, $(3/2^-)^2$, $(5/2^-)$ λ modes and $(1/2^-, 3/2^-)$ ρ modes from Fig.5.12. The λ- and ρ- modes are separated more slowly than Λ_Q as m_Q increases, and the λ dominance is seen at $m_Q \geq 1750$ MeV. The difference comes from the interaction between light quarks which forms the diquark. The diquark in Σ_Q has spin 1 and the spin-spin interaction is repulsive for the λ mode, while the ρ mode has a diquark state of spin 0 and the spin-spin interaction is attractive. Therefore, the difference between the excitation energies of the two modes is small compared to Λ_Q. Thus, the splitting between the excitation energies of two modes is larger for Λ_Q and smaller for Σ_Q compared with the case in which there is no spin-spin force as we see in chapter.3. As a result, the change of the probability of two modes in the Σ_Q case is more slow than the Λ_Q case as shown in Fig.5.14.

In the case of double-heavy baryon, the λ-mode state is composed of the $(QQ)_{\ell=0}$ heavy diquark with the light quark q, while the ρ-mode state has the excited heavy diquark $(QQ)_{\ell=1}$ in the $L = 0$ orbit around q. The combinations of angular momentum are the same as the Σ_Q case which is shown in TABLE 5.6, but the behavior of λ- and ρ modes are different because Ξ_{QQ}, or Ω_{QQ} contains heavy diquark. As mentioned in chapter.3, ω_λ is larger than ω_ρ for the P wave double-heavy baryons and thus ρ modes are dominant. This is shown in Fig.5.13 and Fig.5.15. One sees that the $(1/2)^2$, $(3/2^-)^2$, $(5/2^-)$ λ modes and the $(1/2^-, 3/2^-)$ ρ modes split in the heavy quark region in Fig.5.13, and the ρ modes become dominant for the lowest states at $m_Q \geq m_c$ in Fig.5.15.

5.3.4 Heavy baryons in the heavy quark limit

In this subsection, we investigate the behavior of the single-heavy baryons in the heavy quark limit. We decompose the wave functions of the P-wave single-heavy baryons into the parts with different light spin component j as

$$\Phi^{J=1/2,M}_{\Lambda_Q}(\boldsymbol{\rho},\boldsymbol{\lambda}) = \phi^{J=1/2,M}_{\Lambda_Q,j=0}(\boldsymbol{\rho},\boldsymbol{\lambda}) + \phi^{J=1/2,M}_{\Lambda_Q,j=1}(\boldsymbol{\rho},\boldsymbol{\lambda}) \tag{5.58}$$

$$\Phi^{J=3/2,M}_{\Lambda_Q}(\boldsymbol{\rho},\boldsymbol{\lambda}) = \phi^{J=3/2,M}_{\Lambda_Q,j=1}(\boldsymbol{\rho},\boldsymbol{\lambda}) + \phi^{J=3/2,M}_{\Lambda_Q,j=2}(\boldsymbol{\rho},\boldsymbol{\lambda}) \tag{5.59}$$

$$\Phi^{J=1/2,M}_{\Sigma_Q}(\boldsymbol{\rho},\boldsymbol{\lambda}) = \phi^{J=1/2,M}_{\Sigma_Q,j=0}(\boldsymbol{\rho},\boldsymbol{\lambda}) + \phi^{J=1/2,M}_{\Sigma_Q,j=1}(\boldsymbol{\rho},\boldsymbol{\lambda}) \tag{5.60}$$

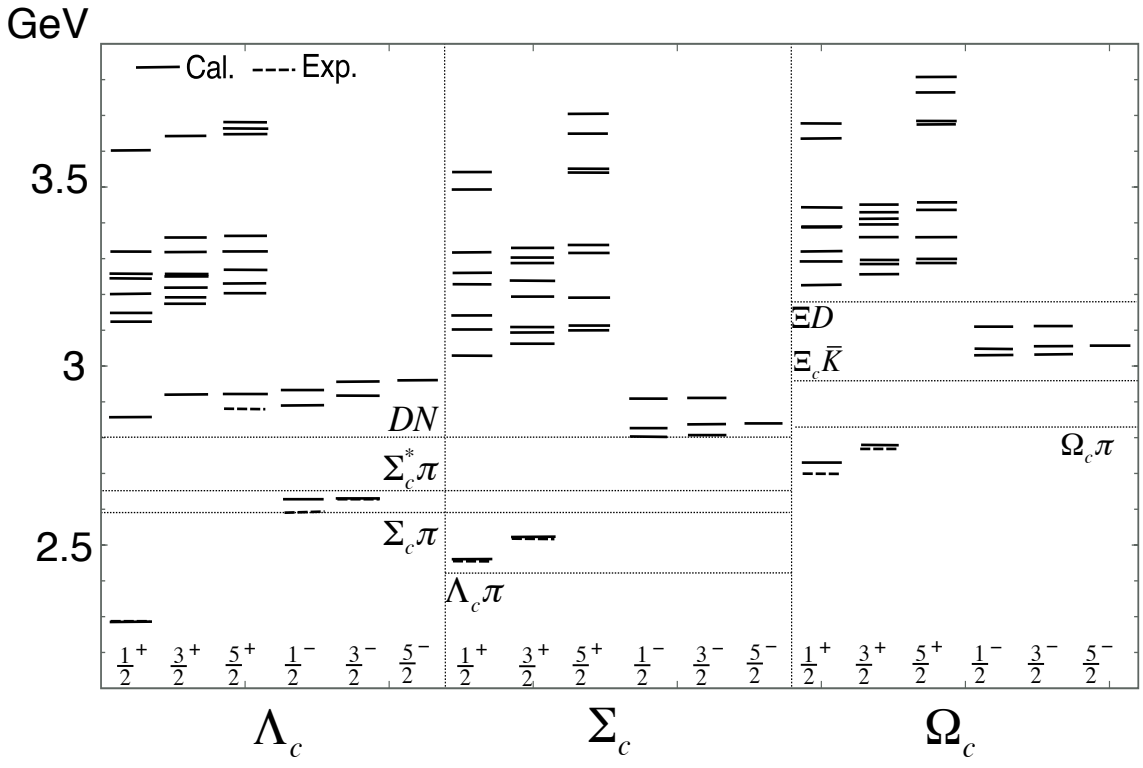

Figure 5.4: Calculated energy spectra of Λ_c, Σ_c, Ω_c for $1/2^+$, $3/2^+$, $5/2^+$, $1/2^-$, $3/2^-$, $5/2^-$(solid line) together with experimental data (dashed line). Several thresholds are also shown by doted line.

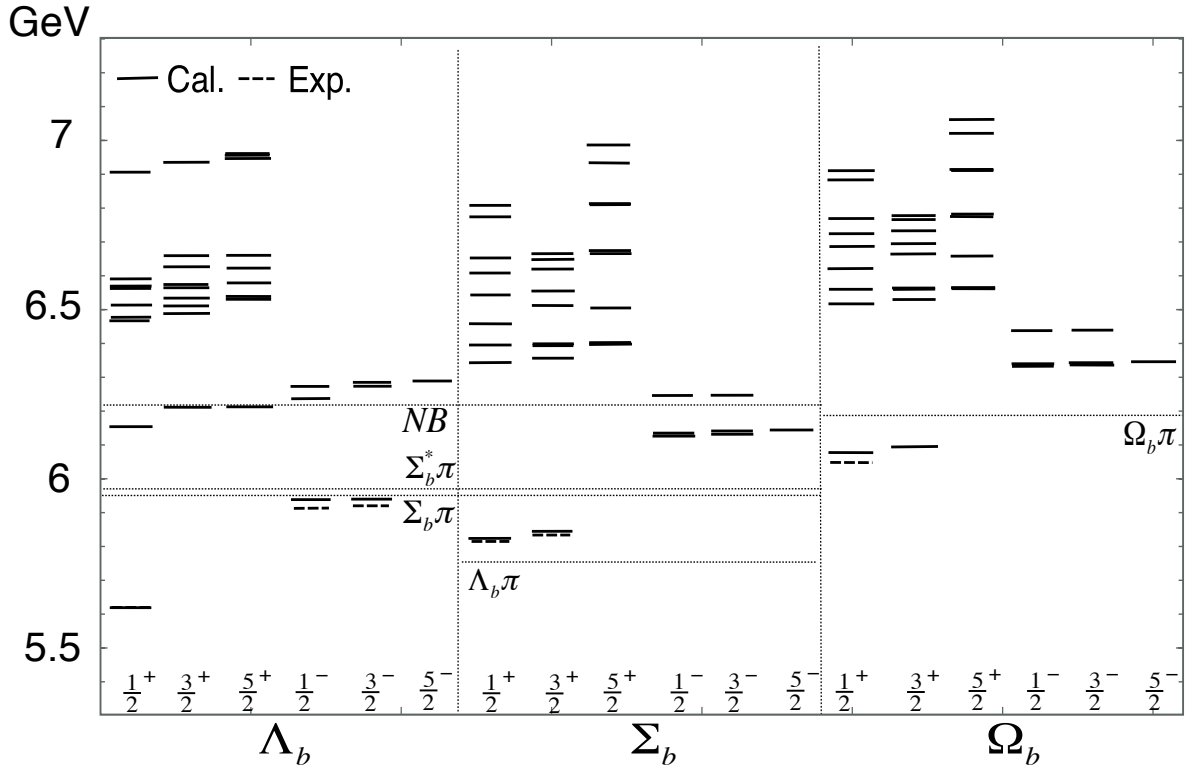

Figure 5.5: Calculated energy spectra of Λ_b, Σ_b, Ω_b for $1/2^+$, $3/2^+$, $5/2^+$, $1/2^-$, $3/2^-$, $5/2^-$ (solid line) together with experimental data(dashed line).Several thresholds are also shown by doted line.

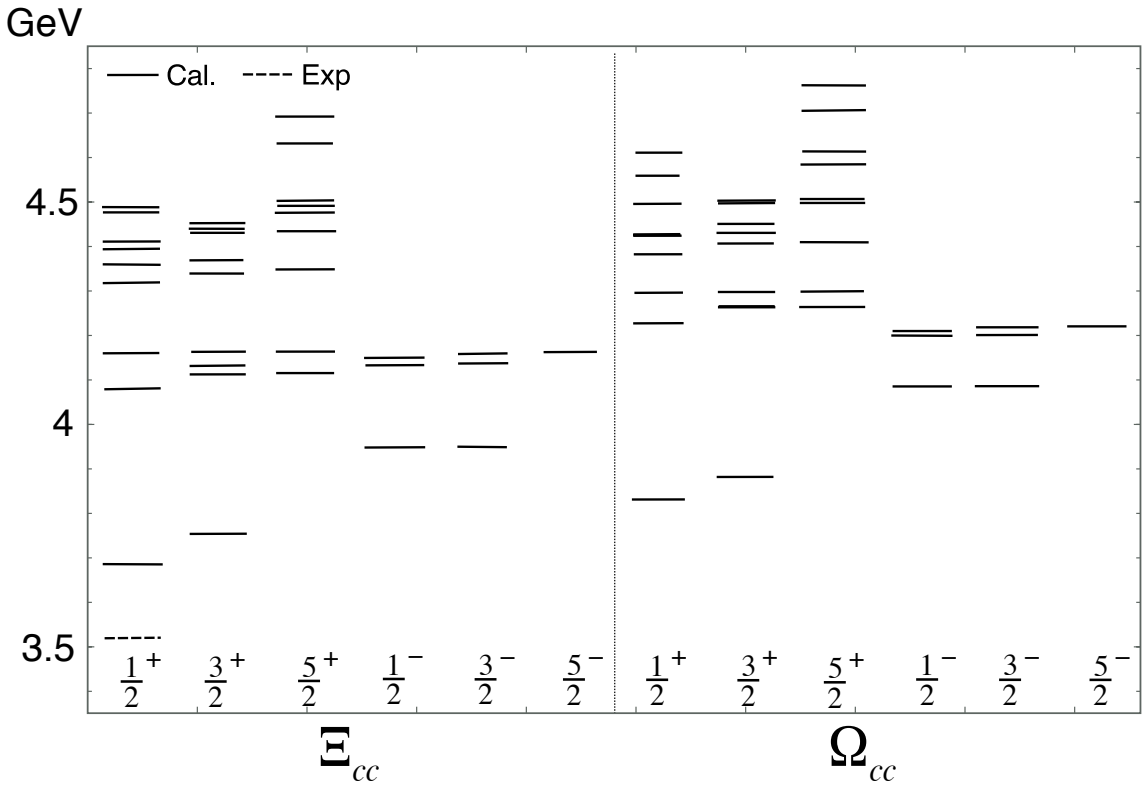

Figure 5.6: Calculated energy spectra of Ξ_{cc}, Ω_{cc} for $1/2^+$, $3/2^+$, $5/2^+$, $1/2^-$, $3/2^-$, $5/2^-$(solid line) together with experimental data (dashed line).

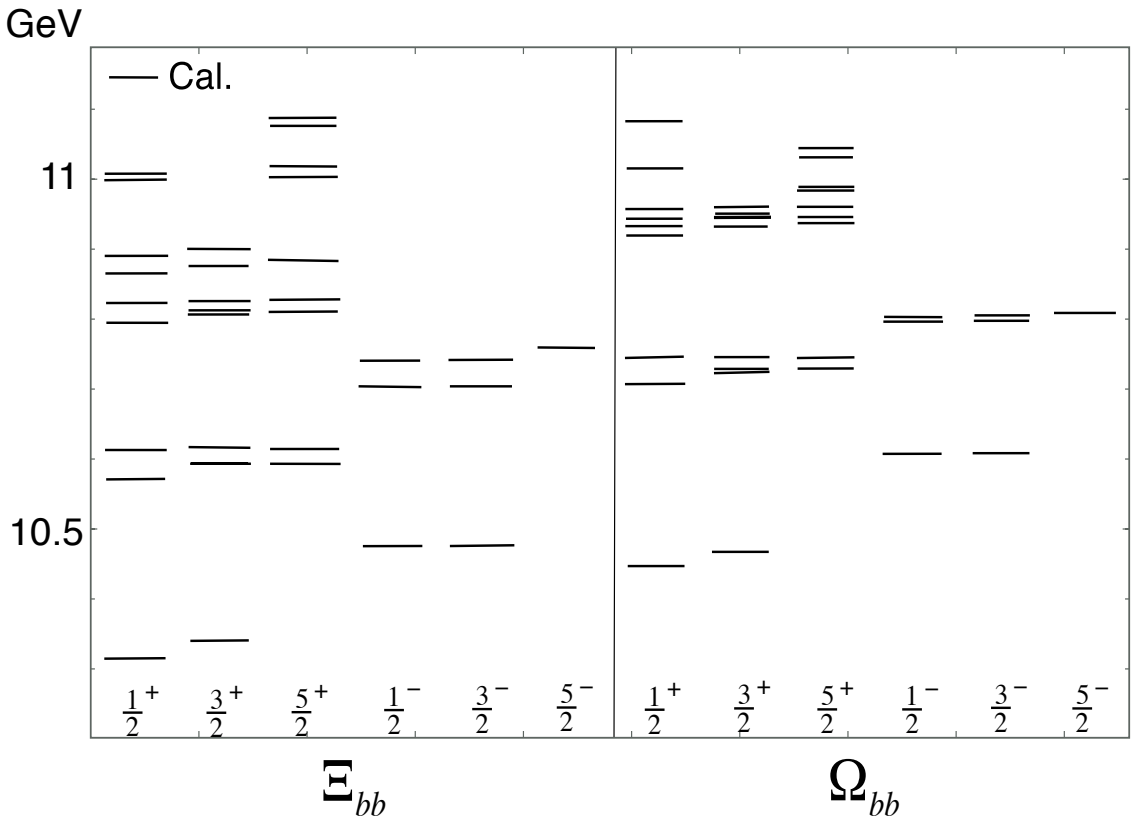

Figure 5.7: Calculated energy spectra of Ξ_{bb}, Ω_{bb} for $1/2^+$, $3/2^+$, $5/2^+$, $1/2^-$, $3/2^-$, $5/2^-$ (solid line) together with experimental data (dashed line).

$$\Phi^{J=3/2,M}_{\Sigma_Q}(\boldsymbol{\rho},\boldsymbol{\lambda}) \quad = \quad \phi^{J=3/2,M}_{\Sigma_Q,j=1}(\boldsymbol{\rho},\boldsymbol{\lambda}) + \phi^{J=3/2,M}_{\Sigma_Q,j=2}(\boldsymbol{\rho},\boldsymbol{\lambda}). \tag{5.61}$$

Here, we take into account only the channel $c = 3$ of the Jacobi coordinates, given in Fig.5.1. The relation between the representation Eq.(5.58)-(5.61) and Eq.(5.11) is shown in Appendix **??**. The heavy quark mass dependences of the probabilities of each j state are shown in the Figs.5.16-5.19 (See Appendix **??** for the definition). The mixings between $j = 0$ and $j = 1$ or $j = 1$ and $j = 2$ above 1 GeV are negligible for the first state of $\Lambda_Q(1/2^-)$ and $\Lambda_Q(3/2^-)$ and the third state of $\Sigma_Q(1/2^-)$ and $\Sigma_Q(3/2^-)$, which correspond to red lines in Figs 5.16-5.17 and green lines in Figs.5.18-5.19. This is because these states are isolated from the other states, as is shown in Fig.5.12. For the other state, two different j components (five λ-modes of Σ_Q and five ρ-modes of Λ_Q) still mix in the charm and bottom mass region, because they lie close to each other within 50 MeV (See Fig.5.12). Above m_Q =14 GeV, one sees no mixing between different j components. In summary, one finds that the second $1/2^-$ state of Λ_Q and the first $1/2^-$ state of $1/2^-$ of Σ_Q are the j=0 singlet state. All the other belong to doublets, $(1/2^-_1, 3/2^-_1)$, $(1/2^-_3, 3/2^-_2)$ and

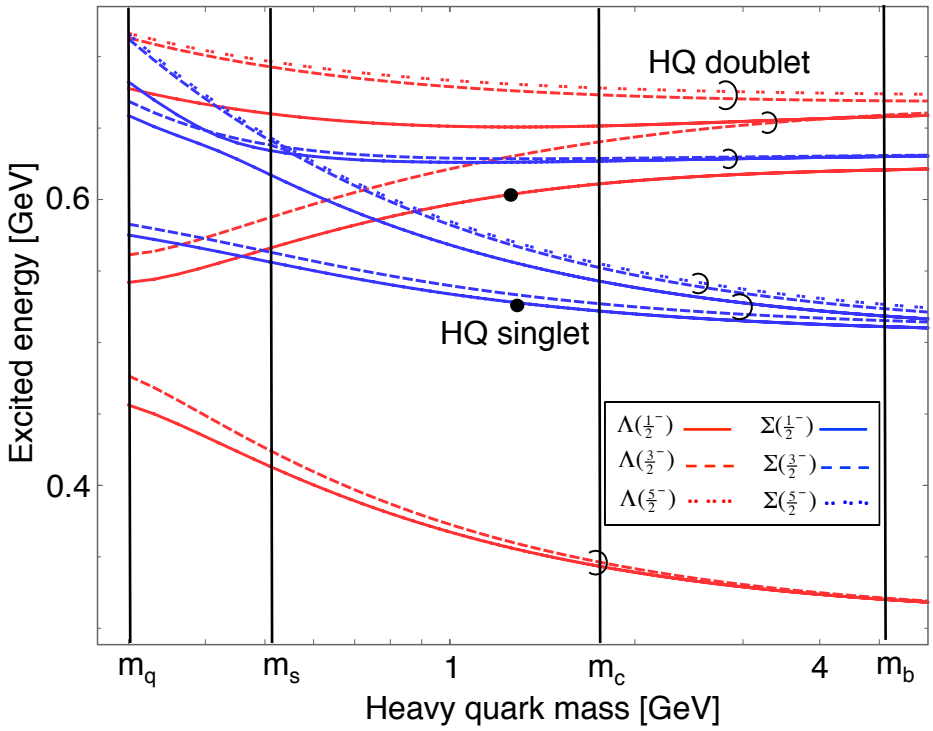

Figure 5.8: Heavy quark mass dependence of excited energy of first state, second state and third state for $1/2^-$(solid line), $3/2^-$(dashed line), $5/2^-$(twined line) of Λ_Q (red line) and Σ_Q (blue line). Bullet denote heavy quark singlet. The pair within a half circle denote heavy quark doublet.

$(3/2^-_3, 5/2^-_1)$ for Λ_Q and $(1/2^-_2, 3/2^-_1)$, $(3/2^-_2, 5/2^-_1)$ and $(1/2^-_3, 3/2^-_2)$ for Σ_Q, as is shown in Fig.5.12.

We next discuss the positive parity states. We focus on the first six positive parity state of single-heavy baryons, corresponding to the states below 3.0 GeV in the charm sector (See Fig.5.4).They consist of the S-wave ((L,ℓ)=(0,0)) component, the (1,1) component, the (2,0) component (ρ-mode) and the (0,2) component (λ-mode). Figs.5.20-5.25 show the probabilities of the each component in the total wave function. One sees that one component becomes dominant avove m_Q =1 GeV. The (0,0) component is dominant for $\Lambda_Q(1/2^+_1)$, $\Lambda_Q(1/2^+_2)$, $\Sigma_Q(1/2^+_1)$, $\Sigma_Q(1/2^+_2)$ and (2,0) component (λ-mode) is dominant for $\Lambda_Q(3/2^+_1)$, $\Lambda_Q(5/2^+_1)$ above 1 GeV (See Figs.5.20-5.25). The lowest six states in the heavy quark region can be written as follows.

$$\Phi_{\Lambda_Q}^{J_n=1/2_1,M}(\boldsymbol{\rho},\boldsymbol{\lambda}) \quad = \quad \phi_{\Lambda_Q,j=0}^{J_n=1/2^+_1,M}(\boldsymbol{\rho},\boldsymbol{\lambda}) \tag{5.62}$$

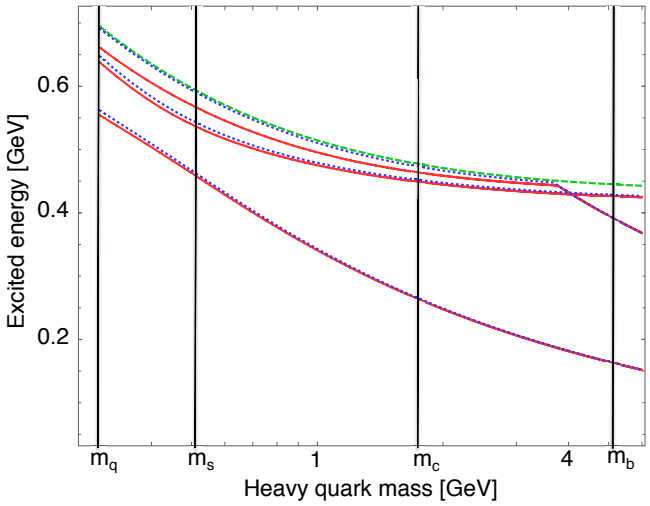

Figure 5.9: Heavy quark mass dependence of excited energy of first state, second state and third state for $1/2^-$(red solid line), $3/2^-$(blue dotted line), $5/2^-$(green dashed line) of Ξ_{QQ}.

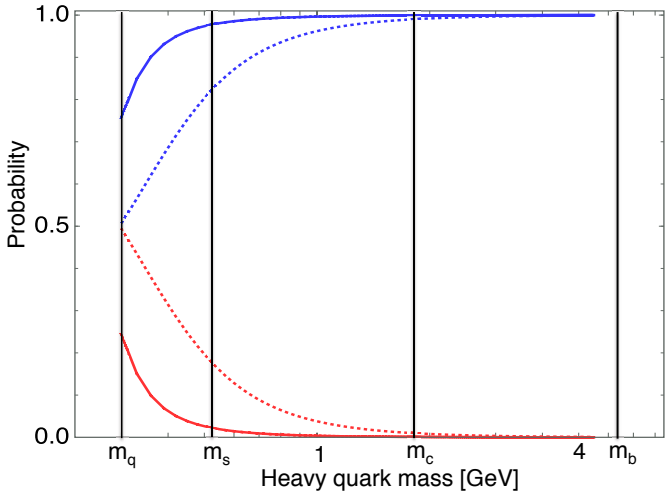

Figure 5.10: The prbability of λ mode (blue line) and ρ mode (red line) of $\frac{1}{2}^-$ for Σ_Q (dotted line), Λ_Q (Solid line).

$$\Phi_{\Lambda_Q}^{J_n=1/2_2,M}(\boldsymbol{\rho},\boldsymbol{\lambda}) \quad = \quad \phi_{\Lambda_Q,j=0}^{J_n=1/2_2,M}(\boldsymbol{\rho},\boldsymbol{\lambda}) \tag{5.63}$$

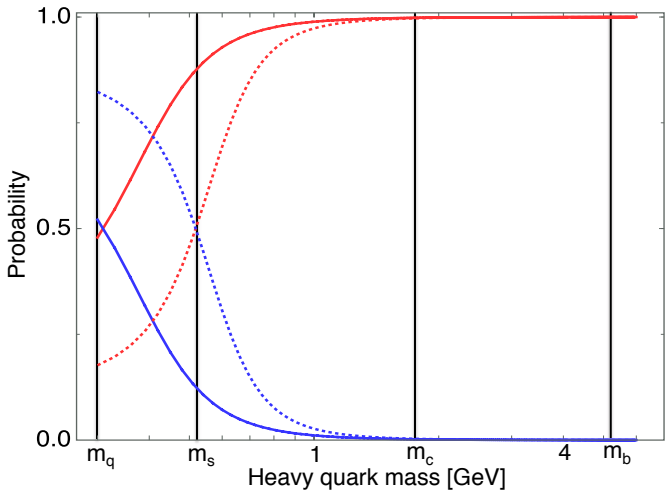

Figure 5.11: The prbability of λ mode (blue line) and ρ mode (red line) of $\frac{1}{2}^-$ for Ξ_{QQ} (Solid line) and Ω_{QQ} (dotted line).

$$\Phi_{\Lambda_Q}^{J_n=3/2_1,M}(\boldsymbol{\rho},\boldsymbol{\lambda}) = \phi_{\Lambda_Q,j=2}^{J_n=3/2_1,M}(\boldsymbol{\rho},\boldsymbol{\lambda}) \tag{5.64}$$

$$\Phi_{\Lambda_Q}^{J_n=5/2_1,M}(\boldsymbol{\rho},\boldsymbol{\lambda}) = \phi_{\Lambda_Q,j=2}^{J_n=5/2_1,M}(\boldsymbol{\rho},\boldsymbol{\lambda}) \tag{5.65}$$

$$\Phi_{\Sigma_Q}^{J_n=1/2_1,M}(\boldsymbol{\rho},\boldsymbol{\lambda}) = \phi_{\Sigma_Q,j=1}^{J_n=1/2_1,M}(\boldsymbol{\rho},\boldsymbol{\lambda}) \tag{5.66}$$

$$\Phi_{\Sigma_Q}^{J_n=3/2_1,M}(\boldsymbol{\rho},\boldsymbol{\lambda}) = \phi_{\Sigma_Q,j=1}^{J_n=3/2_1,M}(\boldsymbol{\rho},\boldsymbol{\lambda}) \tag{5.67}$$

where we use Eq.(5.37) to transform the bases. There are two doublet pairs $(\Lambda_Q(3/2_1^+), \Lambda_Q(5/2_1^+))$ $(j=2)$, $(\Sigma_Q(1/2_1^+), \Sigma_Q(3/2_1^+))$ $(j=1)$ and two singlet states $\Lambda_Q(1/2_1^+)$, $\Lambda_Q(1/2_2^+)$ in the heavy quark limit. Mixings of different j components of the wave function are negligible even in the charm quark region.

5.4 Summary

We have studied the spectrum of the single- and double-heavy baryons and discussed their structures within the framework of a constituent quark model. The potential parameters are determined so as to reproduce the energies of the lowest states $\Lambda(1/2^+)$, $\Sigma(1/2^+)$, $\Sigma(3/2^+)$, $\Lambda(1/2^-)$, $\Lambda(3/2^-)$, $\Lambda_c(1/2^+)$ and $\Lambda_b(1/2^+)$. In the analysis of the baryon wave functions, we have focused on the two characteristic excited modes and investigated the their probabilities as functions of the heavy quark mass. To obtain the precise

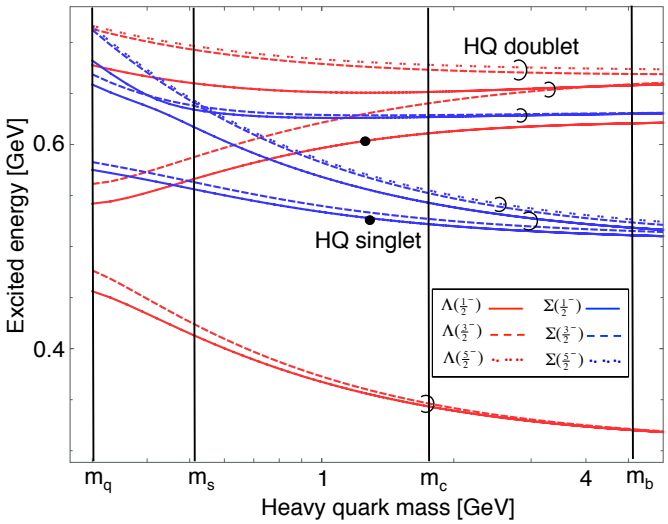

Figure 5.12: Heavy quark mass dependence of excited energy of first state, second state and third state for $1/2^-$(solid line), $3/2^-$(dashed line), $5/2^-$(twined line) of Λ_Q (red line) and Σ_Q (blue line). Bullet denote heavy quark singlet. The pair within a half circle denote heavy quark doublet.

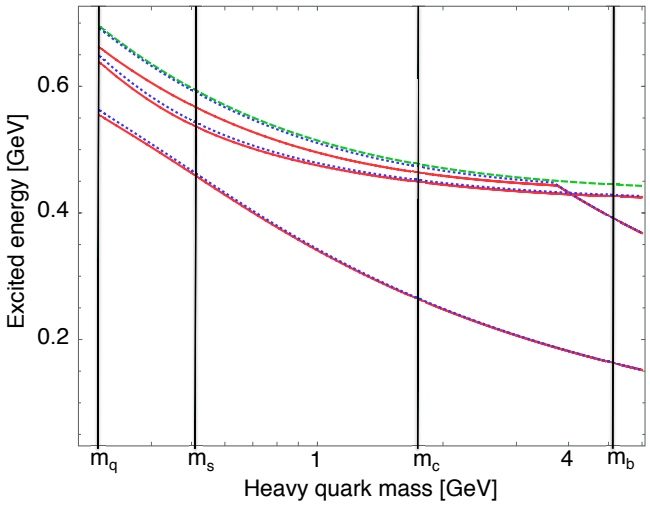

Figure 5.13: Heavy quark mass dependence of excited energy of first state, second state and third state for $1/2^-$(red solid line), $3/2^-$(blue dotted line), $5/2^-$(green dashed line) of Ξ_{QQ}.

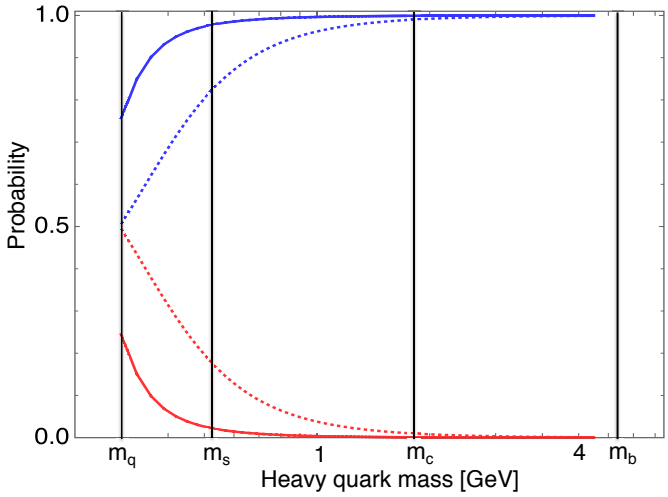

Figure 5.14: The prbability of λ mode (blue line) and ρ mode (red line) of $\frac{1}{2}^-$ for Σ_Q (dotted line), Λ_Q (Solid line).

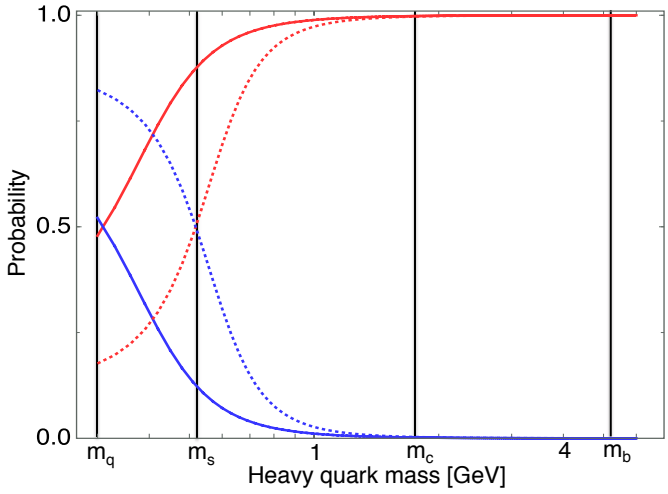

Figure 5.15: The prbability of λ mode (blue line) and ρ mode (red line) of $\frac{1}{2}^-$ for Ξ_{QQ} (Solid line) and Ω_{QQ} (dotted line).

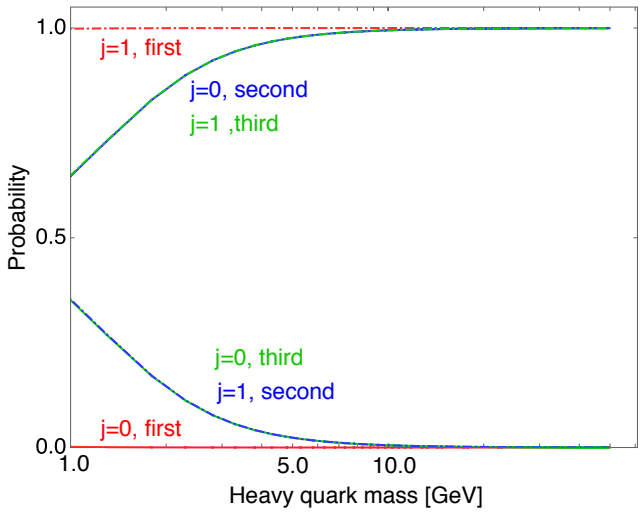

Figure 5.16: The probabilities of j=0 (Solid line) and j=1 (Chain line) for $\Lambda(1/2^-)$. Red, blue, green lines show the first state, second state and third state respectively.

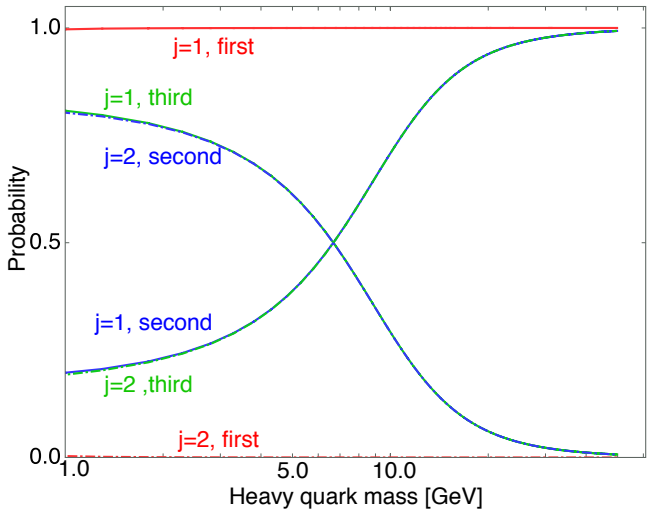

Figure 5.17: The probabilities of j=1 (Solid line) and j=2 (Chain line) for $\Lambda(3/2^-)$. Red, blue, green lines show the first state, second state and third state respectively.

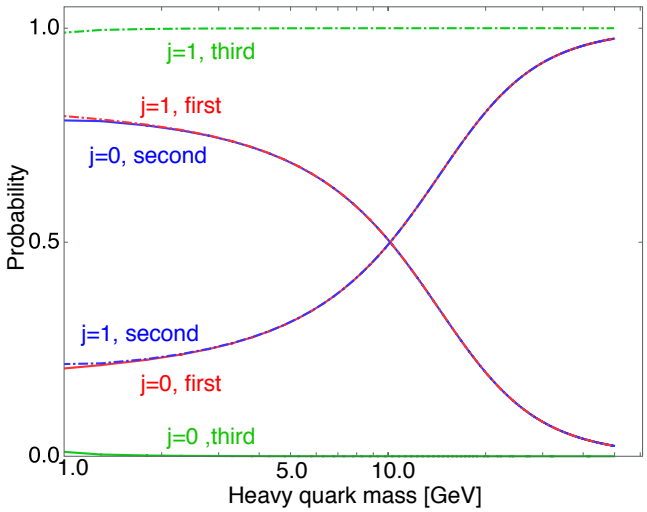

Figure 5.18: The probabilities of j=0 (Solid line) and j=1 (Chain line) for $\Sigma(1/2^-)$. Red, blue, green lines show the first state, second state and third state respectively.

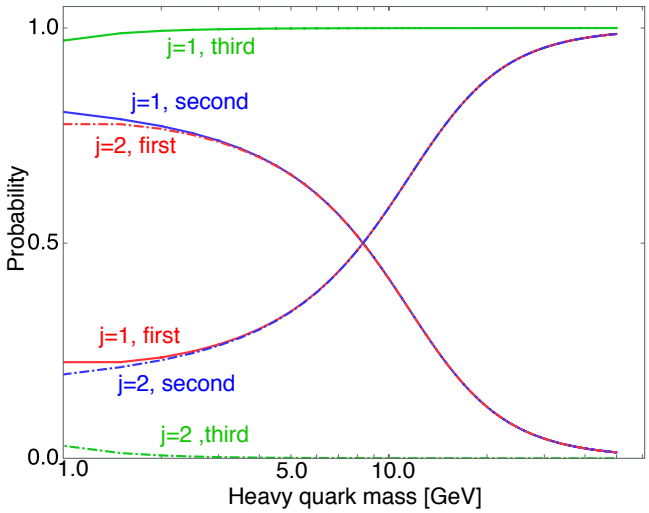

Figure 5.19: The probabilities of j=1 (Solid line) and j=2 (Chain line) for $\Sigma(3/2^-)$. Red, blue, green lines show the first state, second state and third state respectively.

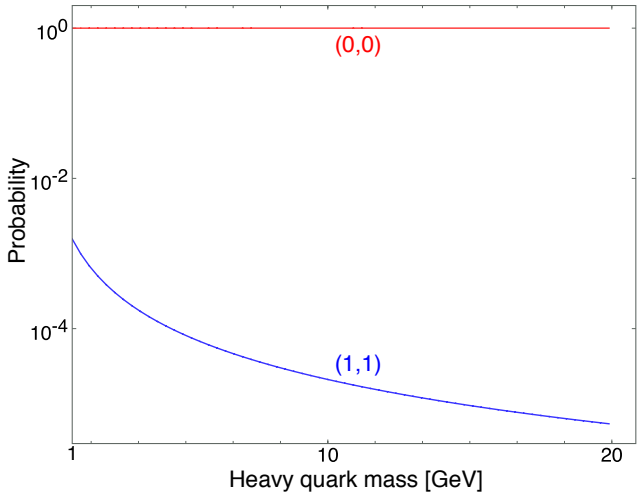

Figure 5.20: The heavy quark mass dependence of the probabilities of the S-wave (0.0) component (Red line) and (1,1) component (blue line) for $\Lambda(1/2^+_1)$.

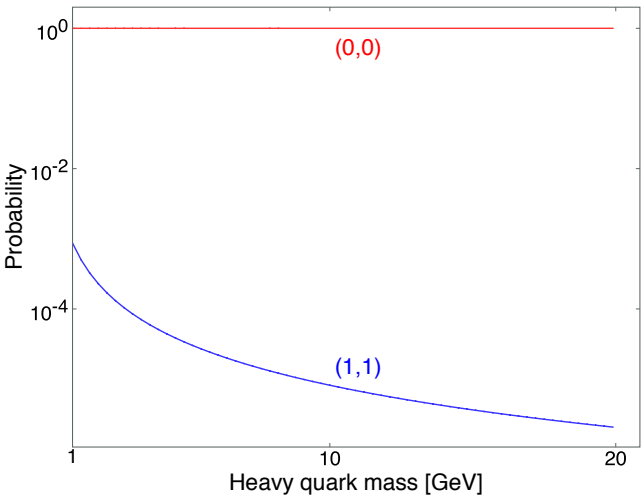

Figure 5.21: The heavy quark mass dependences of the probabilities of the S-wave (0.0) component (Red line) and (1,1) component (blue line) for $\Lambda(1/2^+_2)$.

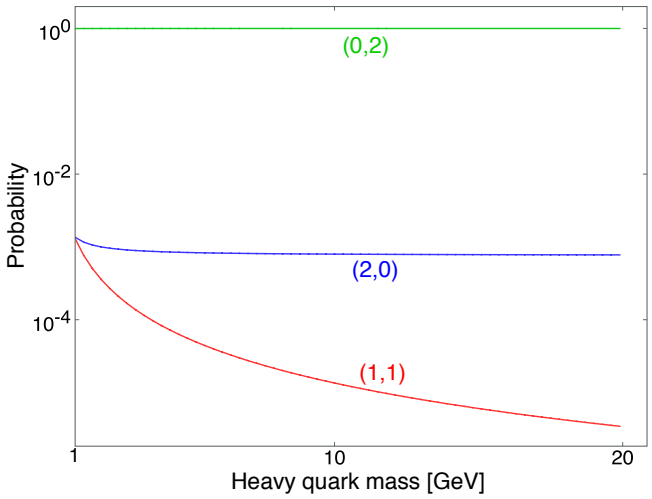

Figure 5.22: The heavy quark mass dependences of the probabilities of (1,1) component (red line), (2,0) component (blue line) and (0,2) component (green line) for $\Lambda(3/2^+_1)$.

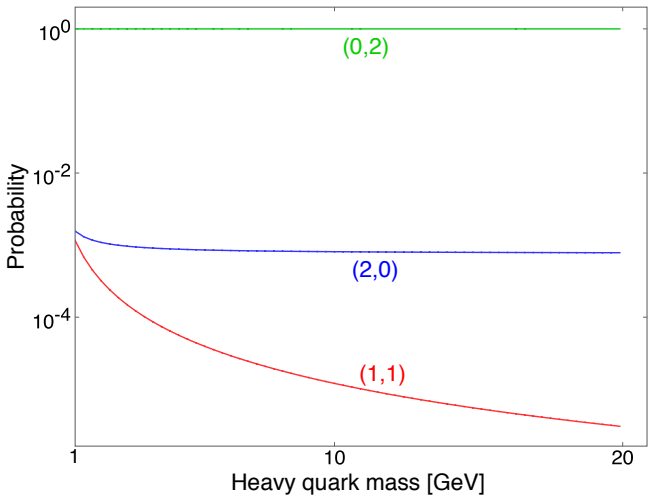

Figure 5.23: The heavy quark mass dependences of the probabilities of (1,1) component (red line), (2,0) component (blue line) and (0,2) component (green line) for $\Lambda(5/2^+_1)$.

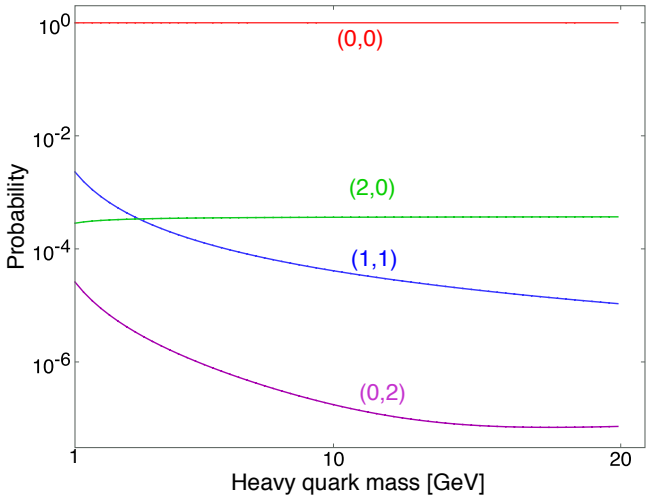

Figure 5.24: The heavy quark mass dependences of the probabilities of the S-wave (0,0) component (red line), (1,1) component (blue line), (2,0) component (green line) and (0,2) component (violet line) for $\Sigma(1/2^+_1)$.

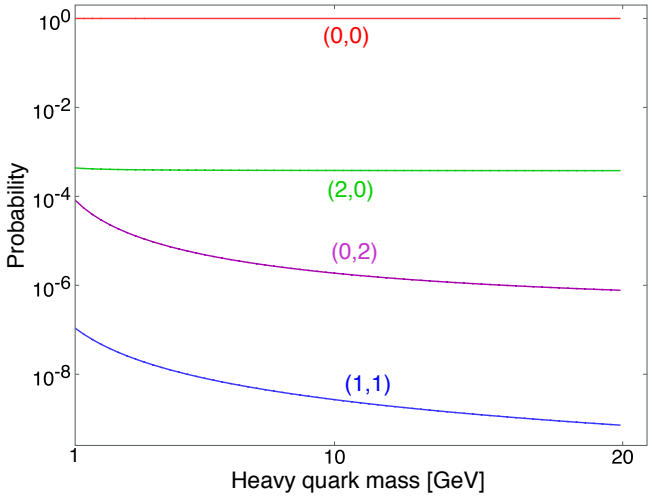

Figure 5.25: The heavy quark mass dependences of the probabilities of the S-wave (l=0,L=0) component (red line), (1,1) component (blue line), (2,0) component (green line) and (0,2) component (violet line) for $\Sigma(3/2^+_1)$.

energy eigenvalues of excited states, we employ the gaussian expansion method, which is one of the best method for three and four body bound states. We have obtained the followings:

(1) Masses of the known Λ_Q, Σ_Q and Ω_Q are in good agreement with the observed data within 50 MeV. Then, we predicted that observed $\Sigma_c(2800)$ can be assigned to $1/2^-_1$, $3/2^-_1$, $1/2^-_2$, $3/2^-_2$ and $5/2^-_1$ state, and Λ_c to $3/2^+_1$, $5/2^-_1$, $1/2^-_2$, $1/2^-_3$ and $3/2^-_2$ and $3/2^-_3$.

(2) In the heavy quark limit, we find six doublets and two singlets for the P-wave single-heavy baryons (See Fig.5.12) and two doublets and two singlets for the first six states of positive parity single-heavy baryons. In the charm sector, the mass differences of these heavy quark spin-doublets are less than 30 [MeV] and in the bottom sector, the differences reduce to less than 10 [MeV].

(3) For the double-heavy baryons, we predict that the mass of the ground Ξ_{cc} state is $\Xi_{cc}(3685)$. This result is consistent with the recent Lattice QCD calculations within 50 MeV. Experimentally, it was reported that a double- charmed baryon was found at the mass 3512 MeV [72]. But other experimental groups, LHC and Belle, have not yet succeeded in the observing the state.

(4) We have investigated the dependences on the heavy quark mass m_Q of the λ and ρ modes to see the features of the negative parity states. Mixings of the ρ and λ modes are suppressed and only one mode dominates. This is because the spin-spin interaction which mainly causes the mixing becomes small in the heavy quark region. It is a future problem to clarify what physical quantities sensitive the differences of the two modes. One possibility is decay patterns. It is conjectured that the λ-mode states decay dominantly to a light baryon and a heavy meson, while the ρ-mode states decay mostly into a light meson and a heavy baryon. Further studies of the decays and productions of these heavy baryons will be useful to verify more on these structures.

Acknowledgments

The completion of this thesis is based on supports from many people. I would like to express my appreciation to them.

I would like to express my sincere gratitude to my supervisor Prof. Makoto Oka for his excellent guidance and strong, ungrudging supports for my research. He has always been willing to help with a smile and given deep insights of physics to me. If it had not been for his much support, I could not have reached completion of this thesis. I think I was very lucky to have such a great supervisor.

I am grateful to Prof. Emiko Hiyama who instructs me in few-body calculations. She have given guidance about complicated few-body calculation method from the basics patiently in four years.

I would like to thank Prof. Atsusi Hosaka for fruitful discussions and good advices from him. He put in an appearance at Tokyo tech many times to discuss the physics. He has been actively interested in my work and kindly given helpful suggestions during the initial phases of this thesis.

I greatly appreciate Dr. Shigehiro Yasui for all the support during the last phase of this thesis.

I would also like to thank Prof. Juan Neves, Prof. Hiroyuki Noumi, Mr. Katsunori Sadato, Mr. Kenta Miyahara for valuable discussions about my research.

I appreciate all the members of nuclear theory group of Tokyo Institute of Technology and strangeness nuclear physics laboratory of RIKEN Nishina Center for their kindness and a lot of help.

This work was supported in part by the Junior Research Associate scholarship at RIKEN. The numerical calculations were carried out on SR16000 at YITP in Kyoto University.

Finally, I would like to express my great appreciation for all the supports and friendships from my family and my friends.

Appendix

E The transformation of the bases

We discuss the wave function in the heavy quark limit in this appendix. For the single-heavy baryons, we take only the channel c=3 of the Jscobi coordinate given in Fig.5.1. The P-wave wave functions of the Λ_Q and Σ_Q baryons are given by the sum of the λ-mode ($^{2S+1}\lambda = {}^2\lambda,\ {}^4\lambda$) and ρ-mode ($^{2S+1}\rho = {}^2\rho,\ {}^4\rho$) components as follows.

$$\begin{aligned}\Phi^{JM}_{\Lambda_Q}(\boldsymbol{\rho},\boldsymbol{\lambda}) &= \psi^{\Lambda_Q}_{{}^2\rho}\sum_{(n,N)} C^{{}^2\rho}_{n,N}\phi_{n,N}(\rho,\lambda) + \psi^{\Lambda_Q}_{{}^4\rho}\sum_{(n,N)} C^{{}^4\rho}_{n,N}\phi_{n,N}(\rho,\lambda) \\ &+ \psi^{\Lambda_Q}_{{}^2\lambda}\sum_{(n,N)} C^{{}^2\lambda}_{n,N}\phi_{n}(\rho,\lambda) \end{aligned} \tag{E.68}$$

$$\begin{aligned}\Phi^{JM}_{\Sigma_Q}(\boldsymbol{\rho},\boldsymbol{\lambda}) &= \psi^{\Sigma_Q}_{{}^2\lambda}\sum_{(n,N)} C^{{}^2\lambda}_{n,N}\phi_{n}(\rho,\lambda) + \psi^{\Sigma_Q}_{{}^4\lambda}\sum_{(n,N)} C^{{}^4\lambda}_{n}\phi_{n,N}(\rho,\lambda) \\ &+ \psi^{\Sigma_Q}_{{}^2\rho}\sum_{(n,N)} C^{{}^2\rho}_{n,N}\phi_{n,N}(\rho,\lambda). \end{aligned} \tag{E.69}$$

Here we extract the parts of the spin and orbital angular momenta for each mode as

$$\psi^{\Lambda_Q}_{{}^2\rho} = [X_{S=1/2,1}[Y_{\ell=1}(\hat{\boldsymbol{\rho}})Y_{L=0}(\hat{\boldsymbol{\lambda}})]_{I=1}]_{JM} \tag{E.70}$$

$$\psi^{\Lambda_Q}_{{}^4\rho} = [X_{S=3/2,1}[Y_{\ell=1}(\hat{\boldsymbol{\rho}})Y_{L=0}(\hat{\boldsymbol{\lambda}})]_{I=1}]_{JM} \tag{E.71}$$

$$\psi^{\Lambda_Q}_{{}^2\lambda} = [X_{S=1/2,0}[Y_{\ell=0}(\hat{\boldsymbol{\rho}})Y_{L=1}(\hat{\boldsymbol{\lambda}})]_{I=1}]_{JM} \tag{E.72}$$

$$\psi^{\Sigma_Q}_{{}^2\lambda} = [X_{S=1/2,1}[Y_{\ell=0}(\hat{\boldsymbol{\rho}})Y_{L=1}(\hat{\boldsymbol{\lambda}})]_{I=1}]_{JM} \tag{E.73}$$

$$\psi^{\Sigma_Q}_{{}^4\lambda} = [X_{S=3/2,1}[Y_{\ell=0}(\hat{\boldsymbol{\rho}})Y_{L=1}(\hat{\boldsymbol{\lambda}})]_{I=1}]_{JM} \tag{E.74}$$

$$\psi^{\Sigma_Q}_{{}^2\rho} = [X_{S=1/2,0}[Y_{\ell=1}(\hat{\boldsymbol{\rho}})Y_{L=0}(\hat{\boldsymbol{\lambda}})]_{I=1}]_{JM} \tag{E.75}$$

Then the corresponding radial parts are expanded by the Gaussian basis as

$$\phi_{n,N}(\rho,\lambda) = N_{n\ell}N_{NL}\rho^{\ell}e^{-\beta_n\rho^2}\lambda^{L}e^{-\gamma_N\lambda^2}, \tag{E.76}$$

where $N_{nl}(N_{NL})$ is the normalization constant. As is discussed in chapter.1, the light spin component j is conserved in the heavy quark limit. Therefore, we transform the bases into those which diagonalize j. We use Eq.(5.37) to transform the bases, and obtain

$$\psi^{\Lambda_Q}_{2_\rho} = \sqrt{\frac{1}{3}}\psi_{j=0,s=1} - \sqrt{\frac{2}{3}}\psi_{j=1,s=1} \tag{E.77}$$

$$\psi^{\Lambda_Q}_{4_\rho} = \sqrt{\frac{2}{3}}\psi_{j=0,s=1} + \sqrt{\frac{1}{3}}\psi_{j=1,s=1} \tag{E.78}$$

$$\psi^{\Lambda_Q}_{2_\lambda} = -\psi_{j=1,s=0} \tag{E.79}$$

$$\psi^{\Sigma_Q}_{2_\lambda} = \sqrt{\frac{1}{3}}\psi_{j=0,s=1} - \sqrt{\frac{2}{3}}\psi_{j=1,s=1} \tag{E.80}$$

$$\psi^{\Sigma_Q}_{4_\lambda} = \sqrt{\frac{2}{3}}\psi_{j=0,s=1} + \sqrt{\frac{1}{3}}\psi_{j=1,s=1} \tag{E.81}$$

$$\psi^{\Sigma_Q}_{2_\rho} = -\psi_{j=1,s=0}. \tag{E.82}$$

for $J = 1/2^-$ and

$$\psi^{\Lambda_Q}_{2_\rho} = -\sqrt{\frac{1}{6}}\psi_{j=1,s=1} + \sqrt{\frac{5}{6}}\psi_{j=2,s=1} \tag{E.83}$$

$$\psi^{\Lambda_Q}_{4_\rho} = -\sqrt{\frac{5}{6}}\psi_{j=1,s=1} - \sqrt{\frac{1}{6}}\psi_{j=2,s=1} \tag{E.84}$$

$$\psi^{\Lambda_Q}_{2_\lambda} = \psi_{j=1,s=0} \tag{E.85}$$

$$\psi^{\Sigma_Q}_{2_\lambda} = -\sqrt{\frac{1}{6}}\psi_{j=1,s=1} + \sqrt{\frac{5}{6}}\psi_{j=2,s=1} \tag{E.86}$$

$$\psi^{\Sigma_Q}_{4_\lambda} = -\sqrt{\frac{5}{6}}\psi_{j=1,s=1} - \sqrt{\frac{1}{6}}\psi_{j=2,s=1} \tag{E.87}$$

$$\psi^{\Sigma_Q}_{2_\rho} = \psi_{j=1,s=0}. \tag{E.88}$$

for $J = 3/2^-$, where

$$\psi_{j,s} = [[[\chi_{1/2}(q)\chi_{1/2}(q)]_s[Y(\hat{\boldsymbol{\rho}})_\ell Y(\hat{\boldsymbol{\lambda}})_L]_I]_j\chi_{1/2}(Q)]_J \tag{E.89}$$

By using Eq.(E.70)-(E.75), Eq.(E.68) and Eq(E.69) is transformed into the bases which is characterized by j.

- $\Lambda_Q(1/2^-, 3/2^-)$

$$\begin{aligned}\phi^{J=1/2,M}_{\Lambda_Q,j=0}(\boldsymbol{\rho},\boldsymbol{\lambda}) &= \psi_{j=0,s=1}\left(\sqrt{\frac{1}{3}}\sum_{(n,N)} C^{2\rho}_{n,N}\phi_{n,N}(\rho,\lambda) + \sqrt{\frac{2}{3}}\sum_{(n,N)} C^{4\rho}_{n,N}\phi_{n,N}(\rho,\lambda)\right) \\ &- \psi_{j=0,s=0}\sum_{(n,N)} C^{2\lambda}_{n,N}\phi_{n,N}(\rho,\lambda)\end{aligned} \tag{E.90}$$

$$\phi^{J=1/2,M}_{\Lambda_Q,j=1}(\boldsymbol{\rho},\boldsymbol{\lambda}) = \psi_{j=1,s=1}\left(-\sqrt{\frac{2}{3}}\sum_{(n,N)} C^{^2\rho}_{n,N}\phi_{n,N}(\rho,\lambda) + \sqrt{\frac{1}{3}}\sum_{(n,N)} C^{^4\rho}_{n,N}\phi_{n,N}(\rho,\lambda)\right) \tag{E.91}$$

$$\begin{aligned}\phi^{J=3/2,M}_{\Lambda_Q,j=1}(\boldsymbol{\rho},\boldsymbol{\lambda}) &= \psi_{j=1,s=1}\left(-\sqrt{\frac{1}{6}}\sum_{(n,N)} C^{^2\rho}_{n,N}\phi_{n,N}(\rho,\lambda) - \sqrt{\frac{5}{6}}\sum_{(n,N)} C^{^4\rho}_{n,N}\phi_{n,N}(\rho,\lambda)\right)\\ &+ \psi_{j=1,s=0}\sum_{(n,N)} C^{^2\lambda}_{n,N}\phi_{n,N}(\rho,\lambda)\end{aligned} \tag{E.92}$$

$$\phi^{J=3/2,M}_{\Lambda_Q,j=2}(\boldsymbol{\rho},\boldsymbol{\lambda}) = \psi_{j=2,s=1}\left(\sqrt{\frac{5}{6}}\sum_{(n,N)} C^{^2\rho}_{n,N}\phi_{n,N}(\rho,\lambda) - \sqrt{\frac{1}{6}}\sum_{(n,N)} C^{^4\rho}_{n,N}\phi_{n,N}(\rho,\lambda)\right) \tag{E.93}$$

- $\Sigma_Q(1/2^-, 3/2^-)$

$$\begin{aligned}\phi^{J=1/2,M}_{\Sigma_Q,j=0}(\boldsymbol{\rho},\boldsymbol{\lambda}) &= \psi_{j=0,s=1}\left(\sqrt{\frac{1}{3}}\sum_{(n,N)} C^{^2\lambda}_{n,N}\phi_{n,N}(\rho,\lambda) + \sqrt{\frac{2}{3}}\sum_{(n,N)} C^{^4\lambda}_{n,N}\phi_{n,N}(\rho,\lambda)\right)\\ &- \psi_{j=0,s=0}\sum_{(n,N)} C^{^2\rho}_{n,N}\phi_{n,N}(\rho,\lambda)\end{aligned} \tag{E.94}$$

$$\phi^{J=1/2,M}_{\Sigma_Q,j=1}(\boldsymbol{\rho},\boldsymbol{\lambda}) = \psi_{j=1,s=1}\left(-\sqrt{\frac{2}{3}}\sum_{(n,N)} C^{^2\lambda}_{n,N}\phi_{n,N}(\rho,\lambda) + \sqrt{\frac{1}{3}}\sum_{(n,N)} C^{^4\lambda}_{n,N}\phi_{n,N}(\rho,\lambda)\right) \tag{E.95}$$

$$\begin{aligned}\phi^{J=3/2,M}_{\Sigma_Q,j=1}(\boldsymbol{\rho},\boldsymbol{\lambda}) &= \psi_{j=1,s=1}\left(-\sqrt{\frac{1}{6}}\sum_{(n,N)} C^{^2\lambda}_{n,N}\phi_{n,N}(\rho,\lambda) - \sqrt{\frac{5}{6}}\sum_{(n,N)} C^{^4\lambda}_{n,N}\phi_{n,N}(\rho,\lambda)\right)\\ &+ \psi_{j=1,s=0}\sum_{(n,N)} C^{^2\rho}_{n,N}\phi_{n,N}(\rho,\lambda)\end{aligned} \tag{E.96}$$

$$\phi^{J=3/2,M}_{\Sigma_Q,j=2}(\boldsymbol{\rho},\boldsymbol{\lambda}) = \psi_{j=2,s=1}\left(\sqrt{\frac{5}{6}}\sum_{(n,N)} C^{^2\lambda}_{n,N}\phi_{n,N}(\rho,\lambda) - \sqrt{\frac{1}{6}}\sum_{(n,N)} C^{^4\lambda}_{n,N}\phi_{n,N}(\rho,\lambda)\right) \tag{E.97}$$

Bibliography

[1] D. Jido, T. Sekihara, Y. Ikeda, T. Hyodo, Y. Kanada-En'yo, and E. Oset, "The nature of Lambda(1405) hyperon resonance in chiral dynamics," Nucl. Phys. **A835** (2010) 59–66, arXiv:1003.4560 [nucl-th].

[2] **Particle Data Group** Collaboration, C. Patrignani et al., "Review of Particle Physics," Chin. Phys. **C40** (2016) no. 10, 100001.

[3] M. Gell-Mann, "A Schematic Model of Baryons and Mesons," Phys. Lett. **8** (1964) 214–215.

[4] **E598** Collaboration, J. J. Aubert et al., "Experimental Observation of a Heavy Particle J," Phys. Rev. Lett. **33** (1974) 1404–1406.

[5] **SLAC-SP-017** Collaboration, J. E. Augustin et al., "Discovery of a Narrow Resonance in e+ e- Annihilation," Phys. Rev. Lett. **33** (1974) 1406–1408. [Adv. Exp. Phys.5,141(1976)].

[6] T. Bohringer et al., "Observation of Upsilon, Upsilon', and Upsilon" at the Cornell electron Storage Ring," Phys. Rev. Lett. **44** (1980) 1111–1114.

[7] M. Voloshin Prog.Part.Nucl.Phys. **61** (2008) 455–511, arXiv:0711.4556 [hep-ph].

[8] S. Ohkoda, Y. Yamaguchi, S. Yasui, K. Sudoh, and A. Hosaka Phys.Rev. **D86** (2012) 014004, arXiv:1111.2921 [hep-ph].

[9] **LHCb** Collaboration, R. Aaij et al. Phys. Rev. Lett. **115** (2015) 072001, arXiv:1507.03414 [hep-ex].

[10] S. H. Lee, S. Yasui, W. Liu, and C. M. Ko Eur.Phys.J. **C54** (2008) 259–265, arXiv:0707.1747 [hep-ph].

[11] L. Maiani, F. Piccinini, A. Polosa, and V. Riquer Phys.Rev. **D71** (2005) 014028, arXiv:hep-ph/0412098 [hep-ph].

[12] A. Selem and F. Wilczek
New trends in HERA physics. Proceedings, Ringberg Workshop, Tegernsee, Germany, October 2-7, 2005 (2006) , arXiv:hep-ph/0602128 [hep-ph].
http://www-library.desy.de/preparch/conf/ringberg/2005/wilczek.ps.gz.

[13] C. Alexandrou, P. de Forcrand, and B. Lucini, "Evidence for diquarks in lattice QCD," Phys. Rev. Lett. **97** (2006) 222002, arXiv:hep-lat/0609004 [hep-lat].

[14] L. Copley, N. Isgur, and G. Karl Phys.Rev. **D20** (1979) 768.

[15] W. Roberts and M. Pervin Int.J.Mod.Phys. **A23** (2008) 2817–2860, arXiv:0711.2492 [nucl-th].

[16] Y. Yamaguchi, S. Ohkoda, A. Hosaka, T. Hyodo, and S. Yasui, "Heavy quark symmetry in multihadron systems," Phys. Rev. **D91** (2015) no. 3, 034034, arXiv:1402.5222 [hep-ph].

[17] S. Weinberg, "Dynamical approach to current algebra," Phys. Rev. Lett. **18** (1967) 188–191.

[18] R. F. Dashen, "Chiral SU(3) x SU(3) as a symmetry of the strong interactions," Phys. Rev. **183** (1969) 1245–1260.

[19] R. F. Dashen and M. Weinstein, "Soft pions, chiral symmetry, and phenomenological lagrangians," Phys. Rev. **183** (1969) 1261–1291.

[20] O. Romanets, L. Tolos, C. Garcia-Recio, J. Nieves, L. L. Salcedo, and R. G. E. Timmermans, "Charmed and strange baryon resonances with heavy-quark spin symmetry," Phys. Rev. **D85** (2012) 114032, arXiv:1202.2239 [hep-ph].

[21] C. Garcia-Recio, V. K. Magas, T. Mizutani, J. Nieves, A. Ramos, L. L. Salcedo, and L. Tolos, "The s-wave charmed baryon resonances from a coupled-channel approach with heavy quark symmetry," Phys. Rev. **D79** (2009) 054004, arXiv:0807.2969 [hep-ph].

[22] T. Yoshida, E. Hiyama, A. Hosaka, M. Oka, and K. Sadato, "Spectrum of heavy baryons in the quark model," Phys. Rev. **D92** (2015) no. 11, 114029, arXiv:1510.01067 [hep-ph].

[23] R. J. Crewther, P. Di Vecchia, G. Veneziano, and E. Witten, "Chiral Estimate of the Electric Dipole Moment of the Neutron in Quantum Chromodynamics," Phys. Lett. **88B** (1979) 123. [Erratum: Phys. Lett.91B,487(1980)].

[24] M. A. Shifman, A. I. Vainshtein, and V. I. Zakharov, "Can Confinement Ensure Natural CP Invariance of Strong Interactions?," Nucl. Phys. **B166** (1980) 493–506.

[25] J. S. Poucher et al., "High-Energy Single-Arm Inelastic e - p and e - d Scattering at 6-Degrees and 10-Degrees," Phys. Rev. Lett. **32** (1974) 118.

[26] M. Gell-Mann, "The interpretation of the new particles as displaced charge multiplets," Nuovo Cim. **4** (1956) no. S2, 848–866.

[27] T. Nakano and K. Nishijima, "Charge Independence for V-particles," Prog. Theor. Phys. **10** (1953) 581–582.

[28] M. Y. Han and Y. Nambu, "Three Triplet Model with Double SU(3) Symmetry," Phys. Rev. **139** (1965) B1006–B1010.

[29] G. Cosme, B. Jean-Marie, S. Jullian, F. Laplanche, J. Lefrancois, A. D. Liberman, G. Parrour, J. P. Repellin, G. Sauvage, and G. Szklarz, "Hadronic production by e+ e- collisions at the energy 990 mev with the orsay storage ring," Phys. Lett. **B40** (1972) 685–688.

[30] H. Burkhardt and B. Pietrzyk, "Update of the hadronic contribution to the QED vacuum polarization," Phys. Lett. **B356** (1995) 398–403.

[31] L. M. Kurdadze, A. P. Onuchin, S. I. Serednyakov, V. A. Sidorov, and S. I. Eidelman, "Observation of multihadronic events in e+ e- collisions at the energy of 1.18-1.34 gev," Phys. Lett. **B42** (1972) 515–518.

[32] L. J. Reinders, H. Rubinstein, and S. Yazaki, "Hadron Properties from QCD Sum Rules," Phys. Rept. **127** (1985) 1.

[33] M. A. Shifman, A. I. Vainshtein, and V. I. Zakharov, "QCD and Resonance Physics. Theoretical Foundations," Nucl. Phys. **B147** (1979) 385–447.

[34] C. D. Roberts and A. G. Williams, "Dyson-Schwinger equations and their application to hadronic physics," Prog. Part. Nucl. Phys. **33** (1994) 477–575, arXiv:hep-ph/9403224 [hep-ph].

[35] G. S. Bali, "QCD forces and heavy quark bound states," Phys. Rept. **343** (2001) 1–136, arXiv:hep-ph/0001312 [hep-ph].

[36] T. Kawanai and S. Sasaki Phys.Rev.Lett. **107** (2011) 091601, arXiv:1102.3246 [hep-lat].

[37] F. Gursey and L. A. Radicati, "Spin and unitary spin independence of strong interactions," Phys. Rev. Lett. **13** (1964) 173–175.

[38] S. Okubo, "Note on unitary symmetry in strong interactions," Prog. Theor. Phys. **27** (1962) 949–966.

[39] C. D. R. L. Chang and D. J. Wilson, "Hadron physics and dynamical chiral symmetry breaking," PoS QCDTNT-II, 039 **15** (2012) .

[40] E. Eichten, K. Gottfried, T. Kinoshita, K. D. Lane, and T.-M. Yan, "Charmonium: Comparison with Experiment," Phys. Rev. **D21** (1980) 203.

[41] T. Barnes, S. Godfrey, and E. S. Swanson, "Higher charmonia," Phys. Rev. **D72** (2005) 054026, arXiv:hep-ph/0505002 [hep-ph].

[42] L. Chang, C. D. Roberts, and D. J. Wilson, "Hadron physics and dynamical chiral symmetry breaking," PoS **QCD-TNT-II2011** (2011) 039, arXiv:1201.3918 [nucl-th].

[43] A. De Rujula, H. Georgi, and S. L. Glashow, "Hadron Masses in a Gauge Theory," Phys. Rev. **D12** (1975) 147–162.

[44] Y. Nambu and G. Jona-Lasinio, "Dynamical Model of Elementary Particles Based on an Analogy with Superconductivity. 1.," Phys. Rev. **122** (1961) 345–358.

[45] Y. Nambu and G. Jona-Lasinio, "DYNAMICAL MODEL OF ELEMENTARY PARTICLES BASED ON AN ANALOGY WITH SUPERCONDUCTIVITY. II," Phys. Rev. **124** (1961) 246–254.

[46] J. Goldstone, "Field Theories with Superconductor Solutions," Nuovo Cim. **19** (1961) 154–164.

[47] S. Weinberg, "Phenomenological Lagrangians," Physica **A96** (1979) 327–340.

[48] J. Gasser and H. Leutwyler, "eta —¿ 3 pi to One Loop," Nucl. Phys. **B250** (1985) 539–560.

[49] J. Gasser and H. Leutwyler, "Chiral Perturbation Theory: Expansions in the Mass of the Strange Quark," Nucl. Phys. **B250** (1985) 465–516.

[50] J. Gasser and H. Leutwyler, "Low-Energy Expansion of Meson Form-Factors," Nucl. Phys. **B250** (1985) 517–538.

[51] **Particle Data Group** Collaboration, K. Nakamura et al., "Review of particle physics," J. Phys. **G37** (2010) 075021.

[52] A. Krause, "Baryon Matrix Elements of the Vector Current in Chiral Perturbation Theory," Helv. Phys. Acta **63** (1990) 3–70.

[53] J. Gasser, M. E. Sainio, and A. Svarc, "Nucleons with Chiral Loops," Nucl. Phys. **B307** (1988) 779–853.

[54] B. Borasoy, "Baryon axial currents," Phys. Rev. **D59** (1999) 054021, arXiv:hep-ph/9811411 [hep-ph].

[55] S. Takeuchi Phys.Rev.Lett. **73** (1994) 2173–2175.

[56] E. Hiyama, Y. Kino, and M. Kamimura Prog.Part.Nucl.Phys. **51** (2003) 223–307.

[57] M. Kamimura, "Nonadiabatic coupled-rearrangement-channel approach to muonic molecules," Phys. Rev. **A38** (1988) 621–624.

[58] H. Kameyama, M. Kamimura, and Y. Fukushima, "Coupled-rearrangement-channel Gaussian-basis variational method for trinucleon bound states," Phys. Rev. **C40** (1989) 974–987.

[59] Y. Kino, H. Kudo, and M. Kamimura, "High precision calculation of anti-protonic helium atomcules and anti-proton mass," Few Body Syst. Suppl. **12** (2000) 40–44. [,40(2000)].

[60] Y. Kino, H. Kudo, and M. Kamimura, "High-accuracy 3-body coupled-channel calculation of metastable states of anti-protonic helium atoms," Nucl. Phys. **A631** (1998) 649C–652C.

[61] S. Funada, H. Kameyama, and Y. Sakuragi, "Halo structure and soft dipole mode of He-6 nucleus in the alpha + n + n cluster model," Nucl. Phys. **A575** (1994) 93–117.

[62] M. Kamimura and H. Kameyama, "Coupled rearrangement channel calculations of muonic molecules and A =3 nuclei," Nucl. Phys. **A508** (1990) 17–28.

[63] E. Hiyama, M. Kamimura, A. Hosaka, H. Toki, and M. Yahiro, "Five-body calculation of resonance and scattering states of pentaquark system," Phys. Lett. **B633** (2006) 237–244, arXiv:hep-ph/0507105 [hep-ph].

[64] E. Hiyama, M. Kamimura, M. Yahiro, A. Hosaka, and H. Toki, "Five-body calculation of resonance and continuum states of pentaquark baryons with quark-quark correlations," Nucl. Phys. **A755** (2005) 411–414. [,274(2005)].

[65] E. Hiyama, K. Suzuki, H. Toki, and M. Kamimura, "Role of quark quark correlation in baryon structure and nonleptonic weak transitions of hyperons," Prog. Theor. Phys. **112** (2004) 99–117, arXiv:nucl-th/0402007 [nucl-th].

[66] K. Suzuki, E. Hiyama, H. Toki, and M. Kamimura, "Roles of quark pair correlations in baryon structure and nonleptonic weak transitions of hyperon," Few Body Syst. Suppl. **12** (2000) 209–213, arXiv:nucl-th/0002047 [nucl-th]. [,209(1999)].

[67] J.-X. Lu, Y. Zhou, H.-X. Chen, J.-J. Xie, and L.-S. Geng, "Dynamically generated $J^P = 1/2^-(3/2^-)$ singly charmed and bottom heavy baryons," Phys. Rev. **D92** (2015) no. 1, 014036, arXiv:1409.3133 [hep-ph].

[68] C. Garcia-Recio, C. Hidalgo-Duque, J. Nieves, L. L. Salcedo, and L. Tolos, "Compositeness of the strange, charm, and beauty odd parity Λ states," Phys. Rev. **D92** (2015) no. 3, 034011, arXiv:1506.04235 [hep-ph].

[69] **PACS-CS Collaboration** Collaboration, Y. Namekawa et al. Phys.Rev. **D87** (2013) no. 9, 094512, arXiv:1301.4743 [hep-lat].

[70] H. Na and S. Gottlieb PoS **LATTICE2008** (2008) 119, arXiv:0812.1235 [hep-lat].

[71] C. Albertus, E. Hernandez, J. Nieves, and J. Verde-Velasco Eur.Phys.J. **A32** (2007) 183–199, arXiv:hep-ph/0610030 [hep-ph].

[72] **SELEX** Collaboration, M. A. Moinester et al., "First observation of doubly charmed baryons," Czech. J. Phys. **53** (2003) B201–B213, arXiv:hep-ex/0212029 [hep-ex].

[73] **BaBar Collaboration** Collaboration, B. Aubert et al. Phys.Rev. **D74** (2006) 011103, arXiv:hep-ex/0605075 [hep-ex].

[74] **BELLE Collaboration** Collaboration, R. Chistov et al. Phys.Rev.Lett. **97** (2006) 162001, arXiv:hep-ex/0606051 [hep-ex].

[75] **LHCb** Collaboration, S. Ogilvy Proceedings, 6th International Workshop on Charm Physics (Charm 2013) (2013) , arXiv:1312.1601 [hep-ex]. https://inspirehep.net/record/1267653/files/arXiv:1312.1601.pdf.

[76] T. Hyodo, D. Jido, and A. Hosaka, "Origin of the resonances in the chiral unitary approach," Phys. Rev. **C78** (2008) 025203, arXiv:0803.2550 [nucl-th].

[77] M. F. M. Lutz and E. E. Kolomeitsev, "Relativistic chiral SU(3) symmetry, large N(c) sum rules and meson baryon scattering," Nucl. Phys. **A700** (2002) 193–308, arXiv:nucl-th/0105042 [nucl-th].

[78] J. A. Oller and U. G. Meissner, "Chiral dynamics in the presence of bound states: Kaon nucleon interactions revisited," Phys. Lett. **B500** (2001) 263–272, arXiv:hep-ph/0011146 [hep-ph].

[79] E. Oset and A. Ramos, "Nonperturbative chiral approach to s wave anti-K N interactions," Nucl. Phys. **A635** (1998) 99–120, arXiv:nucl-th/9711022 [nucl-th].

[80] Y. Nogami, "Possible existence of $\bar{K}$NN bound states," Phys. Lett. **7** (1963) no. 4, 288–289.

[81] T. Sekihara, T. Hyodo, and D. Jido, "Electromagnetic mean squared radii of Lambda(1405) in chiral dynamics," Phys. Lett. **B669** (2008) 133–138, arXiv:0803.4068 [nucl-th].

[82] L. Roca, T. Hyodo, and D. Jido, "On the nature of the Lambda(1405) and Lambda(1670) from their N(c) behavior in chiral dynamics," Nucl. Phys. **A809** (2008) 65–87, arXiv:0804.1210 [hep-ph].

[83] T. Hyodo and W. Weise, "Effective anti-K N interaction based on chiral SU(3) dynamics," Phys. Rev. **C77** (2008) 035204, arXiv:0712.1613 [nucl-th].

[84] Y. Akaishi and T. Yamazaki, "Nuclear anti-K bound states in light nuclei," Phys. Rev. **C65** (2002) 044005.

[85] D. Jido, J. A. Oller, E. Oset, A. Ramos, and U. G. Meissner, "Chiral dynamics of the two Lambda(1405) states," Nucl. Phys. **A725** (2003) 181–200, arXiv:nucl-th/0303062 [nucl-th].

[86] C. Garcia-Recio, J. Nieves, O. Romanets, L. L. Salcedo, and L. Tolos, "Odd parity bottom-flavored baryon resonances," Phys. Rev. **D87** (2013) no. 3, 034032, arXiv:1210.4755 [hep-ph].

[87] J. Hofmann and M. F. M. Lutz, "Coupled-channel study of crypto-exotic baryons with charm," Nucl. Phys. **A763** (2005) 90–139, arXiv:hep-ph/0507071 [hep-ph].

[88] C.-H. Lee, D.-P. Min, and M. Rho, "The Role of Lambda (1405) in kaon - proton interactions," Nucl. Phys. **A602** (1996) 334–346, arXiv:hep-ph/9505283 [hep-ph].

[89] A. Le Yaouanc, L. Oliver, O. Pene, and J. C. Raynal, "Naive quark pair creation model of strong interaction vertices," Phys. Rev. **D8** (1973) 2223–2234.

[90] S. Capstick and W. Roberts, "Quasi two-body decays of nonstrange baryons," Phys. Rev. **D49** (1994) 4570–4586, arXiv:nucl-th/9310030 [nucl-th].

[91] T. Barnes, N. Black, and P. R. Page, "Strong decays of strange quarkonia," Phys. Rev. **D68** (2003) 054014, arXiv:nucl-th/0208072 [nucl-th].

[92] T. Barnes, F. E. Close, P. R. Page, and E. S. Swanson, "Higher quarkonia," Phys. Rev. **D55** (1997) 4157–4188, arXiv:hep-ph/9609339 [hep-ph].

[93] S. Capstick and N. Isgur, "Baryons in a Relativized Quark Model with Chromodynamics," Phys. Rev. **D34** (1986) 2809. [AIP Conf. Proc.132,267(1985)].

[94] S. Godfrey and N. Isgur, "Mesons in a Relativized Quark Model with Chromodynamics," Phys. Rev. **D32** (1985) 189–231.

[95] E. S. Ackleh, T. Barnes, and E. S. Swanson, "On the mechanism of open flavor strong decays," Phys. Rev. **D54** (1996) 6811–6829, arXiv:hep-ph/9604355 [hep-ph].

[96] W. Roberts and B. Silvestre-Brac, "General method of calculation of any hadronic decay in the p wave triplet model," Acta Phys. Austriaca **11** (1992) 171–193.

[97] C. Chen, X.-L. Chen, X. Liu, W.-Z. Deng, and S.-L. Zhu, "Strong decays of charmed baryons," Phys. Rev. **D75** (2007) 094017, arXiv:0704.0075 [hep-ph].

[98] H. G. Blundell and S. Godfrey, "The Xi (2220) revisited: Strong decays of the 1(3) F2 1(3) F4 s anti-s mesons," Phys. Rev. **D53** (1996) 3700–3711, arXiv:hep-ph/9508264 [hep-ph].

[99] F. E. Close and E. S. Swanson, "Dynamics and decay of heavy-light hadrons," Phys. Rev. **D72** (2005) 094004, arXiv:hep-ph/0505206 [hep-ph].

[100] H. Nagahiro, S. Yasui, A. Hosaka, M. Oka, and H. Noumi, "Structure of charmed baryons studied by pionic decays," Phys. Rev. **D95** (2017) no. 1, 014023, arXiv:1609.01085 [hep-ph].

[101] **Belle** Collaboration, Y. Kato et al., "Studies of charmed strange baryons in the ΛD final state at Belle," Phys. Rev. **D94** (2016) no. 3, 032002, arXiv:1605.09103 [hep-ex].

[102] **Belle** Collaboration, Y. Kato et al., "Search for doubly charmed baryons and study of charmed strange baryons at Belle," Phys. Rev. **D89** (2014) no. 5, 052003, arXiv:1312.1026 [hep-ex].